NORTH PACIFIC RESEARCH BOARD PROJECT FINAL REPORT

Life history and population dynamics of four endemic Alaskan skates: determining essential biological information for effective management of bycatch and target species

NPRB Project 715 Final Report

David A. Ebert[1, 2], Jasmine R. Maurer[1], Shaara M. Ainsley[1], Lewis Barnett[1, 3], Gregor M. Cailliet[1, 2]

[1]Pacific Shark Research Center, Moss Landing Marine Laboratories, 8272 Moss Landing Rd., Moss Landing, CA 95039. (831) 771-4419, debert@mlml.calstate.edu

[2]Prinicipal investigator and co-principal investigator

[3]Department of Environmental Science & Policy, University of California, Davis, One Shields Ave, Davis, CA 95616

August 2009

Table of Contents

Abstract

In the Bering Sea, skates (*Bathyraja* spp.) are among the most common bycatch species taken in groundfish fisheries. The susceptibility of skates to fishing pressure has been well documented, however, life history information required for stock assessments and implementation of sustainable management plans is largely unknown for species occurring in Alaskan waters. To address this knowledge gap, the age, growth, longevity, reproductive biology, and demography of four common bathyrajid species (*Bathyraja lindbergi*, *B. maculata, B. minispinosa,* and *B. taranetzi*) were examined. The maximum age estimate for *B. lindbergi* and *B. maculata* was 32, *B. minispinosa* was 37, and *B. taranetzi* was 14. Multiple growth models were applied to evaluate growth characteristics. No significant differences were detected between the growth of females and males for *B. lindbergi*, *B. maculata*, or *B. minispinosa*. Three parameter von Bertalanffy growth functions generated estimates of $k = 0.04$ yr^{-1} $L_\infty = 131.9$ cm TL for *B. lindbergi*, $k = 0.036$ yr^{-1} $L_\infty = 155.6$ cm TL for *B. maculata*, $k = 0.02$ yr^{-1} $L_\infty = 146.9$ cm TL for *B. minispinosa*, and $k = 0.11$ yr^{-1} $L_\infty = 85.4$ and $k = 0.19$ yr^{-1} $L_\infty = 66.4$ cm TL for *B. taranetzi* females and males respectively. Median size at maturity was estimated to be 82.0, 95.5, 67.4, and 61.4 cm TL for female *B. lindbergi*, *B. maculata, B. minispinosa,* and *B. taranetzi*, respectively. Demographic models incorporating uncertainty in vital rates projected annual population growth rates of 11% for *B. lindbergi*, 8% for *B. maculata,* 10% for *B. minispinosa,* and 12% for *B. taranetzi*.

Key Words

Commander skate (*Bathyraja lindbergi*), whiteblotched skate (*Bathyraja maculata*), whitebrow skate (*Bathyraja minispinosa*), mud skate (*Bathyraja taranetzi*), eastern Bering Sea, age, growth, maturity, reproduction, demography

Citation

Ebert, D.A., Maurer, J.R., Ainsley, S.M., Barnett, L.A.K., and Cailliet, G.M. 2009. Life history and population dynamics of four endemic Alaskan skates: determining essential biological information for effective management of bycatch and target species. North Pacific Research Board Final Report 715, 120 p.

Study chronology

June-August 2004: Pacific Shark Research Center researchers participate in NMFS – Alaska Fisheries Science Center Eastern Bering Sea Continental Slope survey to collect vertebral and caudal thorn samples for future skate age, growth, and reproductive biology studies.

November 2006-November 2007: Special collection request approved. Vertebral samples were collected by NMFS-AFSC Fisheries Observer Program from the eastern Bering Sea.

January 2007: Alaska skate identification brochure, the outreach component for the project is completed and distributed. Poster presentation of preliminary results presented at Alaska Marine Science Symposium.

May 2007: NPRB 715 grant proposal approved.

July 2007- December 2008: Clean and prepare vertebral centra for ageing.

October 2007: Additional vertebral samples collected by Jerry Hoff (NMFS-AFSC)

November 2007-November 2008: Special collection request approved. Vertebral samples were collected by NMFS-AFSC Fisheries Observer Program from the eastern Bering Sea.

January 2008: Poster presentation of preliminary results to date presented at Alaska Marine Science Symposium and at Western Groundfish conference.

November 2008-March 2009: Gonad samples sent to Louisiana State University for histological processing and subsequentially returned to MLML.

July-September 2008: Prepare thorns for age estimation.

July 2008: Poster presentations on NBRB #715 presented at American Elasmobranch Society meeting.

September 2008: Oral presentation at Oceana Chondrichthyan Society meeting.

December 2008-May 2009: Complete age estimation and analysis.

December 2008: Oral presentation in public seminar series at Islands and Oceans center in Homer, AK.

June 2009: Oral presentation at 8th Indo Pacific Fish Conference.

July 2009: Oral presentations on NPRB #715 presented at AES meeting.

August 2009: Submission of NPRB #510 final report.

Introduction

Targeting new species and utilizing bycatch are alternative strategies employed by fishers and fishery managers to supplement income lost from global population declines in traditional fish stocks. As a result, elasmobranchs (sharks, skates, and rays) are currently being exploited at their greatest historical rates (FAO 1997; Stevens et al. 2000). Regional evidence of this pattern has been documented on the United States Pacific coast where elasmobranch landings and discard have increased among groundfish fisheries (Alaska Fisheries Science Center (AFSC), Resource Assessment & Conservation Engineering Division (RACE), unpub. data; PacFIN 2004; Leet et al. 2001). The increasing exploitation of this group is especially alarming because their typical biological traits (e.g. long life span, slow growth, low fecundity, and late age at maturity) may severely restrict their ability to sustain fishing pressure or recover from overexploitation (Holden 1974; Cailliet 1990; Walker & Hislop 1998; Stevens et al. 2000; Cailliet & Goldman 2004).

Fishing pressure in the North Atlantic has notably impacted the abundance, population structure, and distribution of several skate species, emphasizing the need for baseline biological information for this poorly known group (Walker & Hislop 1998; Dulvy et al. 2000; Frisk et al. 2002). For example, the common skate (*Dipturus batis*) has reportedly been extirpated in regions of the Irish Sea, as a result of bycatch overexploitation (Brander 1981). Indeed, mortality of discarded skates and rays from trawl fisheries may range between 41-65% with survival rates being greater among shelf species (Stobutzki et al. 2002; Laptikhovsky 2004). Because skates are often discretely distributed, vary widely in length and age at maturity, and generally have low fecundity, populations may be differentially susceptible to exploitation and the potential for altering abundance and populations structure may be great (Walker & Hislop 1998; Dulvy & Reynolds 2002).

Skate landings in Alaskan waters greatly exceed those of all other North American states combined. During 2005 an estimated 23,000 metrics tons of skates, most of it discarded, were taken as bycatch in Alaskan groundfish fisheries in the Bering Sea and Aleutian Islands (Matta et al. 2006). Almost nothing, however, is known about the life histories of the local fauna or the impact of fishery exploitation on these species. Prior to 2005, only two skate species were recognized in National Marine Fisheries Service, Alaska Fisheries Science Center (NMFS-AFSC) taxonomic categories for landings statistics, and fishery observers had only identified skates to gross taxa, e.g. “skate unidentified” (Gaichas et al 2005, Matta et al. 2006). As a result, past species composition and relative abundance of skate landings were essentially unknown, precluding conventional assessments of past abundance and population trends.

Incidental capture and landings of skates have increased in recent years and in 2003, a directed fishery for big (*Raja binoculata*) and longnose (*R. rhina*) skates was developed in the GOA off Kodiak Island (NPFMC 1999; Gaichas et al. 2003). This short-live fishery only lasted until 2005, but more recently an experimental fishery for skates began in March 2009 (Ken Goldman, pers. comm., Alaska Department of Fish and Game). The development of this fishery indicates that interest continues to increase for the development of additional skate fisheries in Alaskan waters. It is highly likely therefore, that directed fisheries for this vulnerable group will eventually expand into other areas of Alaska, e.g. Bering Sea and Aleutian Islands (BSAI), given the relatively large take, amount of currently unutilized biomass and the trend of fisheries expansion into deeper waters (Merrett & Haedrich 1997; Haedrich et al. 2001). *Bathyraja lindbergi*, *B. maculata*, *B. minispinosa*, and *B. taranetzi* are deep-water skates that primarily inhabit deep-shelf and upper slope depths, generally between 200 – 800 m in the Bering Sea (Mecklenburg et al. 2002; Stevenson et al. 2008; Ebert et al. 2006). They may therefore be susceptible to increased exploitation as fisheries expand into deeper waters.

Currently, skates are managed as part of the "other species" category and are attributed an aggregate quota along with taxonomically and biologically dissimilar groups (i.e.; sharks, sculpins, squids, and octopi). As directed fisheries for species in this category develop, the potential for overfishing is a primary concern of fisheries managers (Gaichas et al. 1999, 2005). To protect skate stocks, species-level quotas were established for *R. binoculata* and *R. rhina* soon after the fishery was initiated (Gaichas et al. 2003). Similar measures will be necessary as endemic skate species, including bathyrajids, are targeted. However, before effective management of any species can be undertaken, life history characteristics, especially age, growth, and reproduction must be understood and incorporated into management strategies. Yet the lack of detailed biological information for this group greatly impedes the development of species-specific management strategies (or refined multi-species approaches) and restricts a broader understanding of ecosystem-level interactions and processes. Because many skates, like many elasmobranchs, may possess life history characteristics that make them especially vulnerable to fisheries exploitation, details on these species-specific traits are imperative for developing realistic stock assessments and establishing sustainable skate management in Alaskan waters.

Objectives

The objectives of this study were to determine the age, growth, and reproductive characteristics of four skate species, Commander *Bathyraja lindbergi*, whiteblotched *B. maculata*, whitebrow *B. minispinosa*, and mud *B. taranetzi*, endemic to the Bering Sea and Aleutian Islands. All four species are caught as bycatch in groundfish fisheries. Age and growth studies were conducted on all four species and aspects of their reproductive biology were investigated. The use of caudal thorns was evaluated as an alternative, non-lethal, ageing structure for all four species. Based on the resulting life-history parameters, age-based demographic models were developed for each species to compare and evaluate their potential population growth and resilience. Specific research questions addressed in this study include: 1) what is the age and size at 50% and 100% maturity? 2) What is the size at birth? 3) What are the estimated fecundities? 4) Are caudal thorns useful ageing structures? 5) Do growth parameters of females differ from males? 6) What are the maximum observed and theoretical longevities of selected study species? 7) What are the annual rates of population growth and how do these compare among species?

Methods

Specimens of *Bathyraja lindbergi*, *B. maculata*, *B. minispinosa,* and *B. taranetzi* were collected using a bottom trawl from June to August 2004 during a National Marine Fisheries Service Alaska Fisheries Science Center (NMFS-AFSC) research cruise along the eastern Bering Sea continental slope (EBSCS). The survey area extended the length of the EBSCS from northwest of Unalaska Island (55^{o} 95', 168^{o} 92') to the Navarin Canyon (60^{o} 16', 179^{o} 68') near the U.S.–Russian border. A random stratified sampling design of the area was made by means of 83 pre–determined bottom trawl stations (Hoff & Britt, 2005). Bottom trawls of approximately 30 minutes duration were conducted at each station. Poly nor' eastern trawl equipment with 20.0 cm diameter rubber disc mudsweep roller gear was employed for this survey (Hoff & Britt, 2005). Additional vertebral and caudal thorn samples were collected during 2007 and 2008 by Jerry Hoff (Fishery Biologist, NMFS-AFSC) and through the NMFS-AFSC Fisheries Observer Program.

Biological measurements taken at the time of collection included total length (TL), disc width (DW), inner clasper length, testes length and width, oviducal gland width, uterus width and total weight (nearest gram) whenever possible. Total length was measured to the nearest millimeter (mm) from the tip of the snout to the tail tip and inner clasper length was measured from the point of insertion of the clasper shaft to the tip. Sex and maturity status were also determined for each species. Additionally, the number of mature ova per ovary and maximum ovum diameter were recorded from mature females if the gonads were not damaged.

Ageing structures were collected, with sections of at least eight vertebrae being excised from the area posterior to the cranium between the 5th and 20th vertebra, and five to seven of the anterior most caudal thorns (Fig. 1). For a subset of specimens, a subsample of posterior vertebrae, beginning at least 10 vertebral centra posterior to the end of the anterior vertebral sample (Fig. 1), was collected for use in comparing age structures along the vertebral column. Subsamples of whole reproductive tracts were collected from both sexes and were preserved in 10% formalin for later analysis. Fisheries observers only recorded sex, and did not assign a maturity stage or measure and retain reproductive tracts.

Age and Growth

Vertebrae were prepared for ageing using the gross sectioning technique. Vertebrae were cleaned of excess tissue and three to four individual centra were separated. Two perpendicular measurements of centrum diameter (mm) were recorded to the nearest 0.1 mm from the anterior/posterior surface, and a mean was calculated (MCD) to represent centrum diameter. After the centra were cleaned and measured they were air dried. Two dried centra from each sample were randomly selected and mounted on merchandise tags with a polyester casting resin. Mounted centra were then cut sagitally through the

focus, using a low speed saw (Buehler Isomet, Lake Bluff, IL, USA), to between 0.3 and 0.6 mm thickness. Centra sections were mounted in a thin layer of Cytoseal 60 on a slide. Centra sections were polished with wet sandpaper to between 0.2 and 0.3 mm thickness and viewed and photographed under a dissection microscope using transmitted light. One polished section was used for ageing, the second was set aside as a spare. Mineral oil was brushed on vertebral sections to enhance the band pattern and eliminate surface irregularities for viewing. For a subsample of specimens posterior centra were processed to determine if an ageing bias exists between centra from different locations of the vertebral column. Mean centrum diameter was plotted against TL to verify a positive relationship, the best fit curve was determined by R^2 values of lines fit by SigmaPlot graphical software (SPSS Inc. 2002).

To determine if caudal thorns were an appropriate ageing structure thorn height and base width were measured and plotted against TL. As with MCD, R^2 values fit by SigmaPlot graphical software (SPSS Inc. 2002) were used to determine best fit. Excess tissue was removed from thorns by boiling them and when needed lightly scrubbing with a small brush. Caudal thorns were stained using several techniques to enhance the ridge pattern; alizarin red (LaMarca 1966), crystal violet (Johnson 1979), oil enhancement (Cailliet et al. 1983) and lead micro-topography (Neer and Cailliet 2001). Thorns were aged using a combination of unaltered thorns and oil enhancement for *B. lindbergi*, *B. maculata*, and *B. taranetzi*. Banding patterns in *B. minispinosa* caudal thorns were best visualized after staining in 1% crystal violet for 15 minutes, using a method adapted from Carlson et al. (2003) and Johnson (1979).

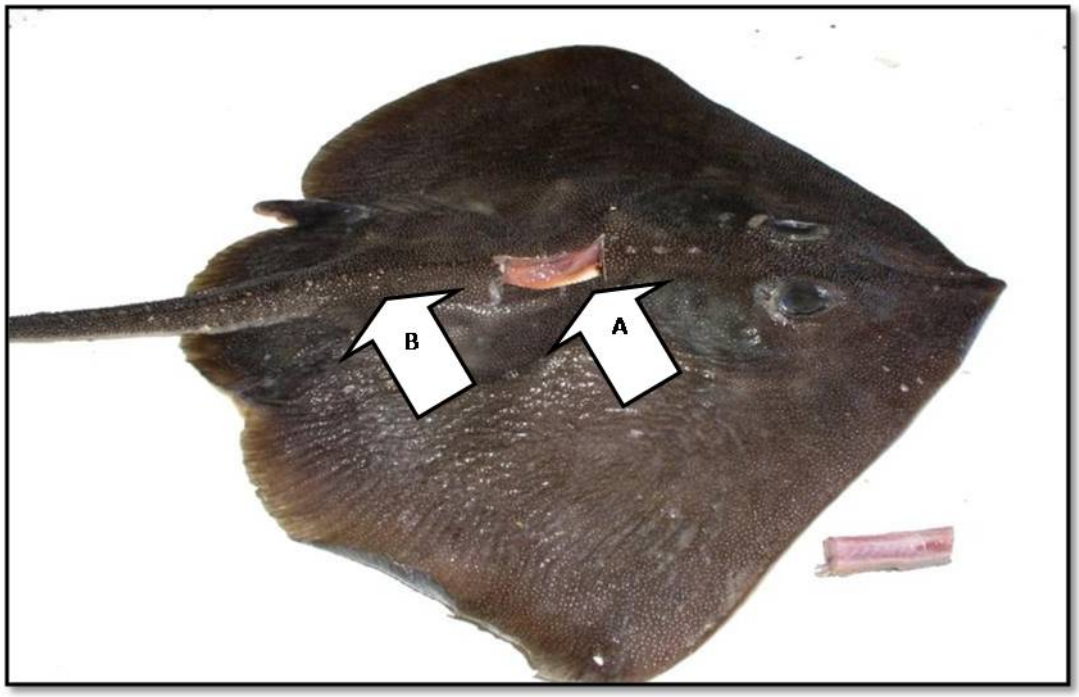

Figure 1.

Vertebrae were excised from anterior (A) and posterior (B) regions of vertebral column. Caudal thorns also were removed from region B.

Age determination

Vertebrae ageing criteria was defined for each species using the following guidelines. The vertebral birthmark (age 0) was defined as the first distinct mark distal to the focus that coincides with an angle change in the corpus calcareum (Walmsley-Hart et al. 1999, Sulikowski et al. 2003), band counts began after this mark. A band pair was defined as one opaque and one translucent band that extended across the corpus calcareum, relative spacing of each band pair also was considered (Fig. 2; Cailliet et al. 2006, McPhie and Campana 2009). Ages were estimated by counting the number of band pairs, which were assumed to represent annual growth, a common assumption for skates (Zeiner and Wolf 1993, Sulikowski et al. 2005a, Frisk and Miller 2006, Matta and Gunderson 2007, Natanson et al. 2007, McPhie and Campana 2009). Bands that did not extend across more than one corpus calcareum follow relative spacing, or have a unique origin and end were considered a check and not counted. Caudal thorn age was assigned by counting band pairs defined as a concentric ridge and an associated broad growth zone on the surface of the thorn. Thorn band counts began below the birthmark defined as the base of the protothorn at the thorns apex (Gallagher and Nolan 1999, Gallagher et al. 2006, Matta and Gunderson 2007).
All vertebrae were assigned a random identification number, to prevent reader bias, and examined three times by the same reader for age estimation. A subset of 20 prepared centra sections were used as a reference set to assure ageing criteria remained constant throughout the ageing process (Campana 2001). The first read was used as a practice read to verify that good ageing criteria had been established and was not included in further analysis. Final age was assigned based on the third read. A fourth read was done when the second and third read differed in age assignment by three or more years. Age estimates were made at least one week apart, with no knowledge of previous band count, length, sex, or date of collection. If the first prepared centra section was not useful for ageing the spare was used. If the second section was not useful for ageing, due to band clarity and not damage from the preparation process, the specimen was not assigned an age. For a subsample of specimens, caudal thorns were examined once for age assignment with no prior knowledge of vertebral age assignment, length, sex, or date of collection.

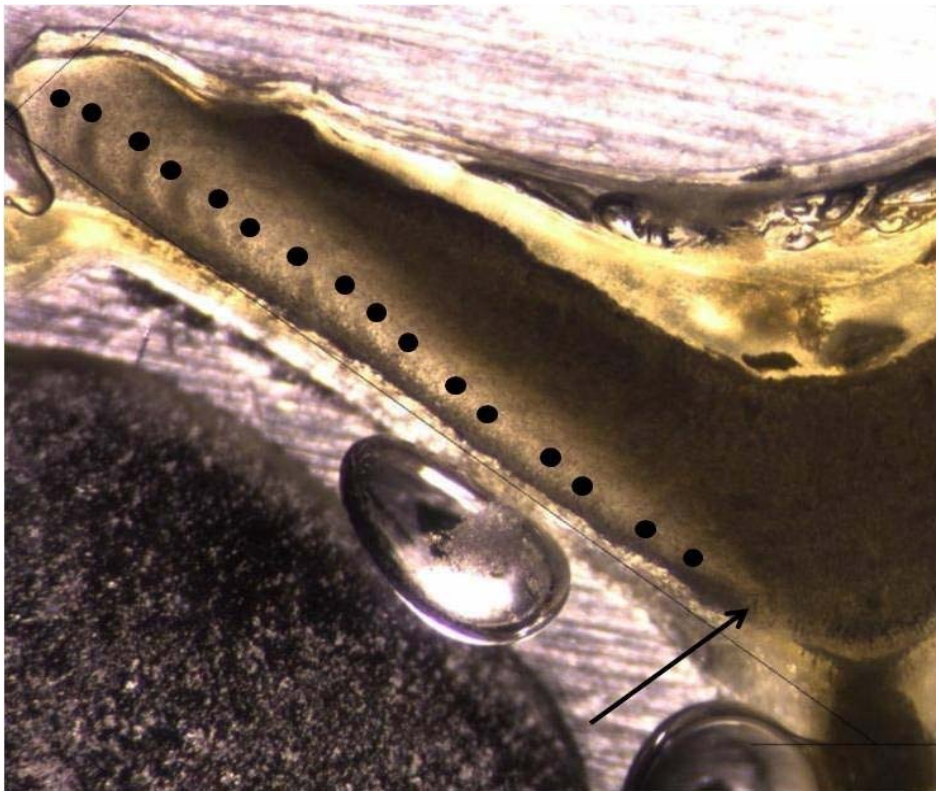

Figure 2.
A vertebral thin section from a 16 year old, 85.5 cm total length *Bathyraja lindbergi*, the arrow identifies the birthmark, signified by an angle change of the corpus calcareum on the vertebral thin section. Band pairs (i.e. one opaque and one translucent band) are indicated by black dots.

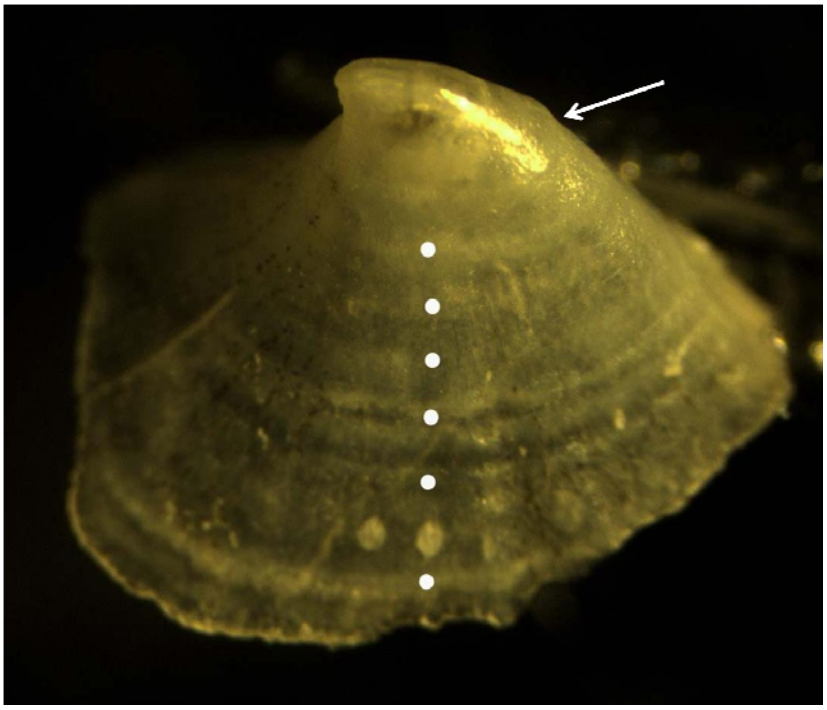

Figure 3.
A caudal thorn with a band pair count of 6 from a 108.4 cm total length *Bathyraja maculata,* the arrow identifies the ridge associated with the protothorn. Band pairs (i.e. one opaque and one translucent band) are indicated by white dots

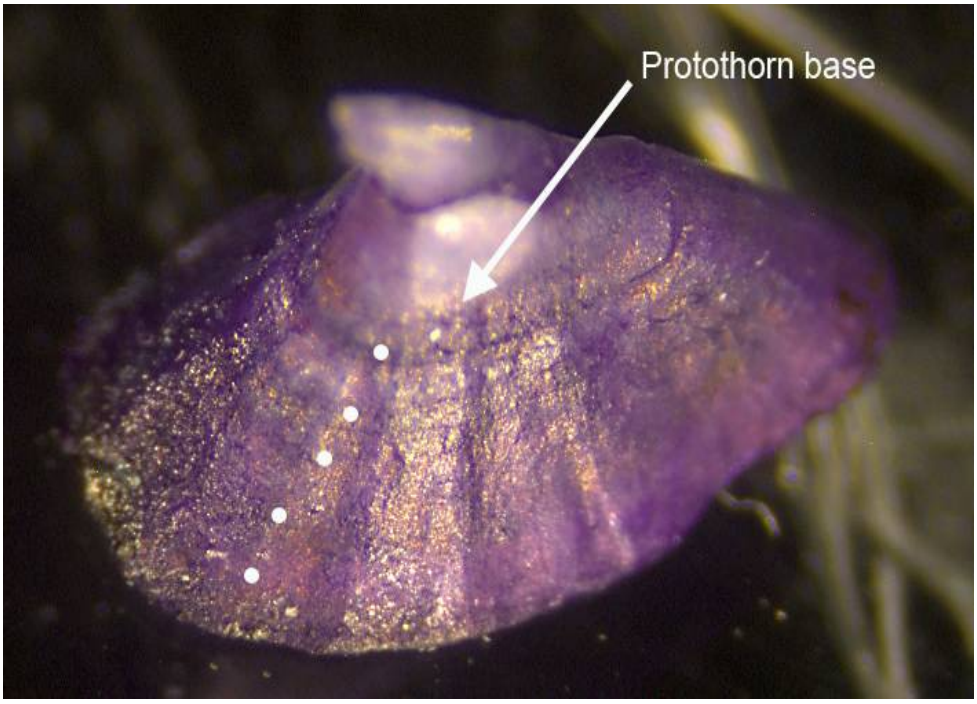

Figure 4.
Caudal thorn from *Bathyraja minispinosa* with an age estimated of 5 years. The caudal thorn was dyed with crystal violet and viewed under reflected light. White dots represent the ridges (band pairs) counted to obtain age estimates. The base of the protothorn is marked by the arrow.

Precision and error analyses

Precision and error analysis were determined to assess reader consistency and repeatability of age assignment of the same centrum. Pair-wise age difference plots were used to examine possible biases between reads and between structures (Campana et al. 1995). Several measures were used to assess reader precision. Index of average percent error (IAPE; Beamish and Fournier 1981), shown below, was used to determine the precision of band counts:

$$\frac{1}{N}\sum_{I=1}^{1}\left(\frac{1}{R}\sum\frac{X_{ij}-X_j}{X_j}\right)*100$$

where N is the number of specimens aged, R is the number of reads, X_{ij} is the ith age estimate of the jth individual and X_j is the average age calculated for the jth fish. Lower IAPE values indicate more precise band counts. Age 0 samples were excluded from the IAPE calculations because they can distort the calculations (Officer et al. 1996).

Coefficient of variation (CV) and index of precision (D) were calculated as additional measures of precision (Chang 1982), and to facilitate comparison with other studies. Coefficient of variation is calculated using standard rather than absolute deviation from the mean, to be more consistent and exhibit less bias. Index of precision (D) calculates the percent error of each observation.

$$CV_j = 100\% * \frac{\sqrt{\sum_{i=1}^{R}\frac{(X_{ij}-X_j)^2}{R-1}}}{X_j} \qquad \text{and} \qquad D_j = \frac{CV_j}{\sqrt{R}}$$

where CV_j and D_j each represent a precision estimate for the j^{th} ageing structure (Chang 1982), which were then averaged among individuals to produce mean CV and D values (Matta 2006).

In addition three chi-square tests of symmetry, Bowkers, McNemars, and Evans-Hoenig tests, were used to determine whether differences between reads and between structures were systematic or due to random error (Hoenig et al. 1995, Evans and Hoenig 1998). For these three tests age values are placed in a contingency table to test the hypothesis that values in the table are symmetrical across the main diagonal (Hoenig et al. 1995, Evans and Hoenig 1998). If a bias is detected these tests can be set up by age groups or individual age classes to determine where age estimations become asymmetric (Hoenig et al. 1995). If a systematic difference exists between the two reads than the test statistic, chi-square value, will tend to be large. The calculation for each test is shown below:

Bowker's test

$$\sum_{b=1}^{N-1}\sum_{a=b+1}^{N}\frac{(n_{ba}-n_{ab})^2}{(n_{ba}+n_{ab})}$$

where possible age values range from 1 to N, *a* is the age estimation for read 2, *b* is the age estimation for read 3, and *n* is the number of centra assigned age *a* on read 2 and age *b* on read 3. Degrees of freedom (df) are equal to the number of comparisons.

McNemar's test

$$\frac{(\sum_{b=1}^{N-1}\sum_{a=b+1}^{N}(n_{ba}-n_{ab}))^2}{\sum_{b=1}^{N-1}\sum_{a=b+1}^{N}(n_{ba}+n_{ab})}$$

For McNemar's test df is equal to 1, other variables are defined above.

Evans-Hoenig test

$$\sum_{p=1}^{N-1}\frac{(\sum_{a=1}^{N-p}(n_{p+a,a}-n_{a,p+a})^2}{\sum_{a=1}^{N-p}(n_{p+a,a}+n_{a,p+a})}$$

where *p* represents the difference between reads, $p=a-b$, df is calculated as number of positive *p* values minus one and other variables are as defined above.

Age verification

The periodicity of growth band deposition can vary among species and with age, and validation of band deposition periodicity should be determined for every species at every size whenever possible. For chondrichthyan fishes, validation methods include: release of known-age marked fish, mark-recapture of chemically tagged fish, bomb carbon dating, and captive rearing (Cailliet and Goldman 2004, Cailliet et al. 2006). The method used and its success vary depending on the funding, equipment available, the ease of capture or recapture, and the size and habitat type of the species. Marginal increment analysis is a technique based on quantifying and classifying the banding pattern of the centra. Although not the most robust, is the most common indirect-validation, verification, technique for age and growth studies of Alaskan skates (Ebert et al. 2007, Matta and Gunderson 2007). In most chondrichthyan species a single year of vertebral growth consists of one opaque and one translucent band (Cailliet and Goldman 2004).

Verification of annual growth band deposition was investigated using centrum edge analysis and marginal increment analysis (MIA) for all four species (Tanaka et al. 1979, Campana 2001, Cailliet and Goldman 2004, and Smith et al. 2007). Centrum edges were classified to one of four categories defined by optical qualities and band width: narrow opaque, broad opaque, narrow translucent and broad translucent. Narrow width is defined as being ≤ 50% of the previous fully formed like band and broad is defined as having width ≥50% of the previous like band (Tanaka et al. 1979, Smith et al. 2007). The proportions of edge types per month were used to detect seasonal difference in edge type. Marginal increment measurements were measured on photos of centra sections using Image-Pro Plus® image analysis software (Media Cybernetic, L.P. 1993-1999). Marginal increment ratio (MIR) was calculated as (Ishiyama 1951, Hayashi 1976, Conrath et al. 2002, and Panfili and Morales-Nin 2002):

MIR = MW/PBW

where MW is marginal width, width of the outer-most band or band pair, and PBW is the penultimate band pair width. The mean MIRs were plotted by month to determine the annual pattern in growth band deposition. Differences among monthly MIRs were compared using a parametric one-way ANOVA, when assumptions were met, or a non-parametric Kruskal-Wallis ANOVA by ranks (Simpfendorfer et al. 2000, Cailliet et al. 2006, Smith et al. 2007).

Growth models

Total length-at-age estimates were used to develop growth models for males and females of each species using several growth functions. To estimate growth model parameters non-linear least squares regression and SigmaPlot graphical software (SPSS Inc. 2002) were used.

A three parameter von Bertalanffy growth function (VBGF; Beverton and Holt 1957) is the most common growth function used in chondrichthyan age and growth studies (Cailliet et al. 2006) and was used as one of six for this study to estimate demographic parameters. The three parameter VBGF is:

$$L_t = L_\infty (1 - e^{(-k(t-t_0))})$$

where L_t is age at length t, L_∞ is asymptotic length, k is the growth coefficient and t_0 is age at theoretical length zero (Ricker 1979). Length at birth will then be calculated as:

$$L_0 = L_\infty (1 - e^{(kt_0)})$$

This model was used to check if the resulting value fell within the range of observed values for length at birth (Cailliet et al. 2006). Using the estimated value for L_0 the data was fit to a two parameter VBGF which is a more biologically significant model (Cailliet and Goldman 2004):

$$L_t = L_\infty (L_\infty - L_0)(e^{(-k+t)})$$

where symbols are defined as above.

The Gompertz size-at-age model also was used as it has been the best fit model for some batoids (Mollet et al. 2002, Neer and Thompson 2005). The collection circumstances for this project did not allow for weight data to be collected as a result TL-at-age will be substituted for weight variables in the Gompertz equation below:

$$L_t = L_\infty(e^{(-ke^{(-gt)})})$$

where L_t, L_∞ and t are defined above, k is a constant such that k*g is the instantaneous growth rate when t=0 and $L_t = L_0$ and g is the instantaneous rate of growth when t = t_0 (Ricker 1979). Gompertz also was used to estimate L_0.

The TL-at-age data also was fit to a logistics model modified from Ricker (1979). The logistic parameters were estimated using:

$$L_t = \frac{L_\infty}{1 + e^{-g(t-t_0)}}$$

where g is the instantaneous rate of growth, t_0 is the inflection point and the other parameters are defined above.

A four parameter Richards growth model (Richards 1959, Neer and Thompson 2005) was fitted to TL-at-age date in the form:

$$L_t = L_\infty[(1 - L_o(e^{-k*t}))]^P$$

where *P* is a shape parameter and others are as previously defined.

The last growth model applied to TL-at-age data was a three parameter polynomial function:

$$L_t = a + b*t + c*t^2$$

where L_t is as previously defined and *a*, *b* and *c* are constants. Polynomial functions were considered because of potential mathematical advantages over the traditional VBGF and do not assume asymptotic growth (Roff 1980).

Growth model goodness-of-fit was assessed by comparisons of several criteria. The coefficient of determination (r^2), significance level ($p < 0.05$), residual mean square error (MSE), and biological significance were all compared to determine which growth model best fit the TL-at-age estimates. Growth curves were tested for differences between the sexes using Likelihood Ratio Test (Kimura 1980, Haddon 2001).

Maturity and reproduction

Maturity was assessed by visual inspection of the reproductive organs and assigned to one of five maturity categories following Ebert (2005; Table 1). The inner clasper length was measured and plotted as a ratio against L_T as a secondary estimator of maturity. An abrupt change in the clasper length to L_T ratio is considered to indicate maturity. Oviducal gland width, maximum ovum diameter, and total number of mature oocytes were plotted as a ratio against L_T, and when possible, season or month to assess size and season-specific influences on these relationships.

Reproductive tracts preserved in formalin for histological assays to verify macroscopic maturity assessment, investigate potential seasonality in the reproductive cycle, and sperm storage ability by females. Sections 3-4 mm thick from testes and oviducal glands were removed using a scalpel and placed in tissue cassettes. Tissue sections were stored in 70% ethanol until final processing. Testes were processed at Louisiana State University (LSU) Veterinary Laboratories using standard hematoxylin and eosin staining (e.g. Maruska et al. 1996). Sperm development in several elasmobranch groups, including skates, has been well described (Maruska et al. 1996, Conrath and Musick 2002, Ebert et al. 2007, 2008b). Hormone analysis by Sulikowski et al. (2005) confirmed that the spermatocyst and spermatid stages were associated with reproductive maturity (stages III through VII; Maruska et al. 1996; Conrath and Musick 2002). These stages were defined as; stage III, spermatocytes; stage IV, spermatids; stage V, immature spermatozoa; stage VI, mature spermatocysts. To determine sperm development stage, slides prepared at LSU were viewed under a compound microscope. A straight line transect across a representative lobe of the testes was used to calculate mean proportion of testes occupied by each maturity stage (Ebert et al. 2007, 2008b). The tightness and organization of sperm packets in the spermatocysts was used to determine maturity (Sulikowski et al. 2005a, b; Ebert et al. 2007, 2008b). Oviducal glands were processed at Northeast Marine Fisheries Science Center, Narragansett, RI also using standard hematoxylin and eosin staining (e.g. Maruska et al. 1996). Oviducal glands were sectioned across several different axes to provide thorough examination of the whole organ.

Age and size at first, 50% and 100% maturity was determined. Fifty percent maturity was determined using maturity ogives described below. Observed maturity levels were classified into binomial data (0=immature, 1=mature; Mollet et al. 2002, Ebert et al. 2007) and binned by size or age class. Females and males were analyzed separately for each species. Using least squares non-linear regression and SigmaPlot graphical software (SPSS Inc. version 8.0 Chicago, IL), a logistic equation was fit in the following form:

$$y = \frac{1}{(1 + e^{-(a+bx)})}$$

where y = maturity status, and x = TL (cm) or age in years. Median TL at maturity (TL_{50}) was calculated using $-a/b$. Additional logistic ogives were developed to determine median age at maturity for each species.

Ovulation cycles may be detected by comparing ova size among months in mature females (Conrath 2004). In females, all mature ova visible on the surface of each ovary were enumerated, and the diameter of the largest ovum was measured to the nearest mm. Mature ova were characterized by their yolky appearance and size, typically exceeding 10 mm in diameter (Ebert 2005). The number of mature ova in left and right ovaries was compared for significant differences using a paired sample *t*-test (Zar 1999). To discern any peaks in reproductive activity, mean maximum ova diameter and number of mature ova were plotted against month of capture. Differences between months in maximum ova diameter and number of mature ova were each tested using parametric one-way ANOVA or non-parametric Kruskal-Wallis tests (Matta 2006). The percentage of mature females with developing egg cases *in utero* was also plotted against each month, and differences in proportion were assessed using a Chi-square (χ^2) test for homogeneity (Zar 1999).

The effects of maternal size and age on reproduction were assessed using multiple regression analysis of ova size and number of mature ova on maternal size and age. Maximum ova diameter and number of mature ova each were regressed against length and age to determine if these factors contribute significantly to variation of ova size and number (Matta 2006).

	Males	Females
Embryo	Taken from egg case	Taken from egg case
Juvenile	Claspers are short and flexible, usually not extending beyond the pelvic fins. Testes are very thin and threadlike without obvious coiling in the epididymis.	Lacks ovarian or oviduct development. The oviducal, or shell gland, appears as a slight bulge in the uterus, which is a thin transparent tube.
Adolescent	Claspers extend beyond the posterior edge of the pelvic fins. Terminal cartilage elements of the claspers are pliable; however they are not fully calcified. Epididymis may be loosely coiled. Seminal fluid/sperm may be present in adolescents	Small somewhat differentiated ovaries that lack vascularization. A noticeable but under-developed oviducal gland. Oviducts are narrow and constricted.
Adult	Claspers are elongated and rigid. Epididymis is highly coiled and testes are enlarged.	Vascularized ovarian eggs present and usually yellowish. Oviducal gland is distinctly differentiated from the oviducts and posterior portion of the oviducts are pendulous.
Gravid	N/A	Egg cases present in utero

Table 1.

Maturity classification of female and male skates as determined by macroscopic inspection of reproductive organs.

Demography

To test the hypothesis that these four skate species have lesser rates of population growth than many elasmobranchs, a time-invariant, density-independent, probabilistic age-structured matrix modeling approach was applied. Vital rate estimates were generated from the assessments of age, growth, and maturity. Vital rates were estimated only for the female portion of the population, as they are the only individuals that contribute new individuals to the population (by reproduction).

Mortality was expressed as age-specific annual survival rates ($S_x = e^{-Mx}$, where M_x is the total instantaneous rate of mortality of individuals of age *x*). M_x was estimated with indirect methods based on other life history parameters, because species-specific catch-at-age data were unavailable. Seven different estimation methods were used. Embryo survival was represented by empirical estimates of egg-case predation rates in the eastern Bering Sea (Hoff 2007). Species-specific embryo survival data were used for *B. minispinosa* and *B. taranetzi* (Table 2). Embryo survival estimates from *B. aleutica* data were used as a proxy for *B. lindbergi* and *B. maculata*, because species-specific data were unavailable. These data provided an adequate surrogate, because all three species inhabit deep environments and have similar egg-case morphology (Hoff 2007).

Birth rates were expressed as age-specific fecundity values (m_x , where $x = \text{age in years}$). Skates are oviparous, so fecundity was defined as the number of eggs extruded female^{-1} year^{-1}. Fecundity estimates was not available for the four species studied, therefore, estimates from other skates were used as a proxy. Only those fecundity estimates that were calculated with a robust method (captive parturition rate or ovarian fecundity estimates accounting for indeterminate spawning mode) were included. Mean fecundities of skates from the Atlantic and Pacific Ocean basins were incorporated (Table 3), giving a range from 32 to 104. Assuming a sex ratio at birth of 1:1, these values were halved to represent the number of female offspring female^{-1} year^{-1} (Table 2).

Density-independent, linear Leslie matrix models (Leslie 1945, Caswell 2001) were constructed using Microsoft Excel® spreadsheet software and PopTools add-in software (Hood 2005). These models incorporated the assumption of a closed population, a standard simplifying assumption made to address the lack of data on rates of potential immigration and emigration. Population growth was estimated by a combination of the rates of birth and death. For each species, a population projection matrix ($\mathbf{A}$) of age-specific survival probabilities (P_x , the probability of surviving from age *x* to *x* + 1) and fertility coefficients (F_x , where *x* = age class) was created to calculate the dominant eigenvalue, the finite annual rate of population growth ($\lambda = e^r$, where *r* = predicted instantaneous rate of population growth per capita; *sensu* Gedamke et al. 2007). Reproductive value ($\mathbf{v}$) and stable-age distribution ($\mathbf{w}$) vectors were calculated as the left and right eigenvectors of the dominant eigenvalue from the projection matrix.

Elasticities, or proportional sensitivities (Caswell et al. 1984, de Kroon et al.1986), of λ were calculated following Caswell (2000) as

$$e_{ij} = \frac{a_{ij}}{\lambda}\frac{\partial\lambda}{\partial a_{ij}},$$

where a_{ij} is the element in row *i* and column *j* of the matrix $\mathbf{A}$. Fertility, juvenile survival, and adult survival elasticities were calculated as the sum of the corresponding matrix-element elasticities. Elasticity ratios of juvenile survival to fertility, adult survival to fertility, and juvenile survival to adult survival were calculated to ease interpretation of possible compensatory effects and generate benchmarks for remediation efforts (Heppell et al. 1999).

Since many Alaskan skates have protracted and asynchronous egg-case deposition seasons (Hoff, 2007), F_x and P_x were calculated for a birth-flow population (Ebert 1999), wherein individuals are constantly entering and leaving a given age class. In this case, individuals just entering age class *x* have F_x and P_x values more appropriate for age class *x* and individuals nearly ready to enter age class *x* + 1 have F_x and P_x values more appropriate for age class *x* + 1. For a given time period from year *t* to *t* + 1, some individuals survive the entire period and some for only a small fraction of the period. On average, a mature individual must survive for half of a given time period to produce offspring. To express this property in the matrix calculations, survival was calculated following Ebert (1999) as

$$P_x = \frac{\ell_x + \ell_{x+1}}{\ell_x + \ell_{x-1}},$$

where,

$$\ell_x = \ell_{x-1} S_x .$$

Fertility coefficients were calculated as the product of averaged m_x values and the survival probability for ½ of a time period ($\ell_{0.5egg} = \sqrt{\ell_{egg}}$, following Caswell 2001). In mathematical terms, the F_x were calculated (modified from Ebert 1999) as

$$F_x = \frac{\ell_{0.5egg}\left(m_x + m_{x+1}P_x\right)}{2}.$$

Species	*Parameter*	*Distribution*	*Min*	*Max*	*Likeliest*	*95% CI*
Bathyraja lindbergi	ω	triangular	31	46	32	
	α	logistic	18	21	17.7	16.2 - 19.2
	m_x	uniform	16	52		
	ℓ_{egg}	triangular	0.65	0.99	0.98	
Bathyraja maculata	ω	triangular	31	46	32	
	α	logistic	18(21)	30(24)	22.5	21.7 - 23.3
	m_x	uniform	16	52		
	ℓ_{egg}	triangular	0.65	0.99	0.98	
Bathyraja minispinosa	ω	triangular	36	53	37	
	α	logistic	23	25	23.5	22.3 - 24.7
	m_x	uniform	16	52		
	ℓ_{egg}	triangular	0.65	0.98	0.87	
Bathyraja taranetzi	ω	triangular	13	20	14	
	α	logistic	8	13(10)	9.2	8.7 - 9.7
	m_x	uniform	16	52		
	ℓ_{egg}	triangular	0.65	0.98	0.81	

Table 2.

Population parameters used in the demographic models of this study, and the probability distribution functions (PDFs) chosen to portray their variability: longevity (ω), age at maturity (α), age-specific fertility (m_x), egg case survival (ℓ_{egg}). Age at maturity values in parentheses indicate actual minimum or maximum values obtained when the range generated using 95% confidence intervals was more restricted than the range bound by first and 100% maturity.

Species	*Mean fecundity*	*Citation*
Amblyraja radiata	41	Parent *et al.* 2008
Dipturus laevis	90	Parent *et al.* 2008
Leucoraja erinacea	33	Holden 1974
Leucoraja naevus	90	du Buit 1976
Leucoraja ocellata	48	Parent *et al.* 2008
Okamejei kenojei	86	Ishihara *et al.* 1997
Raja brachyura	65	Holden *et al.* 1971; Holden 1972; Walker and Hislop 1998
Raja clavata	103	Holden *et al.* 1971; Holden 1975; Ryland and Ajayi 1984
Raja eglanteria	60	Luer and Gilbert 1985
Raja montagui	43	Holden *et al.* 1971; Holden 1972, 1974

Table 3.

Skate fecundity data used to parameterize demographic models in this study.

Two measures of generation time were calculated, the mean age of females generating offspring produced by a cohort during its lifetime (μ_1; Caswell 2001), and the mean age of females generating offspring produced by a population at the stable-age distribution ($\overline{A}$). $\overline{A}$ was calculated from life-table parameters following Cortés (2002). Other population parameters calculated were net reproductive rate (R_0; Caswell 2001), rate of increase per generation (rT; Fowler 1988), and theoretical population doubling time ($t_{\times 2}$; Krebs 2001).

Monte Carlo simulation of the matrix models was used to account for inherent uncertainty of life-history parameters (Cortés 2002). Separate Independent and Identically Distributed (IID) probability density functions (PDFs) were created for each species to represent uncertainty in longevity (ω), age at maturity (α), S_x, and m_x (Tuljapurkar 1997, Cortés 2002, Smith et al. 2008). Because no prior information indicated differing accuracy of specific survival estimates, a uniform PDF was selected for S_x, with the range defined as the range values obtained from all indirect estimation techniques. A skewed triangular PDF was selected for ω, with the most probable value estimated to be maximum observed age (T_{max}). The lower range was defined as

$$\omega_L = T_{max}\left(1 - T_{max} IAPE_{20\%}\right),$$

where $IAPE_{20\%}$ is the index of average percent error calculated from the greatest 20% of age classes. The upper range was defined as

$$\omega_U = T_{max}\left(1.4 + IAPE_{20\%}\right),$$

where the arbitrary constant, 1.4, was used because theoretical longevities calculated from von Bertalanffy growth function parameters were unrealistically great. The nearly linear growth function of these species did not reach an asymptote until an extremely late age. The method used here may also increase the comparability of demographic analysis results among species (Cortés 2002).

Age at maturity (α) was simplified to a knife-edge function, with all age classes younger than age at 50% maturity considered immature, and given a fecundity of zero. The fecundity value for the first mature age class was halved, to reflect that only 50% of individuals would be reproducing during that year, and complete fecundity values were applied to each subsequent age class. A logistic PDF with a mean value equal to the age at 50% maturity estimated from logistic regression was chosen to represent uncertainty in α, with upper and lower limits defined as age at

first and 100% maturity respectively. A uniform PDF was used to represent uncertainty in fecundity, with a range of 16 to 52 for all species (Table 2). The range was defined to encompass the range of mean fecundities of other skates (Table 3).

Simulations (n = 5000) were performed with Microsoft Excel® spreadsheet software and Microsoft Visual Basic for Applications®, in conjunction with Crystal Ball® add-in risk-assessment software (2000 Professional version 5.0, Decisioneering Inc., Denver, USA). Values of each life history parameter were chosen at random from the predetermined PDFs to create replicate matrices. Separate draws for S_x and m_x were taken for each individual age class within a given simulation step. Demographic output parameters were calculated from each replicate matrix, and summarized as means (50th percentile) and 95% confidence intervals (defined as the range of values between the 2.5th and 97.5th percentiles).

Results

Age and growth

A total of 1049 specimens, comprised of all four species, were collected during this study. A total of 293 samples were obtained for *B. lindbergi* from four months, but 20 were discarded due to questions about the correct species identification and three did not have complete associated data. Females (n = 127) ranged in size from 18.2 to 102.1 cm, and males (n = 143) from 17.3 to 94.5 cm (Fig. 5). *Bathyraja maculata* had the lowest sample size with a total of 208 collected from four months. Females (n = 107) ranged in size from 23.7 to 114.5 cm and males (n = 101) from 36.2 to 114.4 (Fig. 6). The largest number of samples, 314, was obtained from all three sources for *B. minispinosa* from ten months, although vertebrae were not collected from 44 of the individuals. Additionally, one individual was later deemed not to be *B. minispinosa* and three other individuals were data deficient. Males sampled (n = 126) ranged from 14.7 to 83.7cm TL, while females (n = 140) ranged from 13.6 to 89.5 cm TL (Fig. 7). Combined sampling efforts collected 234 *B. taranetzi* from eight months. Females (n = 111) ranged in size from 15 to 72.5 cm and males (n = 116) ranged in size from 15.6 to 66.3, an additional 7 were collected for which sex or TL was not recorded (Fig. 8).

Age determination

Bathyraja lindbergi. The Mean Centrum Diameter to Total Length (MCD-TL) relationship was best described by a power function ($MCD = 0.0331 * x^{1.1641}$, $r^2 = 0.97$, n = 158; Fig. 9). Additionally no bias was detected between anterior and posterior band counts using the Bowkers, McNemar, or Evans-Hoenig χ^2 tests of symmetry (n = 23, χ^2 test p>0.05 for all tests; Fig. 10), therefore all age estimates were based on band counts of anterior centra.

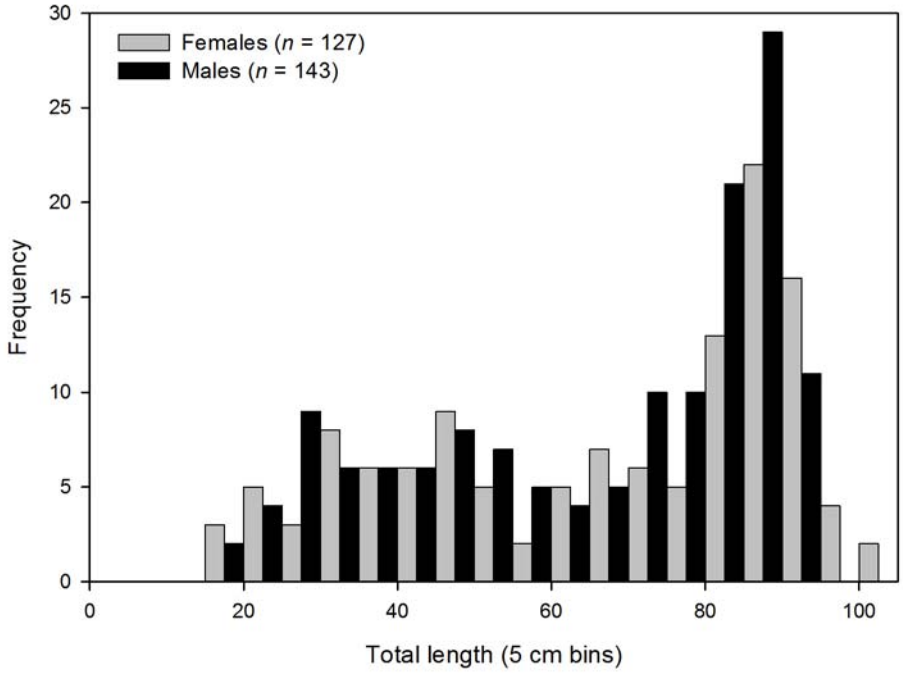

Figure 5.
Length frequencies of male and female *Bathyraja lindbergi* collected from 2004 and 2007.

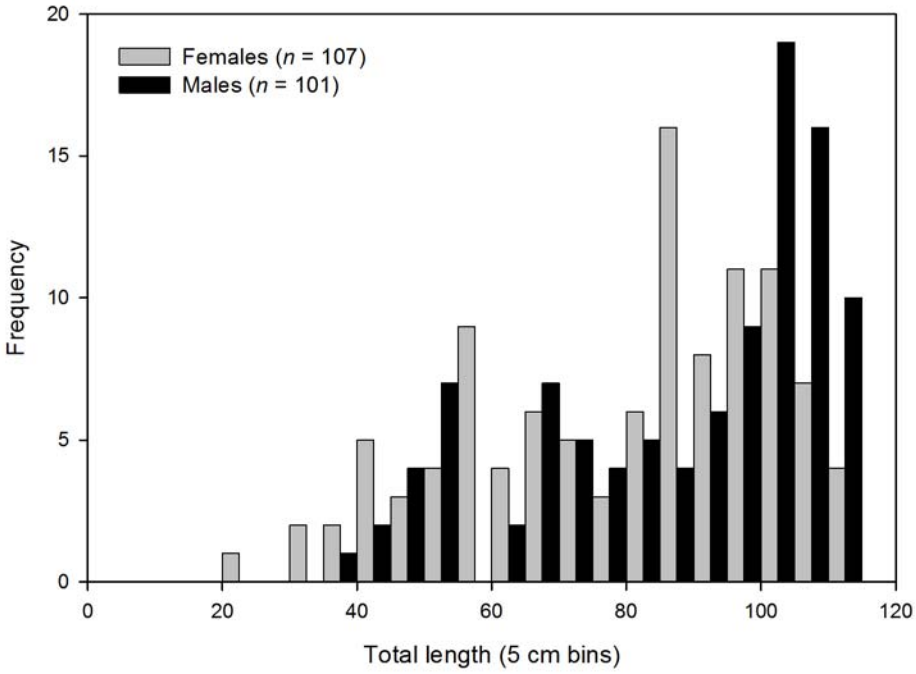

Figure 6.
Length frequencies of male and female *Bathyraja maculata* collected from 2004 and 2007.

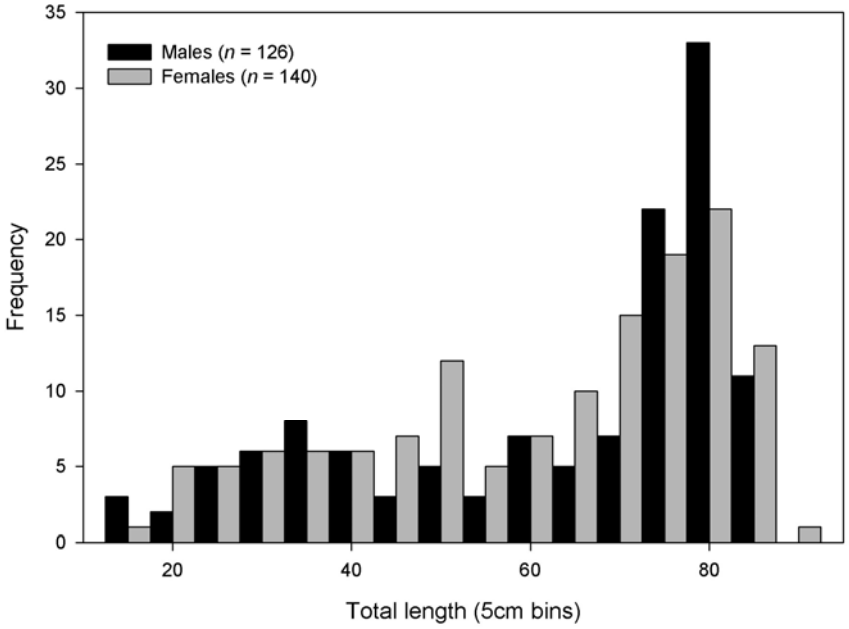

Figure 7.
Length frequencies of male and female *Bathyraja minispinosa* collected from 2004-2006.

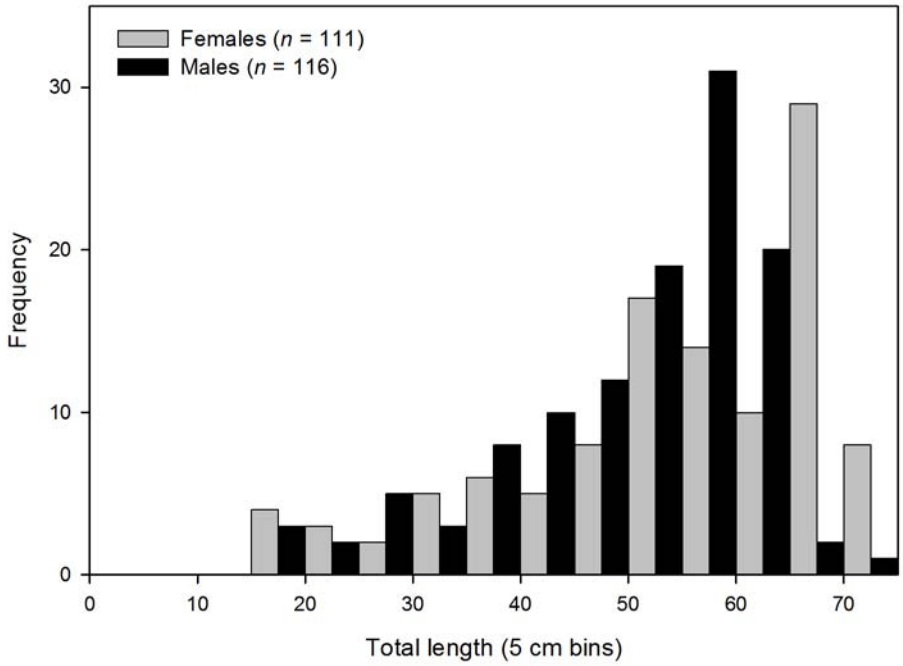

Figure 8.
Length frequencies of male and female *Bathyraja taranetzi* collected from 2004 and 2007.

Caudal thorn height to TL relationship was best described by an exponential model ($y = 4.2757 * e^{(-0.0282*x)}$, n = 47, r² = 0.746; Fig. 11). The relationship between caudal thorn width and TL is best described as a linear relationship ($y = 0.8194 + 0.067 * x$, n = 47, r² = 0.794; Fig. 11). A subsample, n = 54, of caudal thorns representative of the observed size range was used for age estimation. Only 32 individuals had vertebral age estimates that could be used for comparison. A significant bias was detected in age estimates between caudal thorns and vertebral centra by the McNemars and Evans-Hoenig χ^2 tests ($p < 0.03$; Fig. 12). Caudal thorn age estimates in all cases, n = 54, were never greater than 11 (Fig. 13).

Two hundred and nine vertebral centra were prepared for ageing, of those 163 (86%) were assigned a final age and used in further analysis. A portion of the prepared samples (n = 20) were not included in further analysis because they were likely a different species. The remaining 26 samples were excluded in further analysis due to poor slide quality or lack of visible band pairs. The maximum age estimate for *B. lindbergi* was estimated at 32 years from a 96 cm TL female. The maximum age estimate for males was 27 years for an 87.6 cm TL individual.

Bathyraja maculata. MCD-TL is a positive linear relationship (MCD = -0.5297+0.0755x, r² = 0.9703, n = 173; Fig. 14). The Bowkers, McNemars, and Evans-Hoenig χ^2 tests of symmetry did not detect any significant bias among posterior and anterior band counts (p > 0.19 in all cases, n = 22, Fig. 15), therefore all age estimates were based on band counts from anterior centra.

The relationship of caudal thorn height and TL is best described by a power function with a relatively low r² value ($y = 1.0453x^{0.2754}$, r² = 0.413, n = 48, Fig. 16). Caudal thorn base width to TL relationship also is best described by power function ($y = 0.5057x^{0.5745}$, r² = 0.613, n = 48, Fig. 16). A subsample of thorns from the observed size range, n = 58, were cleaned for age estimation. Five thorns were not assigned an age due to damage from preparation, 42 of the remaining 53 individuals also had vertebral age assignments and were used for comparison between the two structures. Significant bias was detected between caudal thorn and vertebral age estimates by the McNemar and Evans-Hoenig χ^2 tests ($p < 0.002$, Fig. 17). Caudal thorn age estimates in all cases, n = 53, were not greater than 9 years (Fig. 18).

Vertebral centra from 155 *B. maculata* were prepared for ageing. Of these seven were discarded due to poor band clarity, the remaining 148, 95.5%, were assigned a final age and used for further analysis. The maximum age estimate for females and males is 32 with TL of 112.2 and 111.1 cm respectively.

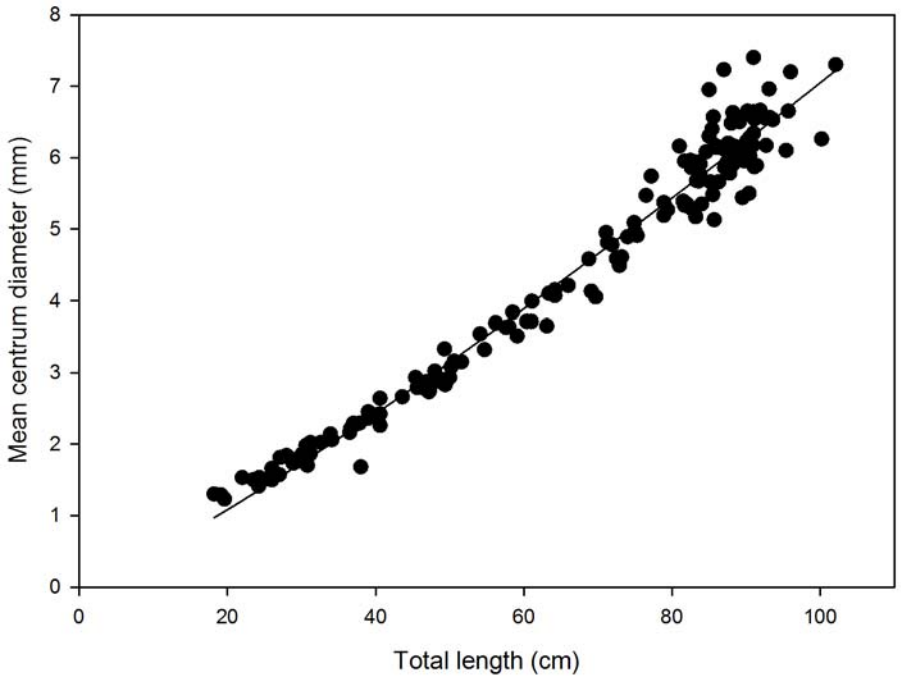

Figure 9.
The relationship between mean centrum diameter and total length for the sexes combined of *Bathyraja lindbergi*.

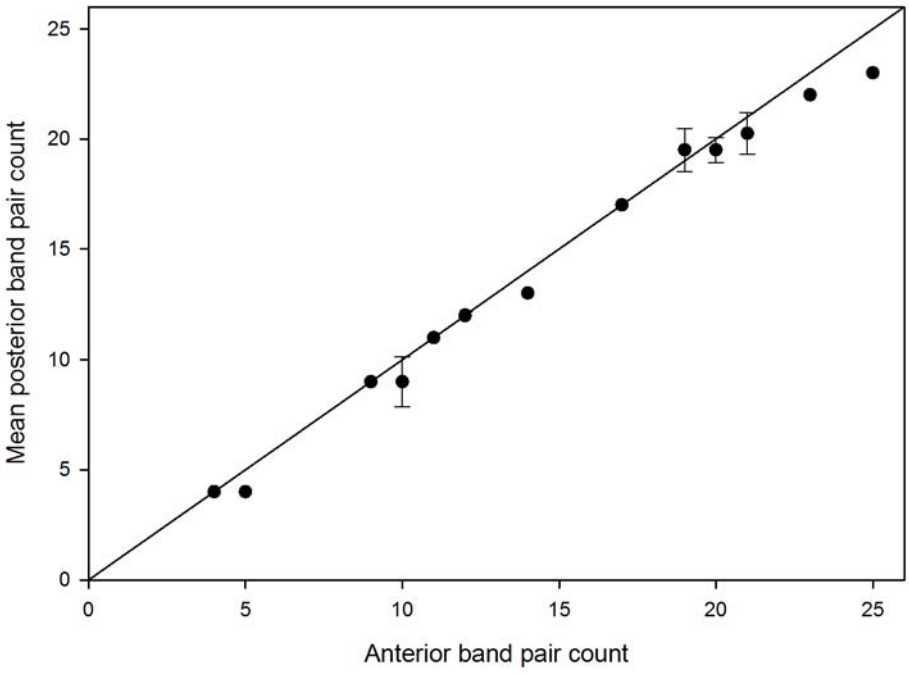

Figure 10.
The relationship between the anterior age estimates from vertebral centra and the mean posterior age estimates of *Bathyraja lindbergi* (*n* = 23). The error bars indicate +/- the 95% confidence intervals.

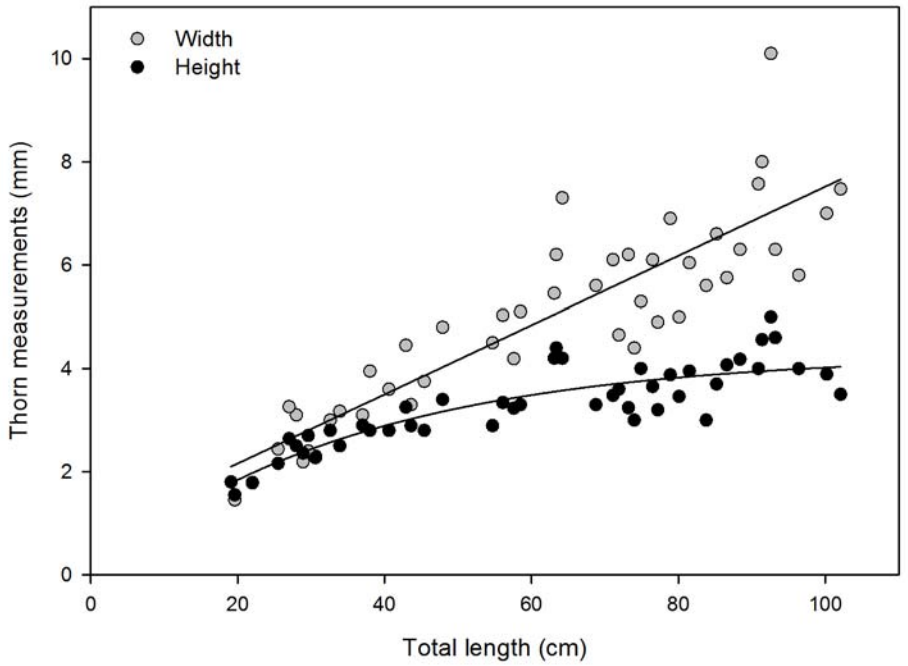

Figure 11.
The relationships between caudal thorn height (n = 47), and width (n = 47) and total length of *Bathyraja lindbergi* sexes combined.

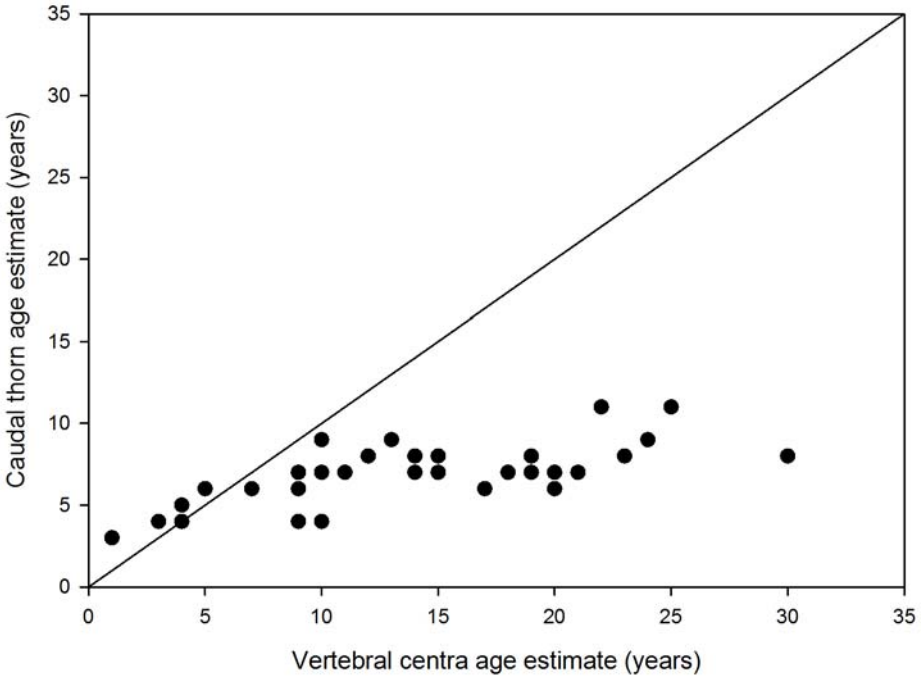

Figure 12.
The relationship between the vertebral centra band counts and the mean caudal thorn band count of *Bathyraja lindbergi* (n = 32). The 45º line represents 1:1 agreement between band counts.

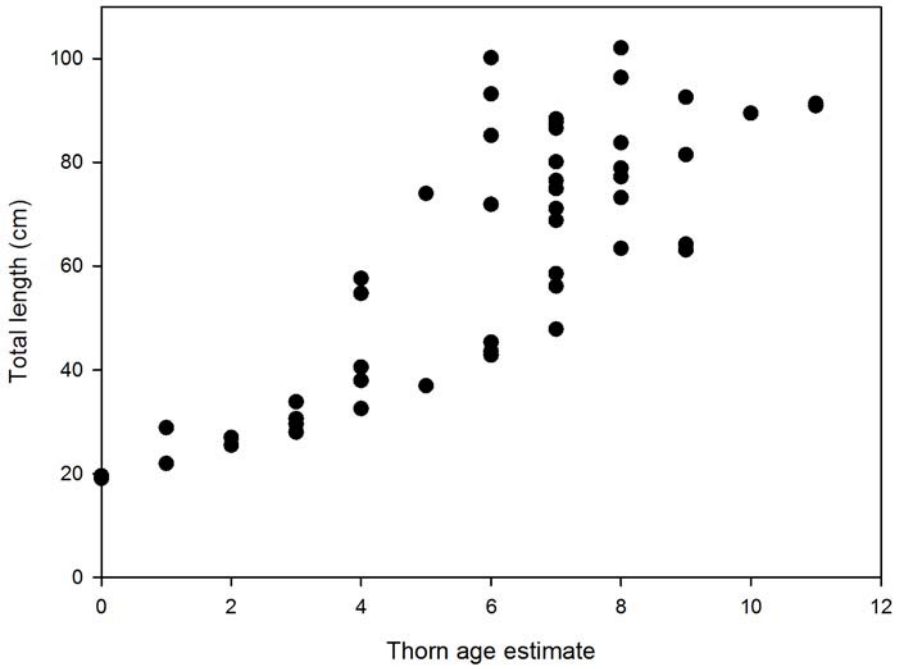

Figure 13.

The relationship of *B. lindbergi* caudal thorn age estimate and TL sexes combined (n = 54).

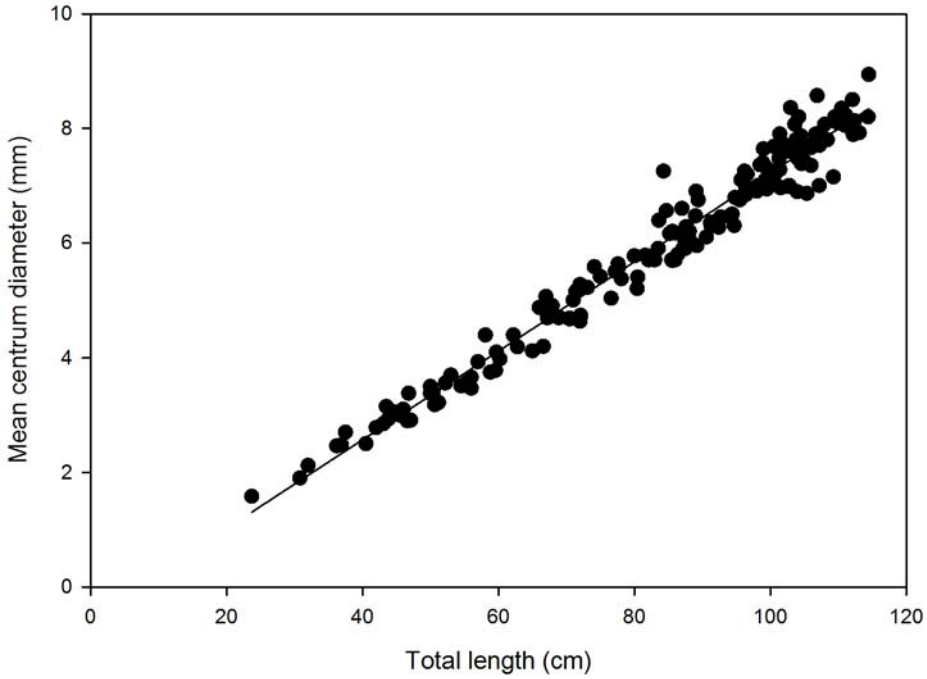

Figure 14.

The relationship between mean centrum diameter and total length for the sexes combined of *Bathyraja maculata*.

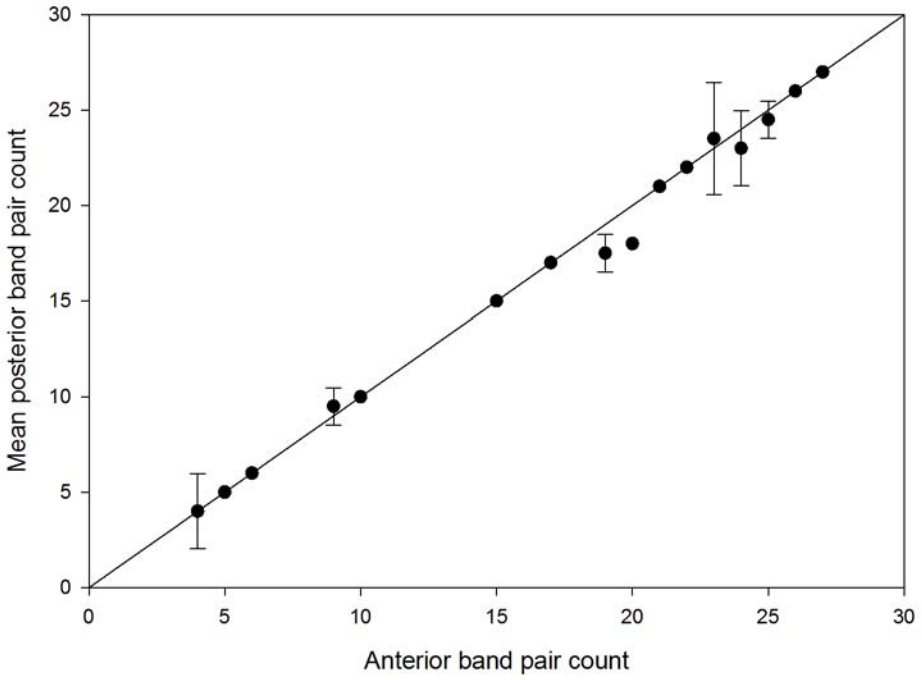

Figure 15.
The relationship between the anterior age estimates from vertebral centra and the mean posterior age estimates of *Bathyraja maculata* (n = 22). The error bars indicate +/- the 95% confidence intervals.

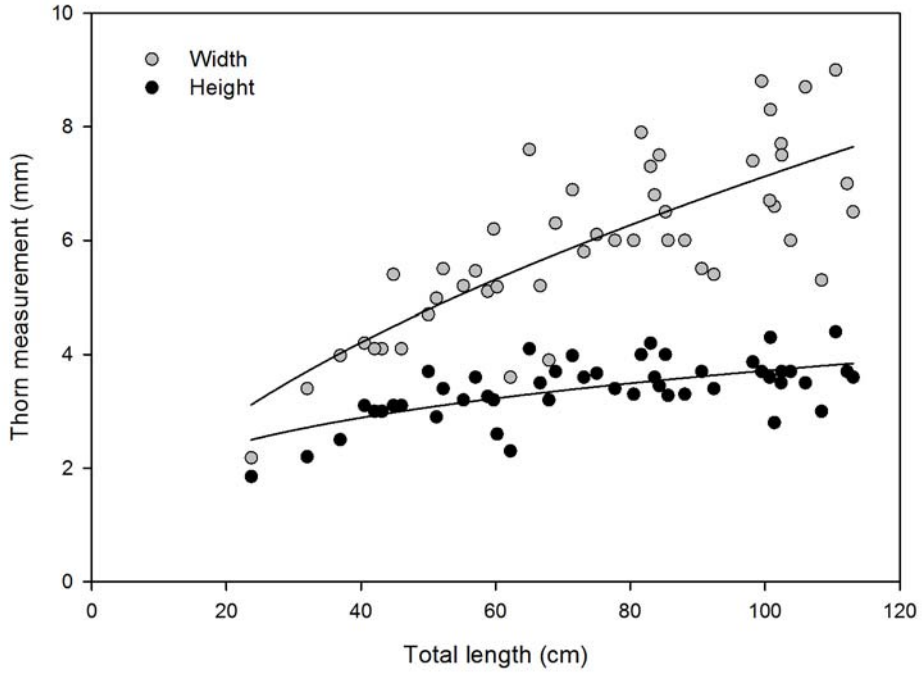

Figure 16.
The relationships between thorn height (n = 48), and width (n = 48) measurements and total length of *Bathyraja maculata* sexes combined.

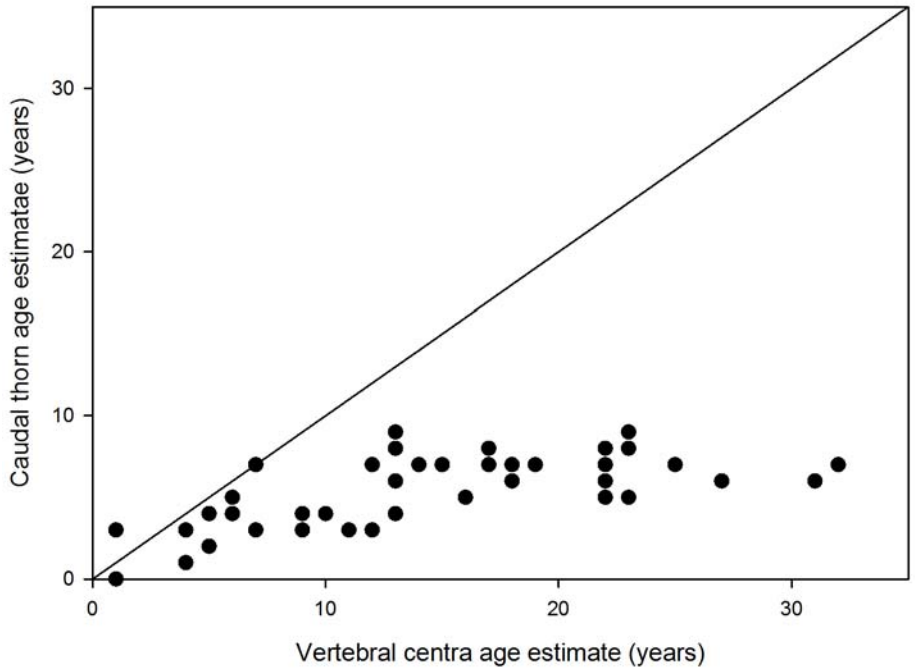

Figure 17.
The relationship between the vertebral centra band counts and the mean caudal thorn band count of *Bathyraja maculata* (*n* = 42). The 45º line represents 1:1 agreement between band counts.

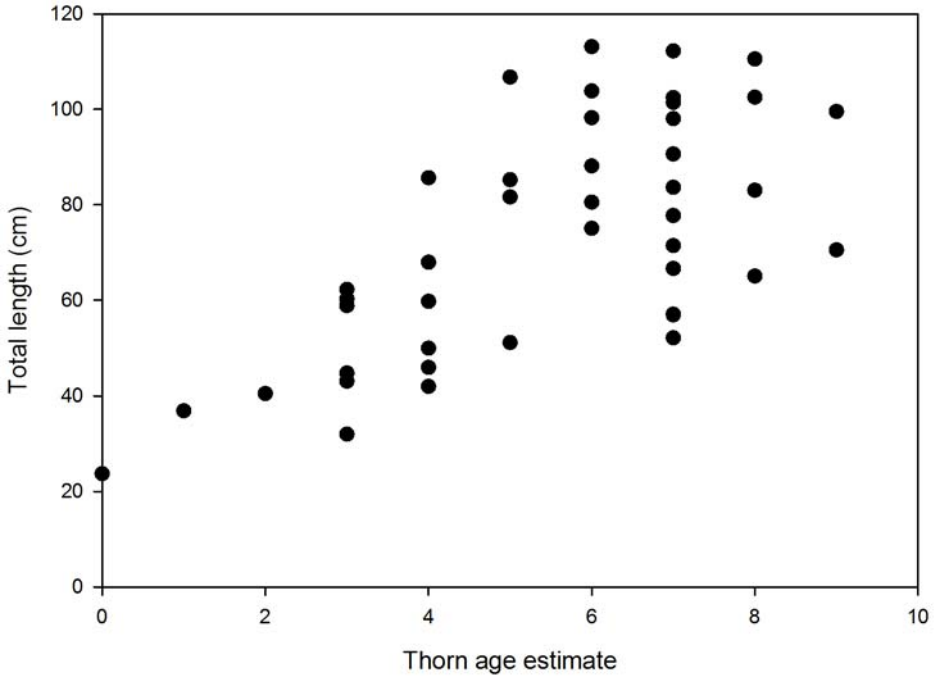

Figure 18.
The relationship of *Bathyraja maculata* caudal thorn age estimate and TL (*n* = 53).

Bathyraja minispinosa. There was a significant increase in MCD with increasing TL ($p < 0.0001$, $r^2 = 0.967$; n = 216; Fig. 19), however the relationship was not linear and was best described by the equation: $y = 0.8294e^{0.0248x}$. The centrum diameter increased at a greater rate in comparison to the TL in larger individuals. Visual assessment of the pair-wise age difference plot comparing the anterior and posterior showed no significant bias ($n = 21$; Fig. 20). However, the analysis using contingency table χ^2 tests of symmetry indicated that not all differences may be attributed to random error (Bowker's, $\chi^2 = 19.0$, df = 17, $p = 0.3285$; McNemar's, $\chi^2 = 4.26$, df = 1, $p = 0.0390$; Evans-Hoenig, $\chi^2 = 7.0$, df = 4, $p = 0.1359$). In Evans and Hoenig (1998) the authors indicate that the McNemar's test, also called the maximally pooled test, detects asymmetry when the individual differences are small but reinforce themselves upon pooling. This suggests that if there is an asymmetry the differences are slight and are likely due to the small sample size, rather than a systematic bias. Since the comparison was inconclusive, the anterior vertebrae were used for the remainder of the ageing study. Anterior vertebrae are the most commonly used and have been validated for other skate species.

Significant, positive non-linear relationships were found between mean thorn height and TL ($y = 0.4591x^{0.4610}$, $r^2 = 0.705$, $p < 0.001$), and mean thorn width and TL ($y = 0.0258x^{1.2387}$, $r^2 = 0.947$, $p < 0.001$; Fig. 21). Caudal thorn age estimates were in agreement with centra age estimates for only the first few years, and then thorn estimates were much younger from age 5 on (Fig. 22). This was reflected in the results of the chi-square analysis of the contingency tables, which found a significant bias between age estimates using the pooled test statistic (McNemars') method ($\chi^2 = 45.0$, df = 1, $p < 0.001$). Ages estimated from caudal thorns never exceeded 18 years (n = 50; Fig. 23).

Out of 263 vertebrae aged, only 187 were deemed usable (71.1%), and two additional vertebrae did not have enough data for analysis, leaving 185 samples. The maximum observed age of 37 was assigned to the largest skate from the study, a mature female (89.5 cm TL). The oldest male was estimated to be 35 years old (76.2 cm TL), while the largest male aged was estimated to be 33 years old (83.7 cm TL).

Bathyraja taranetzi. The MCD-TL relationship is best described by a power function with the equation: $y = 0.0314 * x^{1.2031}$, $r^2 = 0.92$, $n = 160$ (Fig. 24). Comparison of band counts from anterior and posterior centra had no detectable bias (χ^2 tests $p > 0.20$ for all tests, $n = 24$) so anterior bands counts were used for all further analysis (Fig. 25).

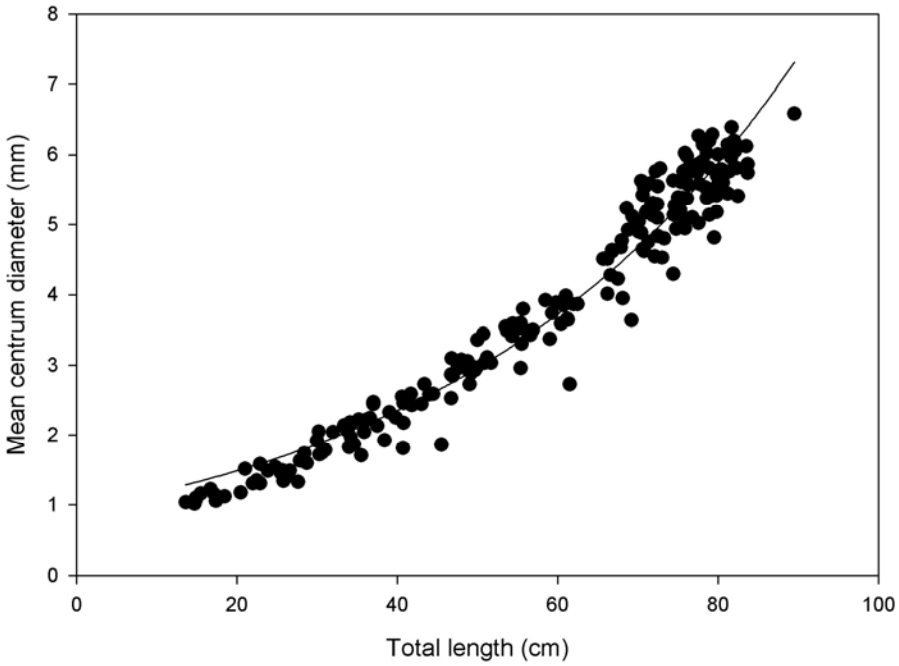

Figure 19.
The relationship between mean centrum diameter and total length for combined sexes of *Bathyraja minispinosa (n* =216).

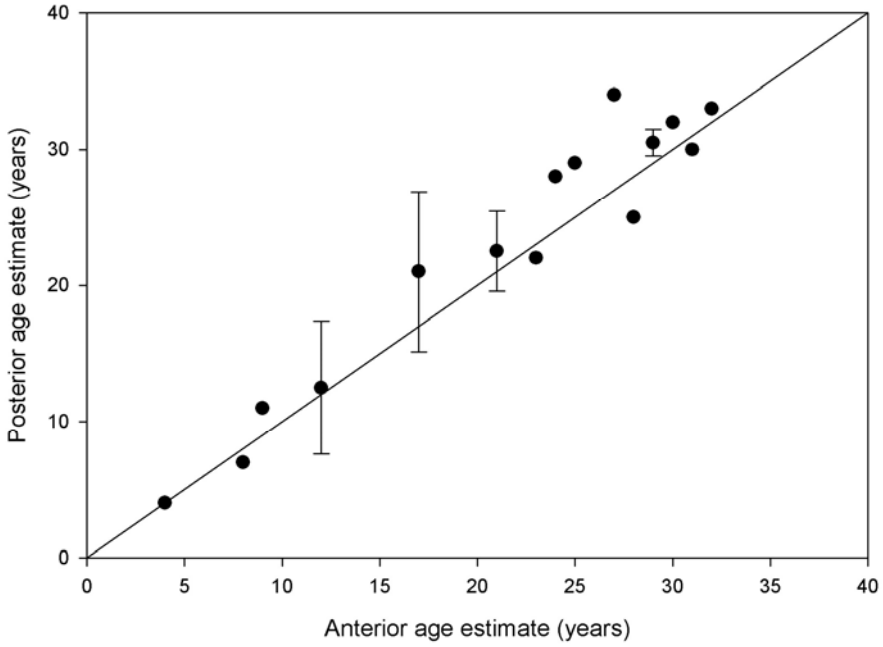

Figure 20.
The relationship between the anterior age estimate and the mean posterior age estimate of vertebral centra of *Bathyraja minispinosa* (*n* = 21). The 45º line represents 1:1 agreement between band counts and the error bars represent 95% confidence intervals.

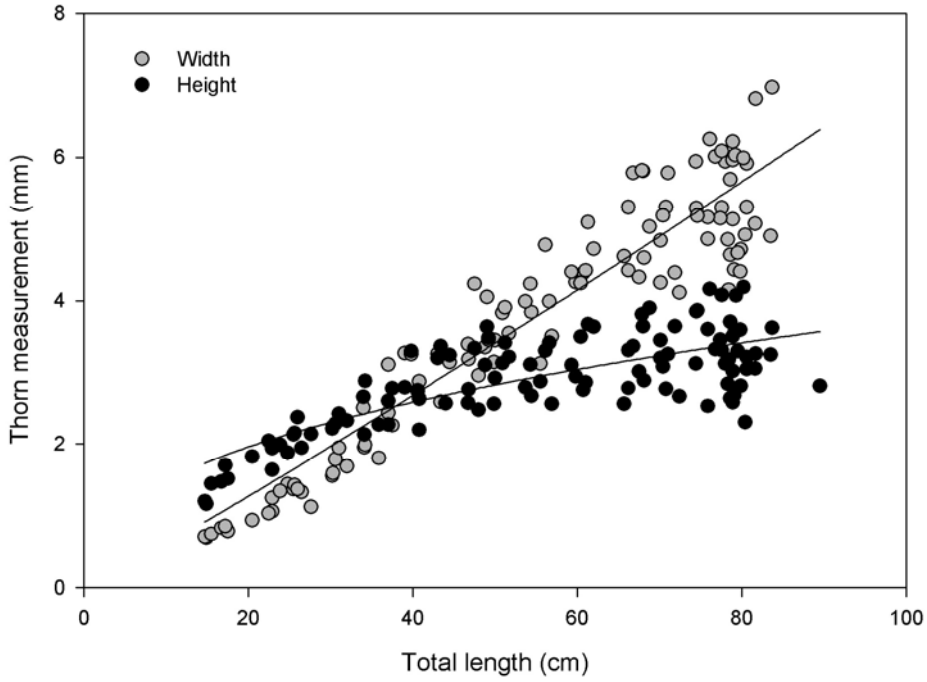

Figure 21.
The relationships between caudal thorn height (n = 113), and width (n = 111) and total length of *Bathyraja minispinosa* sexes combined.

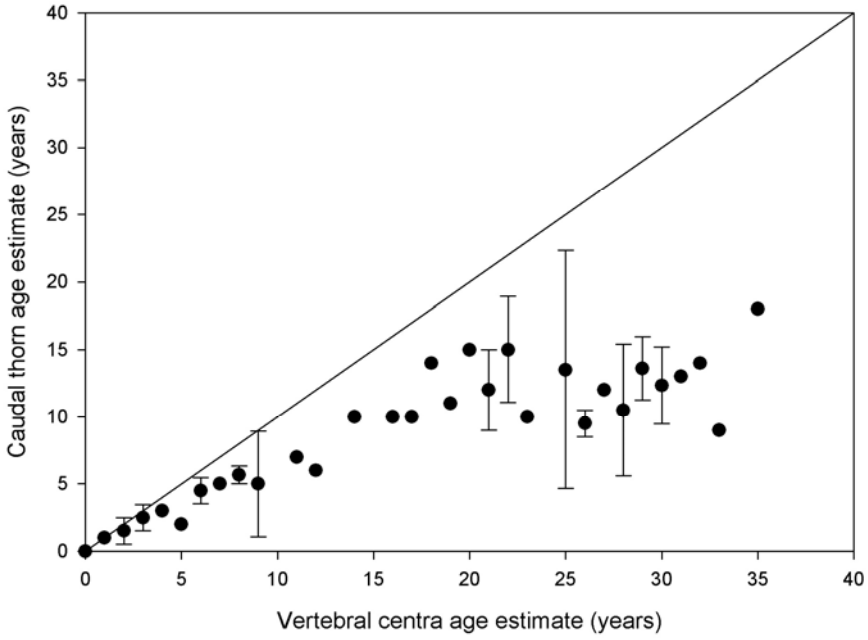

Figure 22.
The relationship between the vertebral centra band counts and the mean caudal thorn band count of *Bathyraja minispinosa* (n = 50). The 45º line represents 1:1 agreement between band counts and the error bars represent 95% confidence intervals.

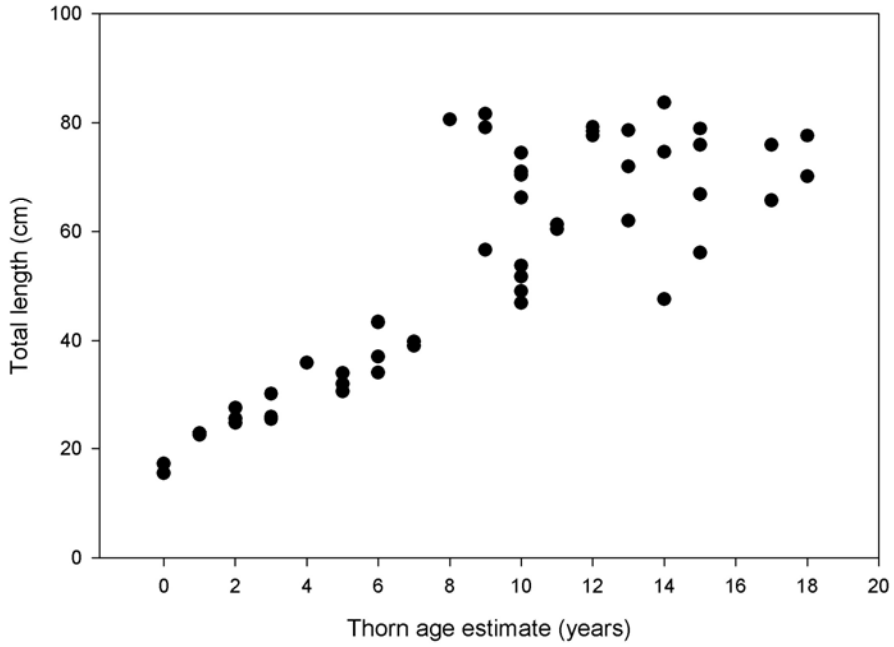

Figure 23.
The relationship of *B. minispinosa* caudal thorn age estimate and TL sexes combined (n = 50).

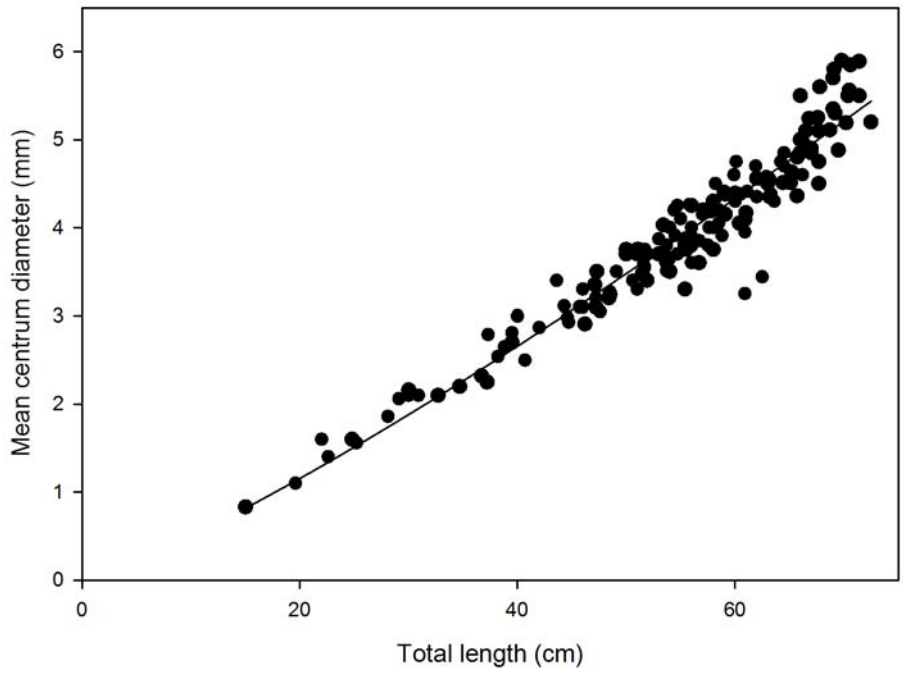

Figure 24.
The relationship between mean centrum diameter and total length of *Bathyraja taranetzi* combined sexes.

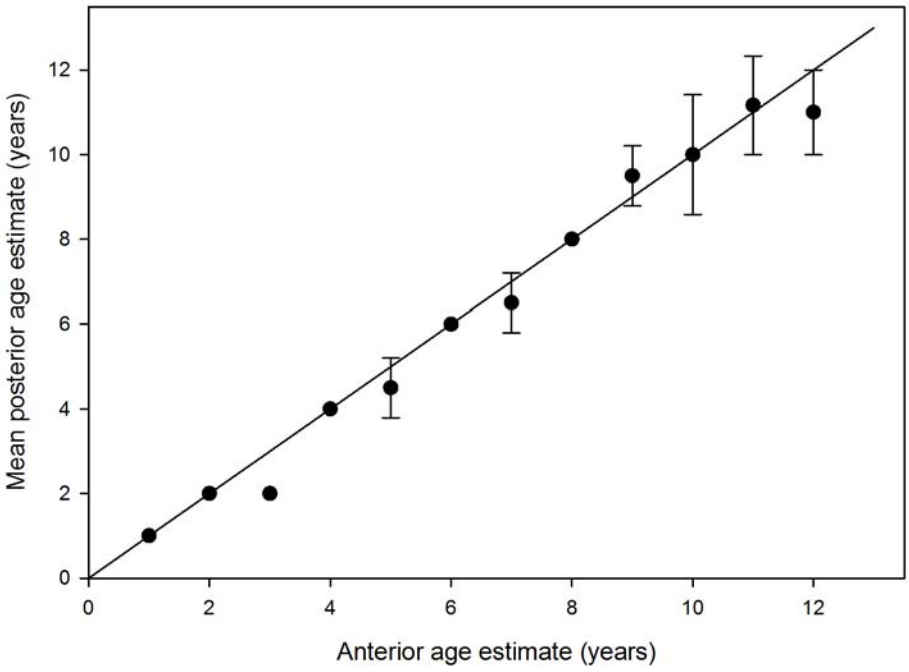

Figure 25.
The relationship between the anterior age estimates from vertebral centra and the mean posterior age estimates of *Bathyraja taranetzi* (*n* = 24). The error bars indicate +/- the 95% confidence intervals.

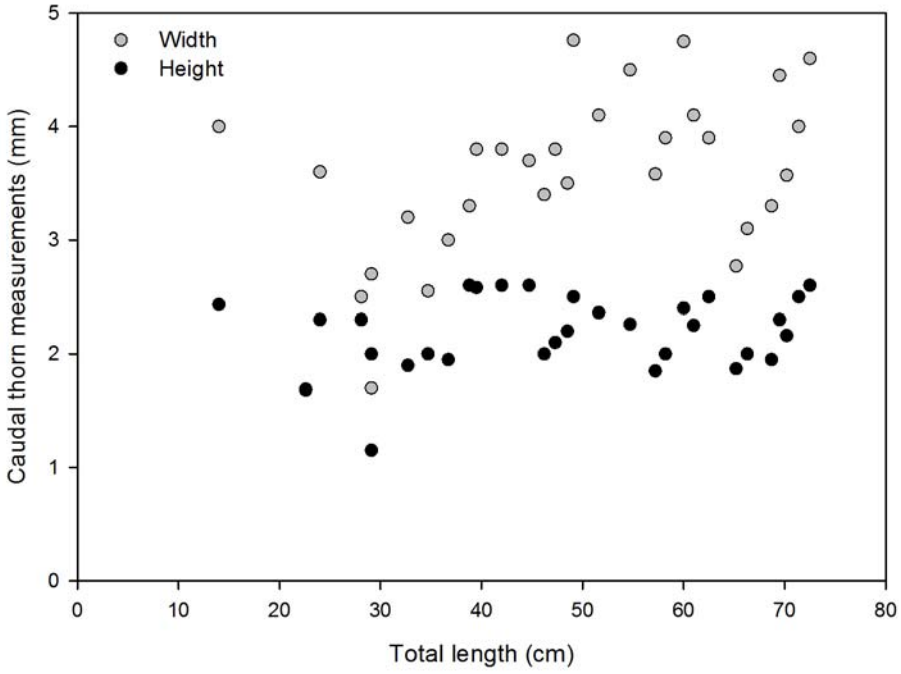

Figure 26.
Caudal thorn height (*n* = 31), and width (*n* = 31) measurements against total length for *Bathyraja taranetzi* combined sexes.

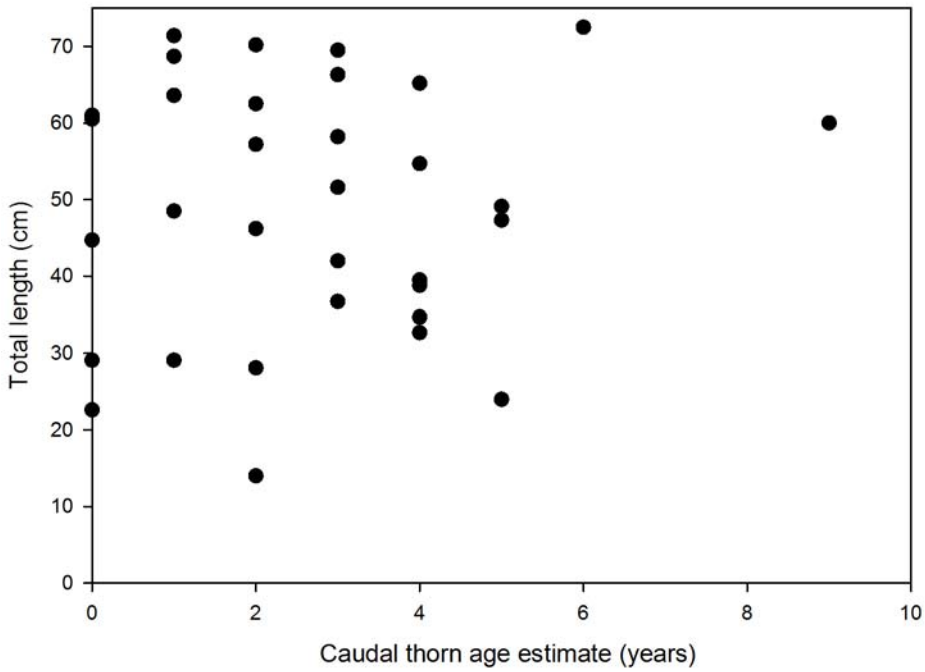

Figure 27.
The relationship of *Bathyraja taranetzi* caudal thorn age estimate and total length (n = 33).

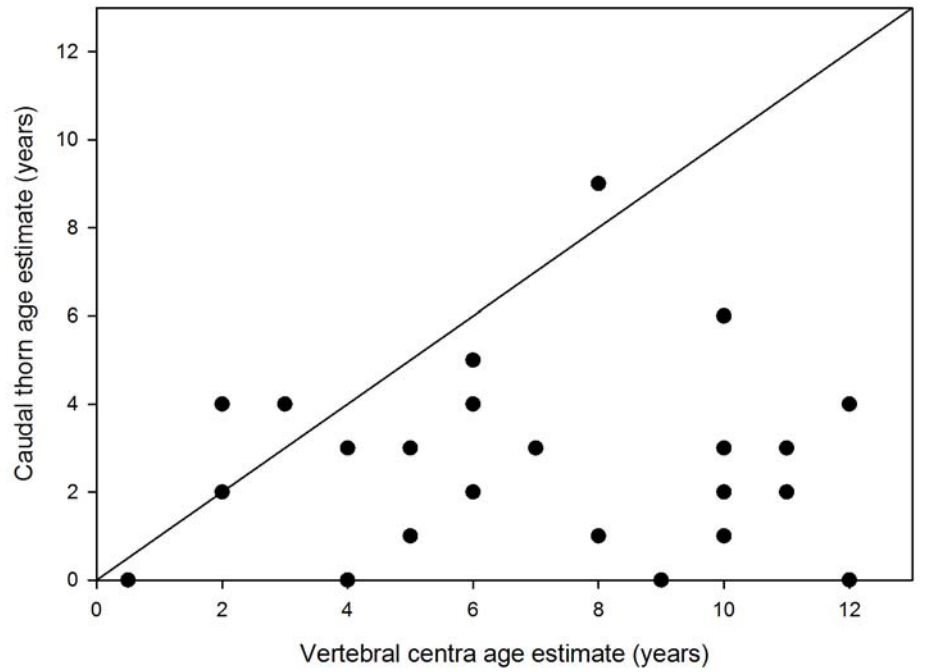

Figure 28.
The relationship between the vertebral centra band counts and the mean caudal thorn band count of *Bathyraja taranetzi* (n = 28). The 45º line represents 1:1 agreement between band counts.

Total length is not a strong predictor of caudal thorn dimensions, accounting for 3.7% and 25.5% of the variability in base width and height respectively (Fig. 26). Similarly, there was no discernable relationship between TL and caudal thorn age estimates (n = 33, Fig. 27). A significant bias between caudal thorn and centra age was detected by the McNemars and Evans-Hoenig χ^2 tests ($p < 0.008$ in both cases, n = 28, Fig. 28).

Age estimation was attempted on 175 prepared vertebral centra; final ages were assigned to 155 (88.6%) used for further analysis. Centra were discarded due to poor band quality and incomplete biological data. Maximum observed age is 14 from a 66.0 cm TL female; the maximum observed age for males is 12 at 61.1, 60.5, and 54.4 cm TL.

Precision and error analysis

Bathyraja lindbergi. Visual examination of age-bias plot did not indicate significant bias between reads (Fig. 29). Average percent error, CV, and D calculations were acceptable among both 2nd, 3rd, and, when used, 4th reads (IAPE = 3.67%, CV = 5.04, D = 3.13; Campana 2001). The Bowkers and Evans-Hoenig χ^2 tests of symmetry did not detect bias between reads ($p >$ 0.05), however McNemars test detected a bias for ages 0-20 indicating that when differences in band counts occurred they were small, ±2 bands, but in the same direction. In this case read 2 produced higher band counts than read three although 80% of all reads agreed ±2 bands and 95% agreed ±3 bands between reads.

Bathyraja maculata. Age-bias plot indicated no obvious bias between reads 2, 3, and 4 as necessary (Fig. 30). Additionally IAPE, CV, and D values all indicated a high level of precision between all reads (IAPE = 3.52%, CV = 4.85, D = 3.20). Chi-square tests of symmetry detected a small bias between ages 11-20; ages 11-15 failed the McNemars test (p = 0.0325) and ages 16-20 failed the Evans-Hoenig test (p = 0.0036). All other ages passed χ^2 tests of symmetry ($p > 0.05$). Percent agreement between 2nd, 3rd, and 4th reads was reasonable with 66.7% agreement ±1, 80% agreement ±2, 88% ±3, and 94.4% ±4 bands.

Bathyraja minispinosa. Estimates of precision were calculated based on reads 2, 3, and 4 when appropriate, excluding individuals with age estimates of zero. The IAPE (4.78%), CV (6.57%) and D (4.02%) all showed an acceptable level of precision among reads. Visual assessment of the pair-wise age difference plot showed no significant bias (Fig. 31), and the contingency table χ^2 tests of symmetry indicated that the differences were due to random error (Bowker's, χ^2 = 97.7, df = 99, p = 0.5190; McNemar's, χ^2 = 0.1244, df = 1, p = 0.7243; Evans-Hoenig, χ^2 = 7.8140, df = 7, p = 0.3493).

Bathyraja taranetzi. Visual examination of age-bias plot did not indicate systematic bias between reads (Fig. 32). Precision was high indicating consistent ageing criteria among all reads (IAPE = 4.53%, CV = 6.31, D = 4.06). In addition, the χ^2 tests of symmetry did not detect any systematic bias between reads ($p > 0.17$ in all cases). Percent agreement supported the same trend, 84% agreed ±1 and 94% agreed ±2 bands among reads.

Age verification

Bathyraja lindbergi. Samples were only collected from four months: June, July, August and October. Only polished centra with high quality edges were used for MIA ($n = 141$) and centrum edge analysis ($n = 143$; Fig. 33). Low sample sizes in August ($n = 13$) and October ($n = 11$) may not be representative of the natural variability in vertebral band formation, in addition to missing samples from eight months, this study was unable to describe the annual pattern of band formation in *B. lindbergi*. However, June ($n = 42$) and July ($n = 78$) mean MIR values were compared using a Mann-Whitney test, and no significant difference was found ($p = 0.581$).

Bathyraja maculata. Samples were only collected from four months: June, July, August and October. Only polished centra with high quality edges were used for MIA ($n = 133$) and centrum edge analysis ($n = 138$; Fig. 34). Low sample sizes in August ($n = 7$) and October ($n = 14$) may not be representative of the natural variability in vertebral band formation, in addition to missing samples from eight months, this study was unable to describe the annual pattern of band formation in *B. maculata*. However, June ($n = 49$) and July ($n = 68$) mean MIR values were compared using a two sample t-test, no significant difference was found ($p = 0.943$).

Bathyraja minispinosa. A total of 125 vertebrae were measured for marginal increment analysis and assigned edge types. While samples were available from 10 months, sample sizes per month varied greatly. An ANOVA was conducted excluding months with sample sizes less than 14, and results indicated that there was no significant difference in the mean MIR values among the months of June, July, August, and October ($F_{3,112} = 1.452$, $p = 0.231$; Fig. 35). The results of the edge analysis indicates that the opaque band is deposited during the late summer and early fall as greater than 60% of the edges were opaque during this time period.

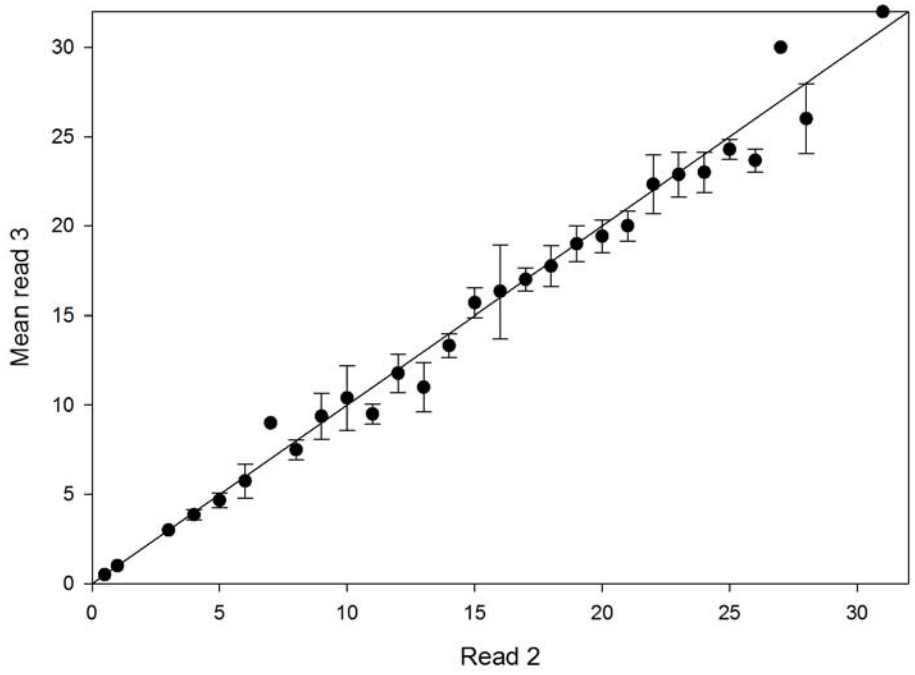

Figure 29.
Age bias plot of age estimates between Read 2 and Read 3 of *Bathyraja lindbergi* vertebral centra (*n* = 209). The 45º line represents 1:1 agreement between band counts. The error bars indicate +/- the 95% confidence intervals.

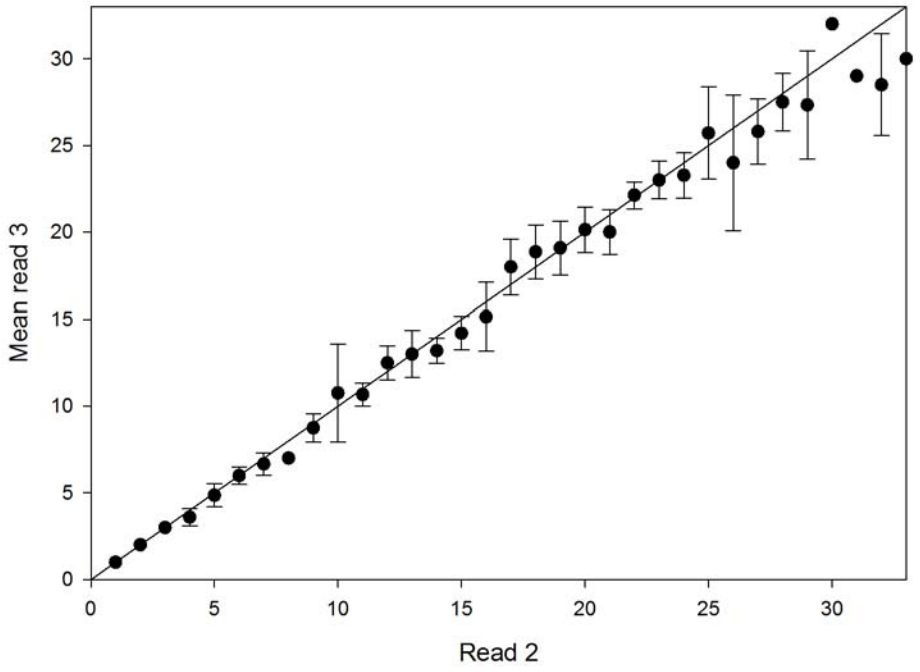

Figure 30.
Age bias plot of age estimates between Read 2 and Read 3 of *Bathyraja maculata* vertebral centra (*n* = 148). The 45º line represents 1:1 agreement between band counts. The error bars indicate +/- the 95% confidence intervals.

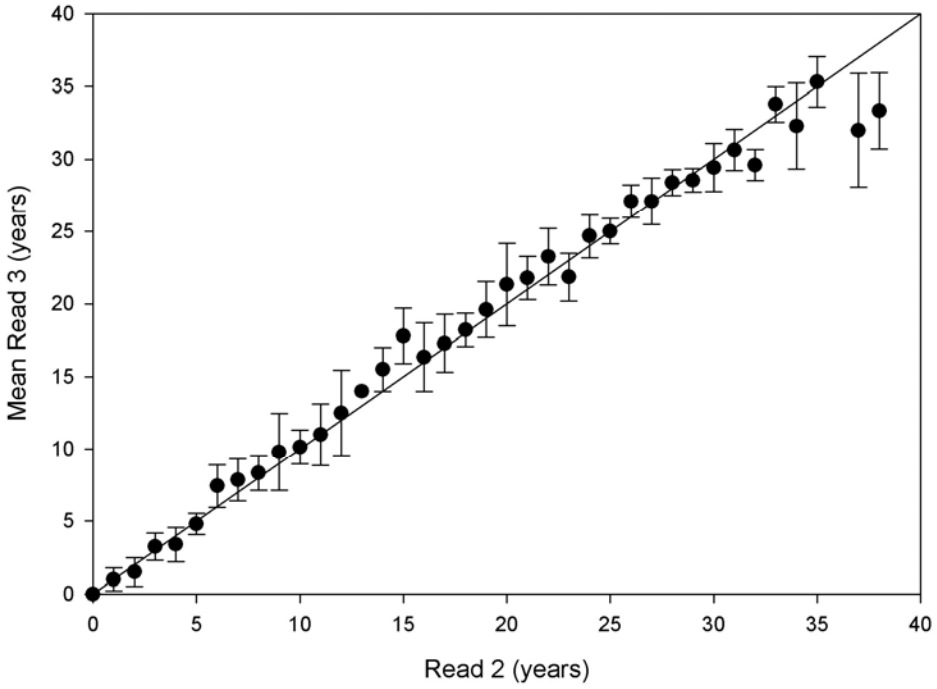

Figure 31.
The relationship between Read 2 and Read 3 of vertebral centra of *Bathyraja minispinosa* (*n* = 261). The 45º line represents 1:1 agreement between band counts and the error bars represent 95% confidence intervals.

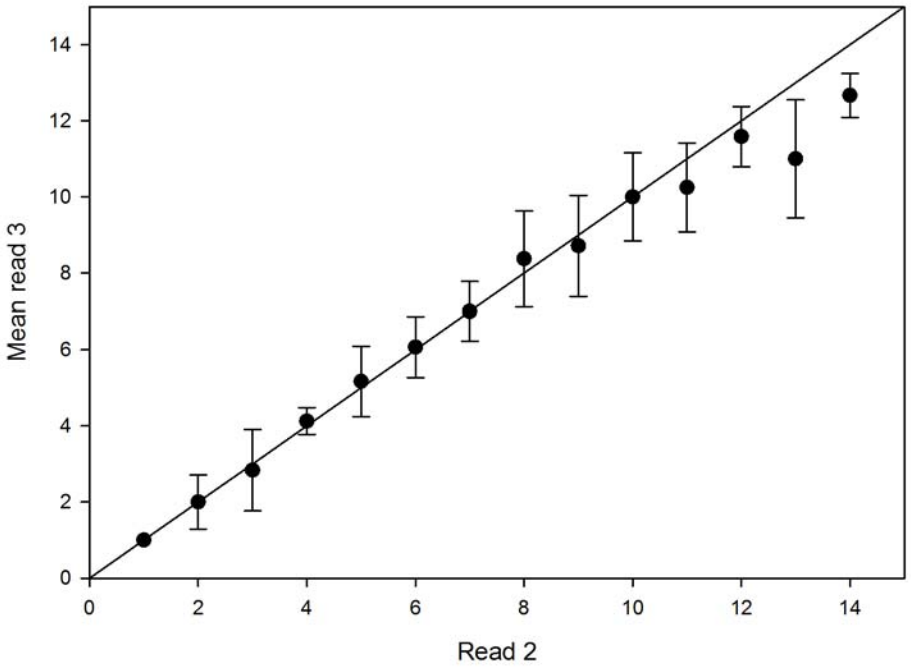

Figure 32.
Age bias plot of age estimates between Read 2 and Read 3 of *Bathyraja taranetzi* vertebral centra (*n* = 155). The 45º line represents 1:1 agreement between band counts. The error bars indicate +/- the 95% confidence intervals.

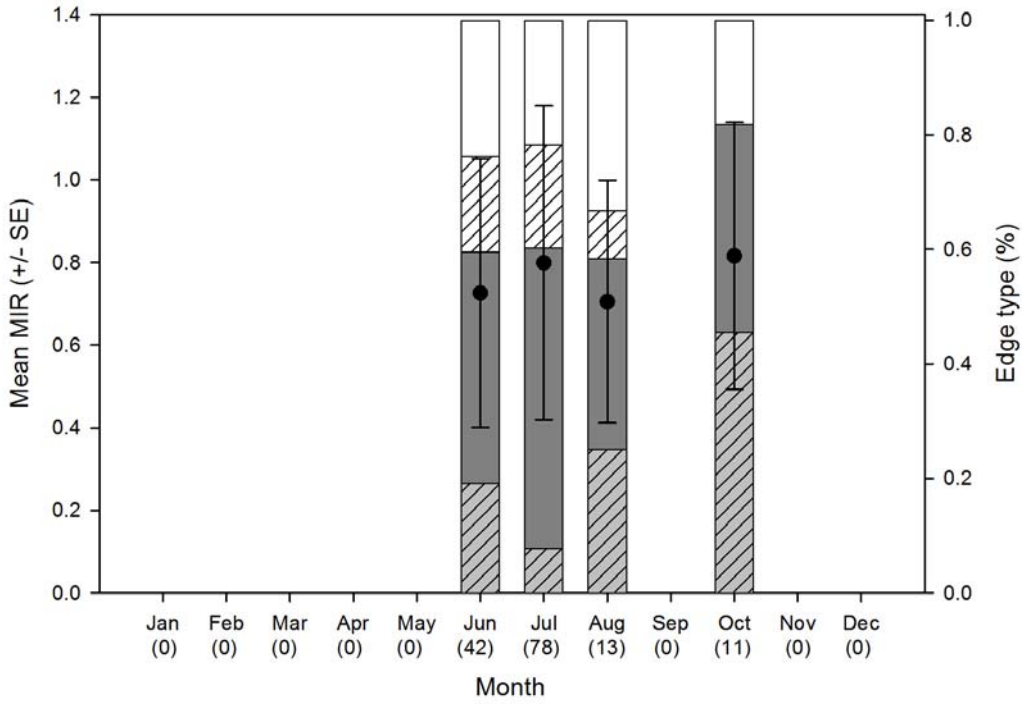

Figure 33.

Monthly variation in *Bathyraja lindbergi* centrum edge type and mean marginal increment ratio (MIR) ± 1 standard error (n = 144) determined from pooled sexes. Sample sizes are depicted below the month in parentheses. Striped light grey, narrow opaque edge; dark grey, broad opaque edge; striped white, narrow translucent edge; white, broad translucent edge.

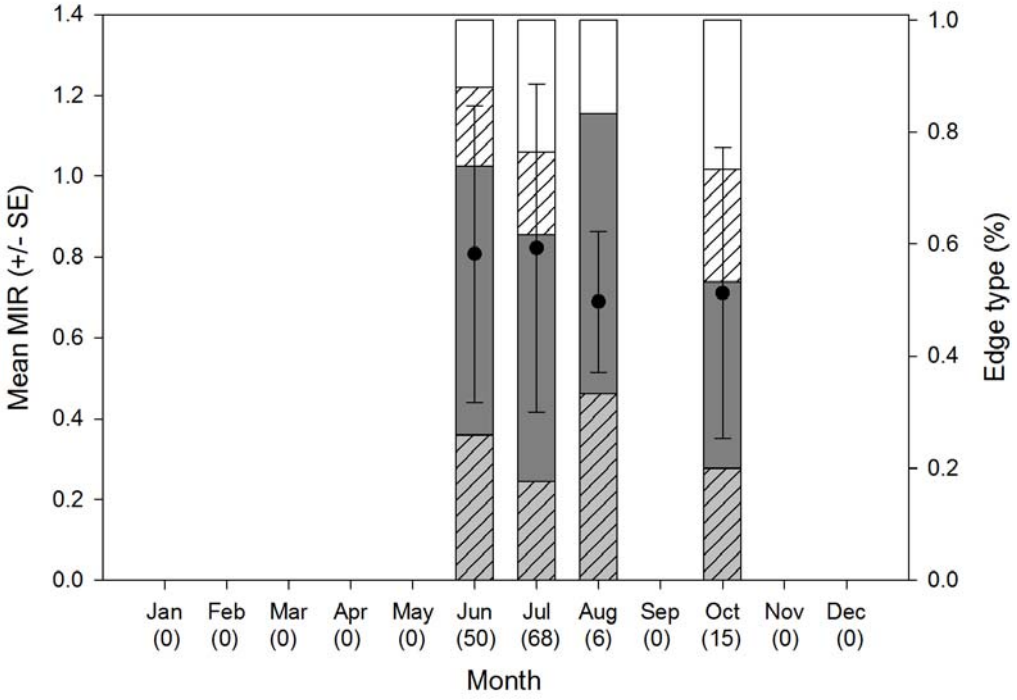

Figure 34.
Monthly variation in *Bathyraja maculata* centrum edge type and mean marginal increment ratio (MIR) ± 1 standard error (n = 139) determined from pooled sexes. Sample sizes are depicted below the month in parentheses. Striped light grey, narrow opaque edge; dark grey, broad opaque edge; striped white, narrow translucent edge; white, broad translucent edge.

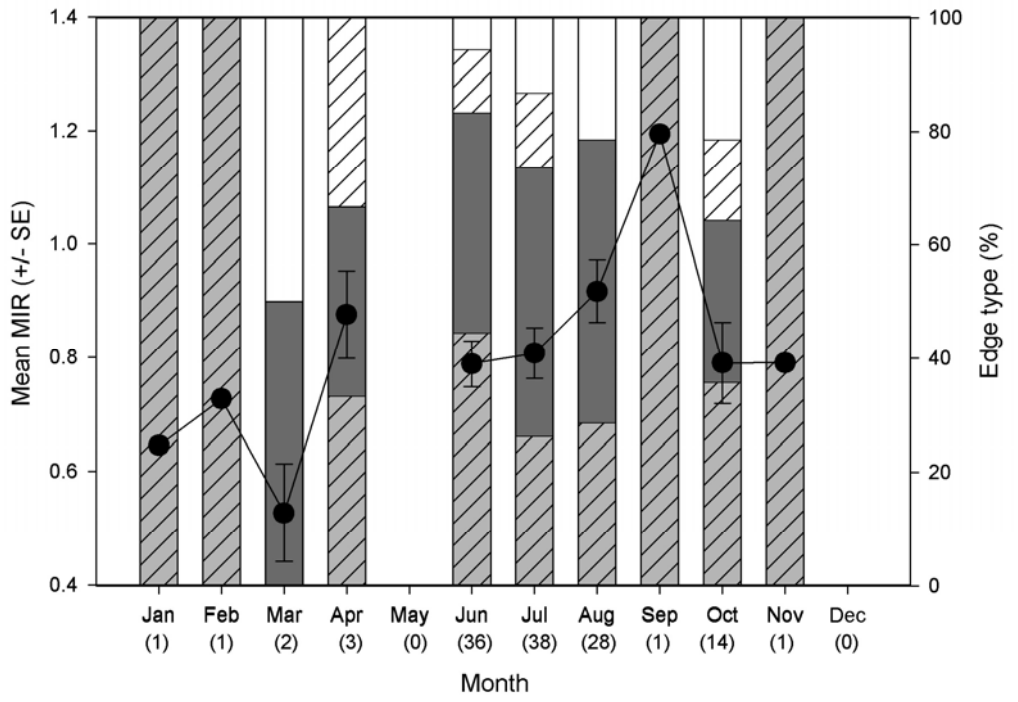

Figure 35.

Monthly variation in *Bathyraja minispinosa* centrum edge type and mean marginal increment ratio (MIR) ± 1 standard error (n = 125) determined from pooled sexes. Monthly sample sizes are depicted below the month in parentheses. Striped light grey, narrow opaque edge; dark grey, broad opaque edge; striped white, narrow translucent edge; white, broad translucent edge.

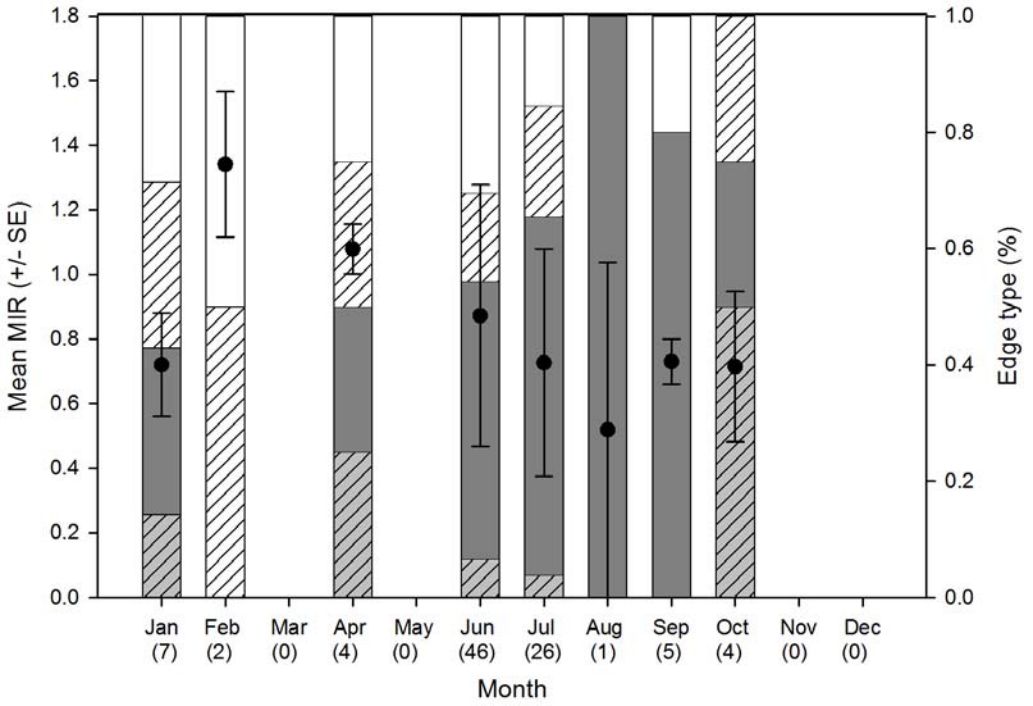

Figure 36.

Monthly variation in *Bathyraja taranetzi* centrum edge type and mean marginal increment ratio (MIR) ± 1 standard error (n = 95) determined from pooled sexes. Sample sizes are depicted below the month in parentheses. Striped light grey, narrow opaque edge; dark grey, broad opaque edge; striped white, narrow translucent edge; white, broad translucent edge.

Bathyraja taranetzi. Samples were collected from eight months. Only polished centra with high quality edges were used for MIA (n = 91) and centrum edge analysis (n = 91; Fig. 36). Low sample sizes in January (n = 4), February (n = 2), April (n = 3), August (n = 1), September (n = 5), and October (n = 4) may not be representative of the natural variability in vertebral band formation, in addition to missing samples from four months, this study was unable to describe the annual pattern of band formation in *B. taranetzi*. However, June (n = 46) and July (n = 26) mean MIR values were compared using a two sample t-test, no significant difference was found (p = 0.105).

Growth parameter estimates

Bathyraja lindbergi. Age estimates from vertebral centra ranged from 0 to 32 years for females (n = 88) and 1 to 27 for males (n = 75). The largest observed female was 102.1 cm TL and had a band count of 30. The greatest band count for a female, 32 was from a 96.0 cm TL individual. The largest observed male was 92.7 cm TL and had a band count of 20, compared to the maximum age estimate for a male, 27, from a 87.6 cm TL individual.

Although maximum age estimates differed there was no detectable difference in male and female growth curves (p > 0.78 for all curves) so sexes were combined to create final growth curves (Fig. 37). All growth models fit to age-at-length data had high explanatory power (r^2 > 0.90). The 3-parameter VBGF and Gompertz growth models produced greater estimates of size at hatching, 21.5 and 24.5 cm respectively, than has been observed (17 to 19 cm TL, J. Hoff pers. comm.). The Gompertz and Logistic growth models determined realistic L_∞ values, 109.6 and 101.6 cm respectively. The best statistical fit is obtained using the polynomial growth function (Table 4). Results of all six growth models are presented for the sake of comparison.

Bathyraja maculata. Band counts from female and male vertebral centra provided minimum longevity estimate of 32 years from individuals of 112.2 and 111.1 cm TL, respectively. Female age estimates (n = 85) ranged from 1 to 32 years over an observed size range of 23.7 to 114.5 cm TL. For males (n = 63) the age estimates ranged from 3 to 32 from the observed size range of 36.2 to 114.4 cm TL. The largest observed female had a band count of 29, while the largest observed male had a band count of 23.

There was not a significant difference in male and female growth curves, thus sexes were combined to create final growth curves (p > 0.96 all models; Fig. 38). The 3-parameter VBGF calculated a greater size at hatching than observed, 17 to 19 cm TL, at 22.6 cm TL (J. Hoff pers. comm.). The Gompertz model calculated size at hatching is greater than observed size at hatching and the smallest free living individual collected for this study at 26.4 cm. The estimates

of L_∞ ranged from 118.3 cm to 155.6 cm from the logistic and 3-parameter VBGF respectively (Table 5).

Bathyraja minispinosa. Estimated ages ranged from 0 to 37 (n = 97) for females and 0 to 35 (n = 88) for males. The maximum band count of 37 years was assigned to the largest skate from the study, a mature female (89.5cmTL). The male with the highest band count was estimated to be 35 years old (76.2cmTL), while the largest male aged was estimated to be 33 years old (83.7cmTL).

The results of a likelihood ratio test following Kimura (1980) and Haddon (2001) found that there was no difference between male and female growth curves for any of the models, therefore sexes were pooled ($p > 0.3736$ for all curves; Fig 39). All growth models fit the data well ($r^2 > 0.9570$, $p < 0.001$; Table 6), however according to established criteria, the Gompertz model was deemed the best fit. The L_∞ estimates from the standard 3-paramter VBGF was much greater than the reported maximum sizes for the species (Table 6). Additionally, size at hatching calculated from the 3-parameter VBGF and Gompertz were slightly greater (VB: 16.4 cm TL; Gompertz: 18.1 cm TL) than the observed size of 14 to 15 cm TL (J. Hoff pers. comm.).

Bathyraja taranetzi. Age estimates ranged from 1 to 14 for females from an observed size range of 25.2 to 72.5 cm TL ($n = 78$), and age estimates for males ranged from 0 to 12 from an observed size range of 19.6 to 66.3 cm TL ($n = 77$). The largest female had a final band count of 10 and the largest male had a final band count of 11. The greatest band count, 14, for a female was from a 66 cm TL individual. Four males shared the greatest band count, 12, their TL's were: 54.4, 54.5, 60.5, and 61.1 cm.

Likelihood ratio results indicated female and male growth curves were significantly different ($p < 0.004$ all curves), so they were examined separately (Figs. 40 & 41). Female 3-parameter VBGF and Gompertz estimated greater size at hatching, 18.5 and 20.3 cm TL respectively, than observed which is 13 to 15 cm TL at birth (J. Hoff pers. comm.). Calculated size at hatching from male 3-parameter VBGF and Gompertz were similar to observed at 14.3 and 16.8 cm TL respectively. Similarly L_∞ estimates from female growth models range from 76.3 to 86.0 cm and are greater than L_∞ estimates from male growth curves which range from 61.6 to 75.8 cm (Table 7).

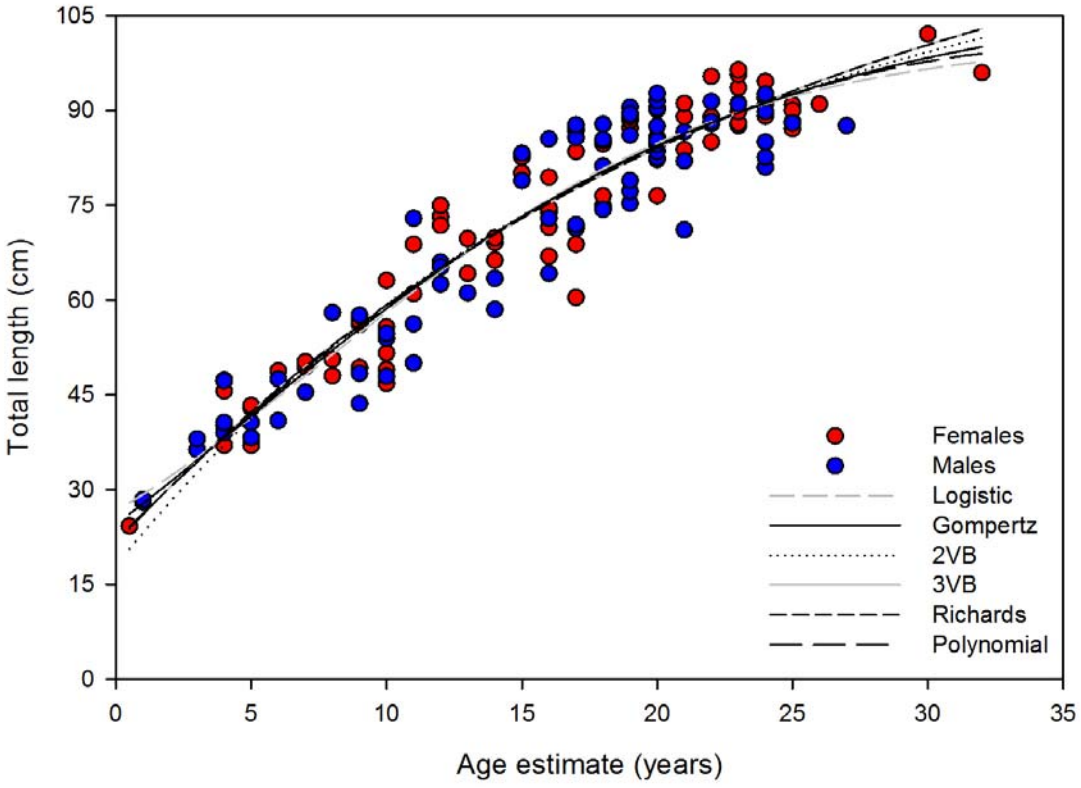

Figure 37.
Six different growth models fitted to age-at-length data for combined sexes of *Bathyraja lindbergi* (*n* = 163).

Growth Model		L_∞	k	t_0	L_0	g	p	a	b	c	r^2	MSE	SEE	p
	Males	136.1	0.0389	-4.5293	21.99	-	-	-	-	-	0.8885	42.48	6.518	<0.0001
3-Parameter VBGF	Females	128.5	0.0445	-3.997	20.95	-	-	-	-	-	0.9163	29.29	5.412	<0.0001
	Pooled	**131.9**	**0.0417**	**-4.2661**	21.50	-	-	-	-	-	0.9033	34.79	5.898	<0.0001
	Males	122.2	0.0500	-	18	-	-	-	-	-	0.8864	42.69	6.533	<0.0001
2-Parameter VBGF	Females	121.7	0.0513	-	18	-	-	-	-	-	0.9155	29.24	5.408	<0.0001
	Pooled	**122.1**	**0.0505**	-	18	-	-	-	-	-	0.9019	35.08	5.923	<0.0001
	Males	108.9	1.5030	-	24.40	0.0877	-	-	-	-	0.9454	40.46	6.360	<0.0001
Gompertz	Females	109.7	1.4907	-	24.71	0.0877	-	-	-	-	0.9191	28.32	5.322	<0.0001
	Pooled	**109.7**	**1.4974**	-	24.54	**0.0873**	-	-	-	-	0.9072	33.38	5.778	<0.0001
	Males	100.0	0.1368	7.7159	-	-	-	-	-	-	0.8982	38.80	6.229	<0.0001
Logistic	Females	102.7	0.1300	7.8468	-	-	-	-	-	-	0.9203	27.89	5.281	<0.0001
	Pooled	**101.7**	**0.1327**	**7.8296**	-	-	-	-	-	-	0.9097	32.48	5.699	<0.0001
	Males	122.5	0.0389	-	0.838	-	0.1904	-	-	-	0.8885	43.08	6.564	<0.0001
Richards	Females	119.9	0.0445	-	0.837	-	0.0688	-	-	-	0.9163	29.64	5.445	<0.0001
	Pooled	**136.3**	**0.0417**	-	**0.836**	-	**-0.0322**	-	-	-	0.9033	35.01	5.917	<0.0001
	Males	-	-	-	-	-	-	21.5593	4.3588	-0.0621	0.8918	41.24	6.421	<0.0001
Polynomial	Females	-	-	-	-	-	-	22.0440	4.3216	-0.0594	0.9185	28.52	5.340	<0.0001
	Pooled	-	-	-	-	-	-	**21.9420**	**4.3071**	**-0.0593**	0.9059	33.84	5.818	<0.0001

Table 4.

Parameters for each growth model for males, females, and combined sexes of *Bathyraja lindbergi*. VBGF, von Bertalanffy growth function; L_∞, asymptotic length; k, growth coefficient; t_0, theoretical age at 0 length; L_0, length at birth; g, instantaneous growth rate; p, shape parameter; a, b, and c, are constants.

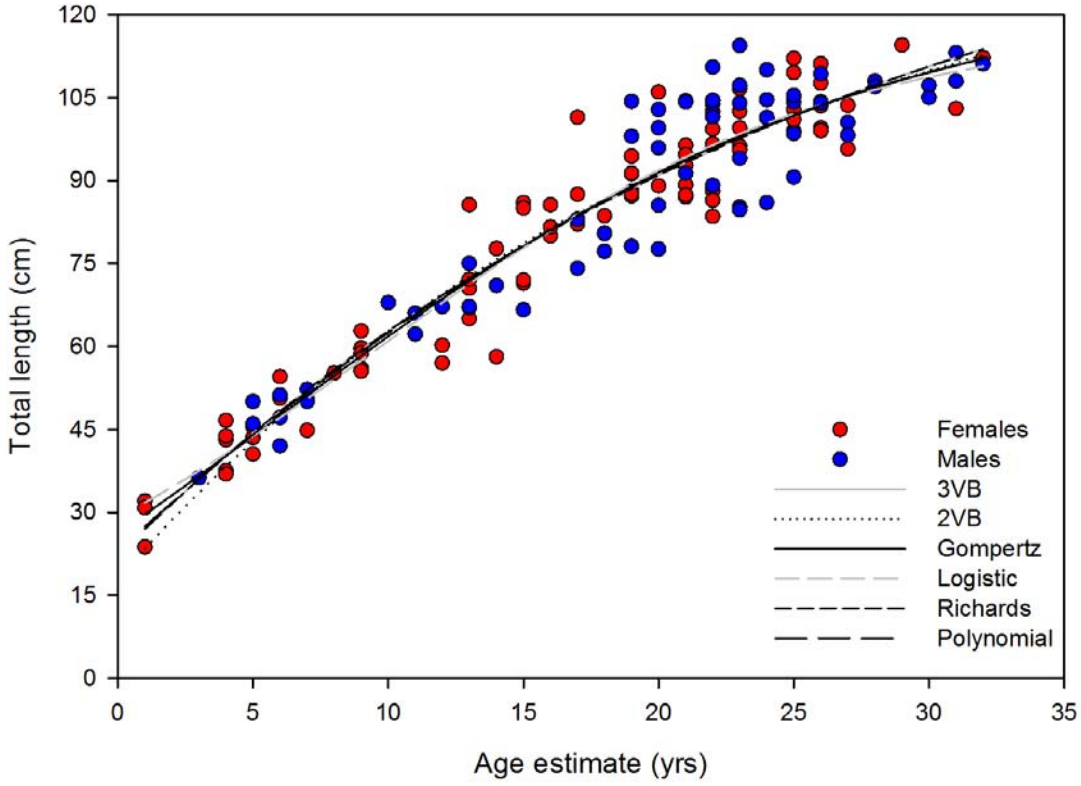

Figure 38.
Six different growth models fitted to age-at-length data for combined sexes of *Bathyraja maculata* (n = 148).

Growth Model		L_∞	k	t_0	L_0	g	p	a	b	c	r^2	MSE	SEE	p
3-Parameter VBGF	Males	147.7	0.0408	-3.5695	20.01	-	-	-	-	-	0.8761	58.98	7.680	<0.0001
	Females	160.5	0.0340	-4.5529	23.01	-	-	-	-	-	0.9340	38.82	6.067	<0.0001
	Pooled	**155.6**	**0.0362**	**-4.2507**	**22.20**	-	-	-	-	-	0.9134	45.31	6.731	<0.0001
2-Parameter VBGF	Males	142.8	0.0444	-	18	-	-	-	-	-	0.8759	58.11	7.623	<0.0001
	Females	142.7	0.0443	-	18	-	-	-	-	-	0.9315	37.74	6.143	<0.0001
	Pooled	**142.9**	**0.0443**	-	**18**	-	-	-	-	-	0.9119	45.74	6.764	<0.0001
Gompertz	Males	127.6	1.5798	-	26.27	0.0781	-	-	-	-	0.8788	57.70	7.596	<0.0001
	Females	127.7	1.5771	-	26.39	0.0775	-	-	-	-	0.9356	35.88	5.990	<0.0001
	Pooled	**127.7**	**1.5783**	-	**26.36**	**0.0777**	-	-	-	-	0.9155	44.18	6.646	<0.0001
Logistic	Males	119.4	0.1156	9.6093	-	-	-	-	-	-	0.8807	56.82	7.538	<0.0001
	Females	117.4	0.1205	9.3525	-	-	-	-	-	-	0.9360	35.70	5.975	<0.0001
	Pooled	**118.3**	**0.1183**	**9.4841**	-	-	-	-	-	-	0.9164	43.73	6.613	<0.0001
Richards	Males	143.0	0.0322	-	0.8643	-	0.0322	-	-	-	0.8762	59.98	7.745	<0.0001
	Females	144.0	0.0341	-	0.8565	-	0.1073	-	-	-	0.9340	37.27	6.105	<0.0001
	Pooled	**148.7**	**0.0362**	-	**0.8572**	-	**0.0456**	-	-	-	0.9134	45.63	6.755	<0.0001
Polynomial	Males	-	-	-	-	-	-	21.718	4.644	-0.0575	0.8783	57.98	7.614	<0.0001
	Females	-	-	-	-	-	-	23.574	4.388	-0.0504	0.9350	36.23	6.0191	<0.0001
	Pooled	-	-	-	-	-	-	**23.000**	**4.476**	**-0.0530**	0.9149	44.53	6.6732	<0.0001

Table 5.

Parameters for each growth model for males, females, and combined sexes of *Bathyraja maculata*. VBGF, von Bertalanffy growth function; L_∞, asymptotic length; k, growth coefficient; t_0, theoretical age at 0 length; L_0, length at birth; g, instantaneous growth rate; p, shape parameter; a, b, and c, are constant

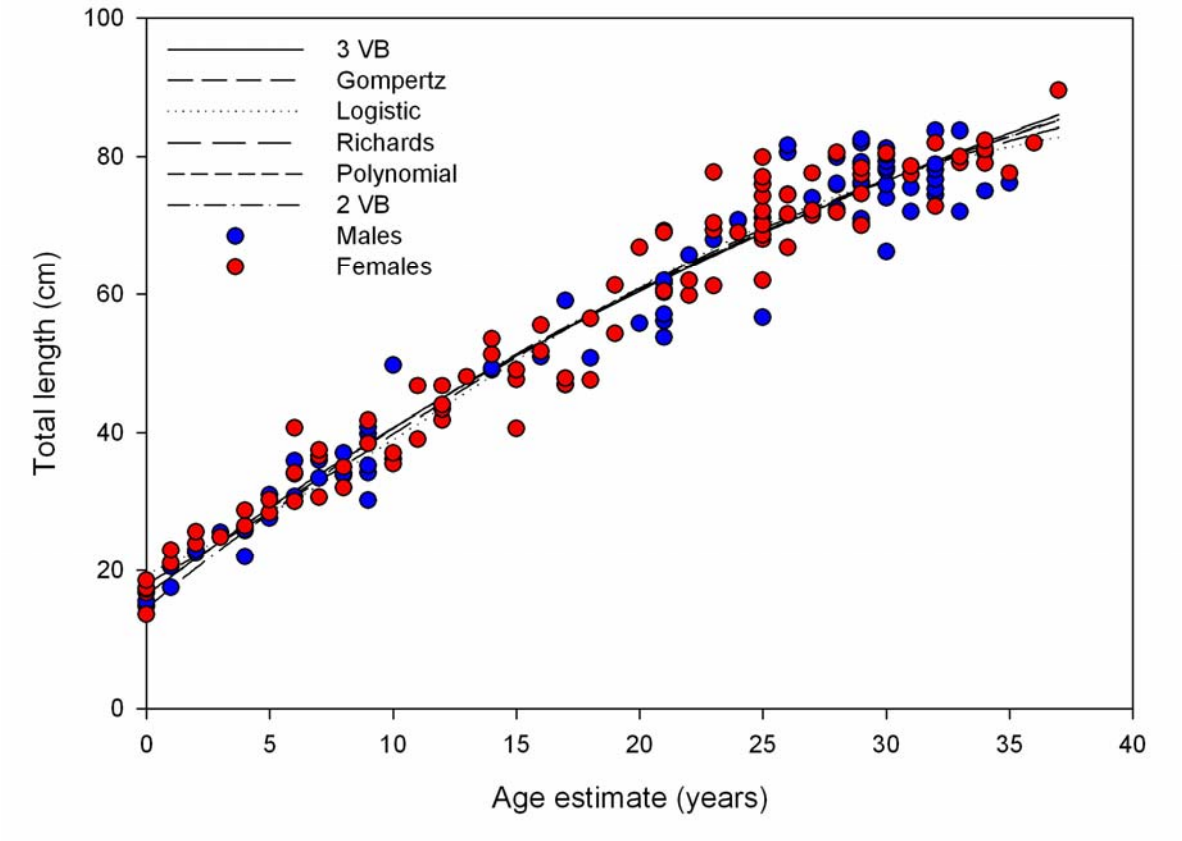

Figure 39.
Six different growth models fitted to age-at-length data for combined sexes of *Bathyraja minispinosa* (n = 185).

Growth Model		L_∞	k	t_0	L_0	g	p	a	b	c	r^2	MSE	SEE	p
3-Parameter VBGF	Males	129.0	0.0255	-4.8565	15.03	-	-	-	-	-	0.9601	19.46	4.411	<0.0001
	Females	171.9	0.0162	-6.6565	17.57	-	-	-	-	-	0.9552	18.92	4.350	<0.0001
	Pooled	**146.9**	**0.0206**	**-5.7604**	16.44	-	-	-	-	-	0.9576	19.15	4.376	<0.0001
2-Parameter VBGF	Males	125.3	0.0270	-	14.5	-	-	-	-	-	0.9609	19.26	4.389	<0.0001
	Females	137.5	0.0236	-	14.5	-	-	-	-	-	0.9534	19.87	4.457	<0.0001
	Pooled	**130.8**	**0.0254**	-	14.5	-	-	-	-	-	0.9571	19.47	4.412	<0.0001
Gompertz	Males	94.8	1.7228	-	16.93	0.0687	-	-	-	-	0.9611	18.97	4.355	<0.0001
	Females	106.2	1.7186	-	19.04	0.0561	-	-	-	-	0.9564	18.43	4.293	<0.0001
	Pooled	**100.2**	**1.7134**	-	18.06	**0.0618**	-	-	-	-	0.9586	18.69	4.323	<0.0001
Logistic	Males	86.5	0.1099	11.8472	-	-	-	-	-	-	0.9606	19.19	4.380	<0.0001
	Females	93.1	0.0956	13.3722	-	-	-	-	-	-	0.9564	18.40	4.289	<0.0001
	Pooled	**89.6**	**0.1022**	**12.5704**	-	-	-	-	-	-	0.9584	18.78	4.333	<0.0001
Richards	Males	90.5	0.0256	-	0.8833	-	0.3544	-	-	-	0.9610	19.69	4.437	<0.0001
	Females	104.2	0.0162	-	0.8976	-	0.5002	-	-	-	0.9561	19.12	4.373	<0.0001
	Pooled	**96.5**	**0.0206**		**0.8883**		**0.4205**	-	-	-	0.9581	19.25	4.388	<0.0001
Polynomial	Males	-	-	-	-	-	-	15.1273	2.8151	-0.0262	0.9617	19.09	4.369	<0.0001
	Females	-	-	-	-	-	-	17.5784	2.4697	-0.0163	0.9565	18.7660	4.332	<0.0001
	Pooled	-	-	-	-	-	-	**16.4472**	**2.6225**	**-0.0207**	0.9586	18.9207	4.350	<0.0001

Table 6.

Parameters for each growth model for males, females, and combined sexes of *Bathyraja minispinosa*. VBGF, von Bertalanffy growth function; L∞, asymptotic length; k, growth coefficient; t0, theoretical age at 0 length; L0, length at birth; g, instantaneous growth rate; p, shape parameter; a, b, and c, are constant.

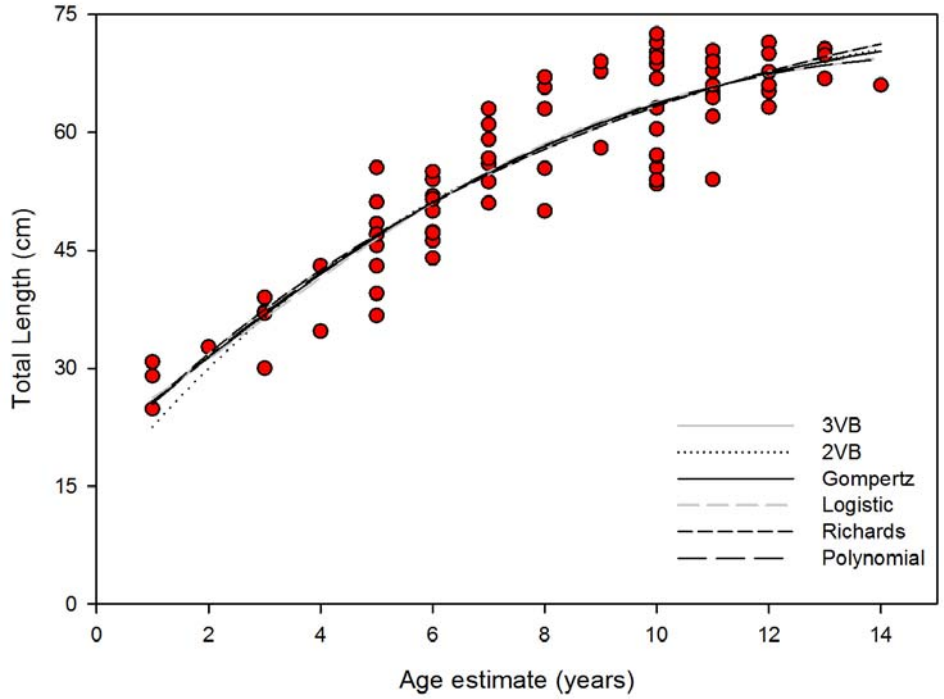

Figure 40.
Six different growth models fitted to female *Bathyraja taranetzi* length-at-age data (*n* = 78).

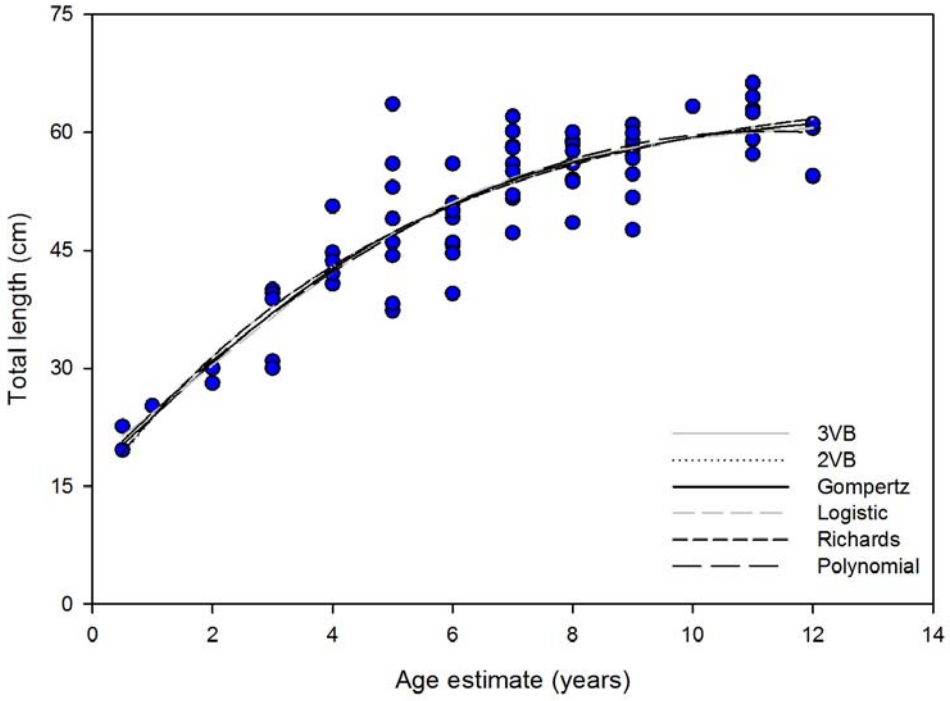

Figure 41.
Six different growth models fitted to male *Bathyraja taranetzi* length-at-age data (*n* = 77)

Growth Model		L_∞	k	t_0	L_0	g	p	a	b	c	r^2	MSE	SEE	p
3-Parameter VBGF	Males	66.5	0.1995	-1.2161	14.3	-	-	-	-	-	0.7917	24.32	4.931	<0.0001
	Females	85.4	0.1108	-2.2034	18.5	-	-	-	-	-	0.8264	26.62	5.160	<0.0001
	Pooled	78.1	0.1325	-1.9006	17.3	-	-	-	-	-	0.8038	27.23	5.218	<0.0001
2-Parameter VBGF	Males	66.3	0.2020	-	14	-	-	-	-	-	0.7917	23.99	4.899	<0.0001
	Females	80.1	0.1382	-	14	-	-	-	-	-	0.8228	26.83	5.179	<0.0001
	Pooled	74.8	0.1559	-	14	-	-	-	-	-	0.8014	27.38	5.232	<0.0001
Gompertz	Males	63.2	1.3237	-	16.8	0.3020	-	-	-	-	0.7949	23.94	4.893	<0.0001
	Females	76.3	1.3230	-	20.3	0.1982	-	-	-	-	0.8309	25.93	5.093	<0.0001
	Pooled	71.8	1.2949	-	19.9	0.2192	-	-	-	-	0.8053	27.01	5.197	<0.0001
Logistic	Males	61.6	0.0414	2.0717	-	-	-	-	-	-	0.7951	23.92	4.891	<0.0001
	Females	72.3	0.2871	2.9688	-	-	-	-	-	-	0.8341	25.45	5.045	<0.0001
	Pooled	68.8	0.3055	2.6345	-	-	-	-	-	-	0.8054	26.99	5.196	<0.0001
Richards	Males	75.9	0.1996	-	0.7845	-	-0.13263	-	-	-	0.7917	24.65	4.965	<0.0001
	Females	86.1	0.1109	-	0.7833	-	-0.0077	-	-	-	0.8194	26.98	5.194	<0.0001
	Pooled	86.1	0.1325	-	0.7774	-	-0.0979	-	-	-	0.8038	27.41	5.236	<0.0001
Polynomial	Males	-	-	-	-	-	-	16.9735	7.6805	-0.3416	0.7959	23.83	4.882	<0.0001
	Females	-	-	-	-	-	-	19.0122	6.6598	-0.2192	0.8306	25.98	5.097	<0.0001
	Pooled	-	-	-	-	-	-	18.9138	6.7019	-0.2363	0.8053	27.02	5.199	<0.0001

Table 7.

Parameters for each growth model for males, females, and combined sexes of *Bathyraja taranetzi*. VBGF, von Bertalanffy growth function; L_∞, asymptotic length; k, growth coefficient; t_0, theoretical age at 0 length; L_0, length at birth; g, instantaneous growth rate; p, shape parameter; a, b, and c, are constant

Maturity and reproduction

Bathyraja lindbergi. Reproductive data was collected for 115 female and 141 male *B. lindbergi*. The largest immature female was 87.5 cm TL and the smallest mature female was 81.5 cm TL. The largest immature male was 88.0 cm TL and the smallest mature male was77.0 cm TL. Median size at maturity was estimated at 78.9 and 80.4 cm TL for females and males respectively (Fig. 42). The corresponding median ages at maturity were estimates as 18.5 years for females and 16.9 years for males (Fig.43).

Measures of inner clasper length and oviducal glands also were used to indicate the onset of maturity. Inner clasper length ranged from 8 to 216 mm, with an abrupt increase near 71 cm TL (Fig. 44). Similarly in females, oviducal width had a sharp increase near 71 cm TL, and oviducal measurement ranged in size from 2 to 63 mm (Fig. 45).

Each of the five testes collected in 2004 were prepared for histological examination. All five individuals had mature sperm present and were classified as mature males at the time of collection (Fig. 44). Examination of prepared oviducal glands did not show any evidence of sperm storage.

There was no difference in mature ova counts in the left and right ovaries (Mann-Whitney non-parametric test: $U = 996$, $p = 0.788$, $n = 31$). A one-way ANOVA did not indicate a significant difference in number of mature ova ($F = 0.886$, $p = 0.424$, $n = 31$; Fig. 46) or in maximum ova diameter ($KW = 2.927$, $df = 2$, $p = 0.231$, $n = 32$; Fig. 47) among months.

There was no relationship between number of mature ova or maximum ova size with TL (number of mature ova: $r^2 < 0.001$; maximum ova diameter: $r^2 < 0.04$; Fig. 48) or age estimate (number mature ova: $r^2 < 0.001$; maximum ova diameter: $r^2 = 0.24$; Fig. 49). A total of 10 gravid females were observed during the summer months, June-August (Fig. 50).

Bathyraja maculata. Reproductive data was recorded for 95 females and 93 males of *B. maculata*. The largest immature female was 99.3 cm TL and the smallest mature female observed was 96.4 cm TL. For males the largest immature observation was 102.4 cm TL and the smallest mature male was 89.1 cm TL. Median size at maturity was 95.47 and 92.6 cm TL for females and males respectively (Fig. 51). The estimates for median age at maturity were 22.5 and 20.7 years respectively for females and males (Fig. 52).

Inner clasper length in males ranged from 17 to 275 mm and oviducal width ranged from 1 to 79 mm in females; both increased with TL. A sharp increase of oviducal-TL relationship corresponding with the onset of maturity is observed near 83 cm TL for females, in males a sharp increase of inner clasper to TL is observed at 91 cm TL (Figs. 53 & 54).

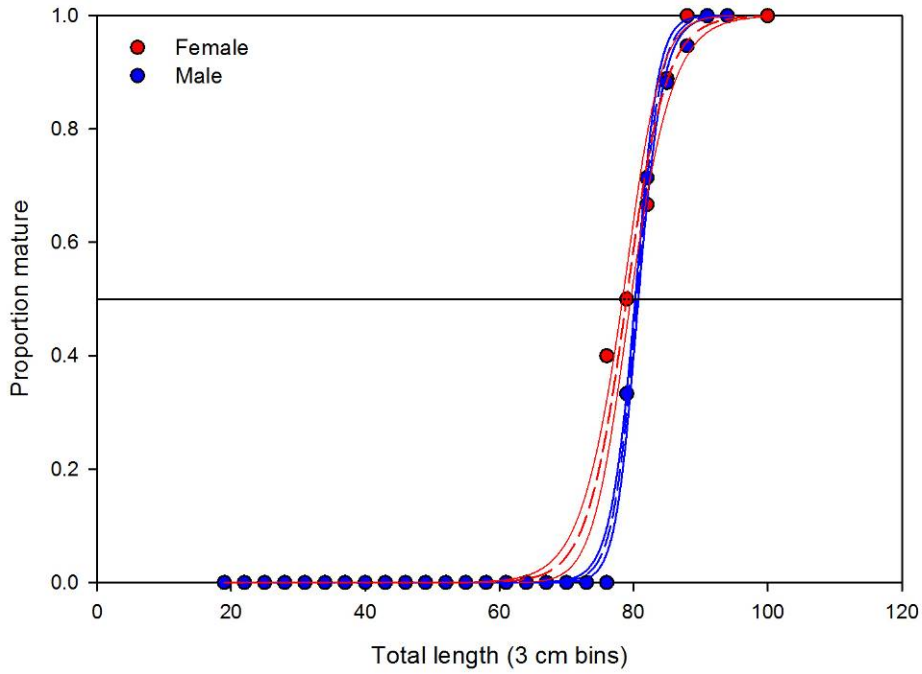

Figure 42.
Estimated median size at maturity for female and male *Bathyraja lindbergi*. Size at 50% maturity corresponds to 78.9 cm and 80.4 cm total length for females and males respectively.

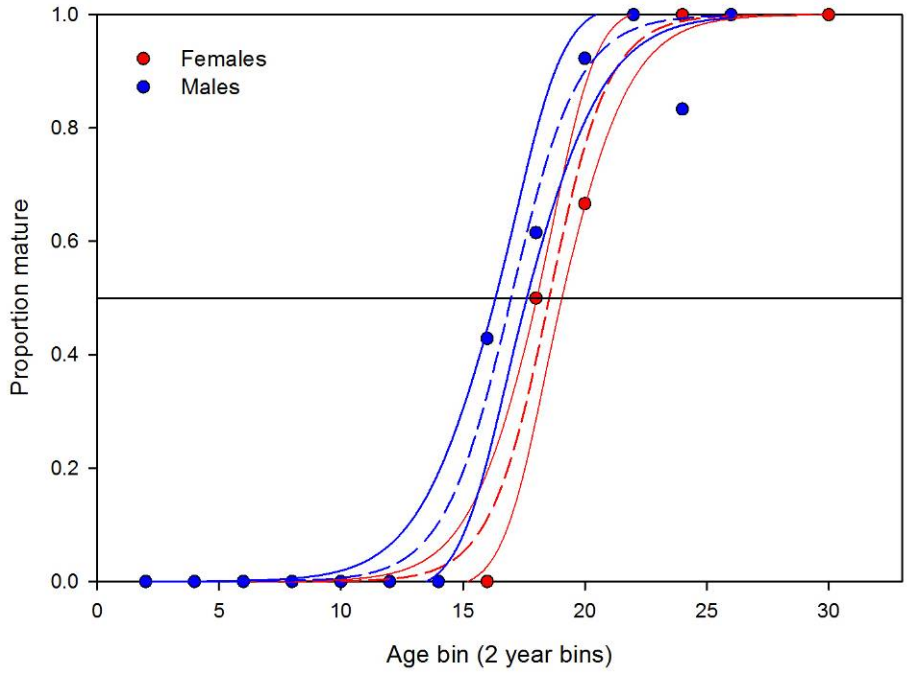

Figure 43.
Estimated median age at maturity for female and male *Bathyraja lindbergi*. Age at 50% maturity corresponds to 18.5 and 16.9 years for females and males respectively.

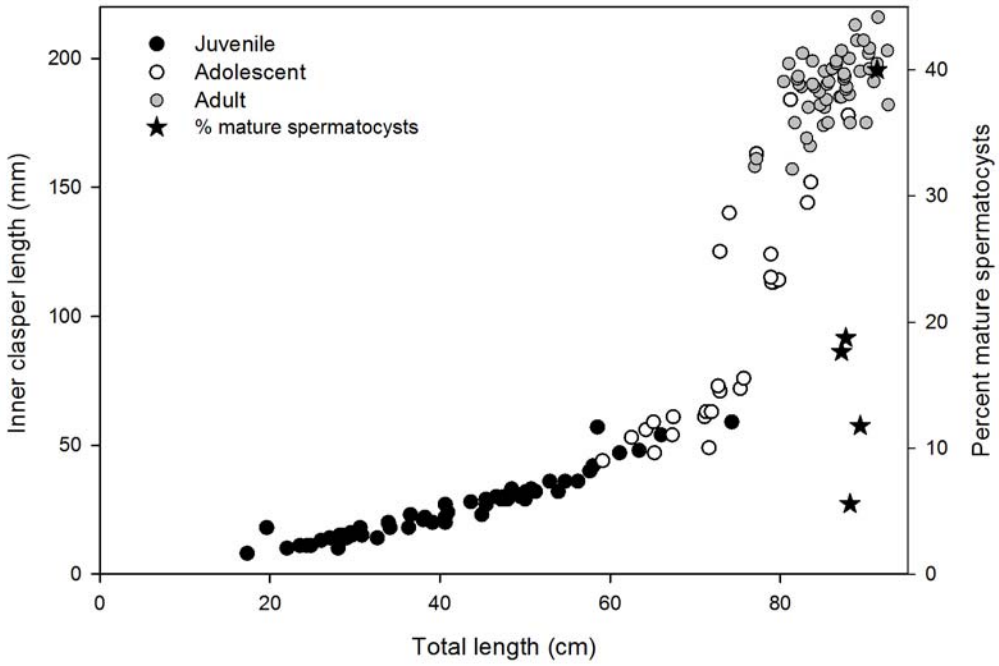

Figure 44.
Relationship between percent mature spermatocysts (n = 5), or inner clasper length (n = 137) based on reproductive classifications of male *Bathyraja lindbergi* and total length.

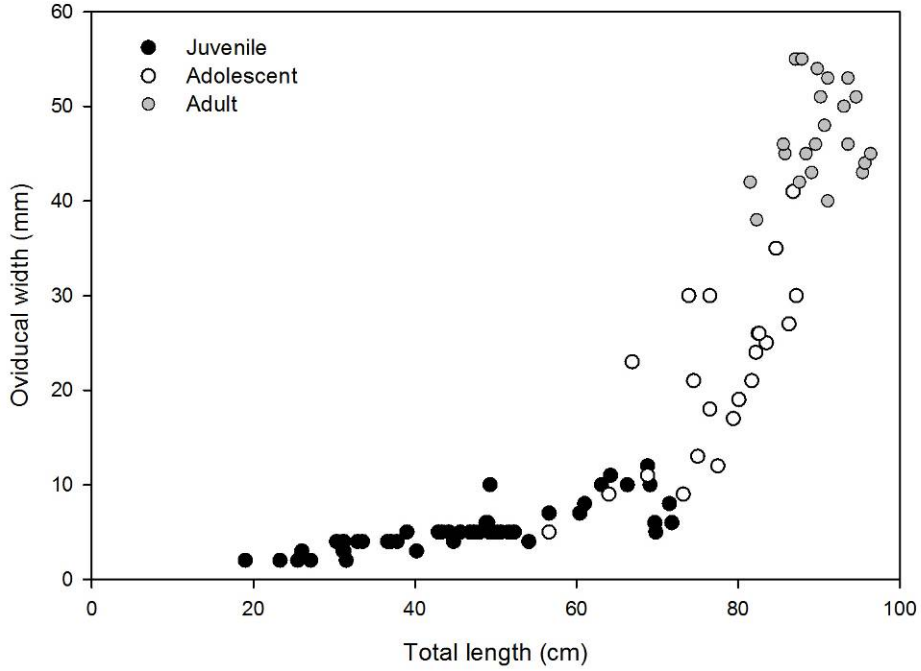

Figure 45.
Relationship between oviducal gland width (n = 95) and total length based on reproductive classifications of female *Bathyraja lindbergi*.

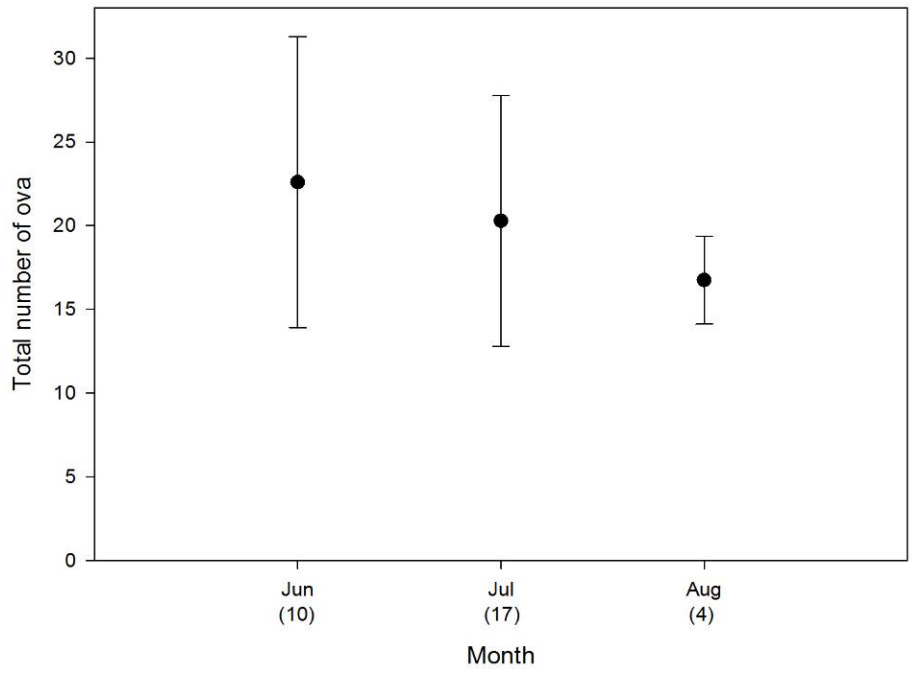

Figure 46.
Relationship between total number of ova (n = 31) and month based on the examinations of mature female *Bathyraja lindbergi*. Sample sizes are depicted below the month in parentheses. Error bars represent ± one standard deviation.

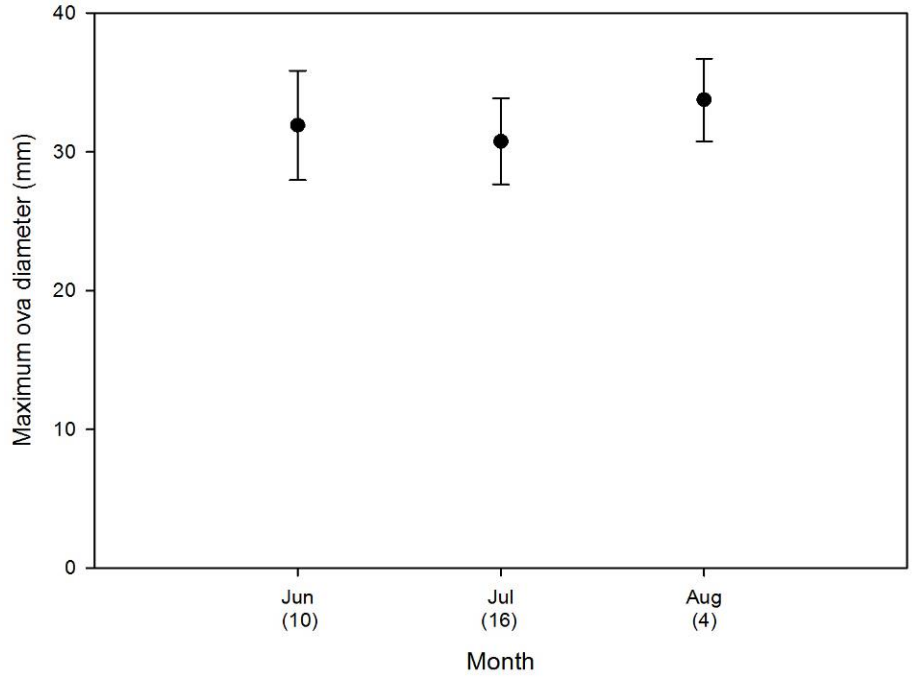

Figure 47.
Relationship between mean maximum ova diameter (n = 30) and month based on the examinations of mature female *Bathyraja lindbergi*. Sample sizes are depicted below the month in parentheses. Error bars represent ± one standard deviation.

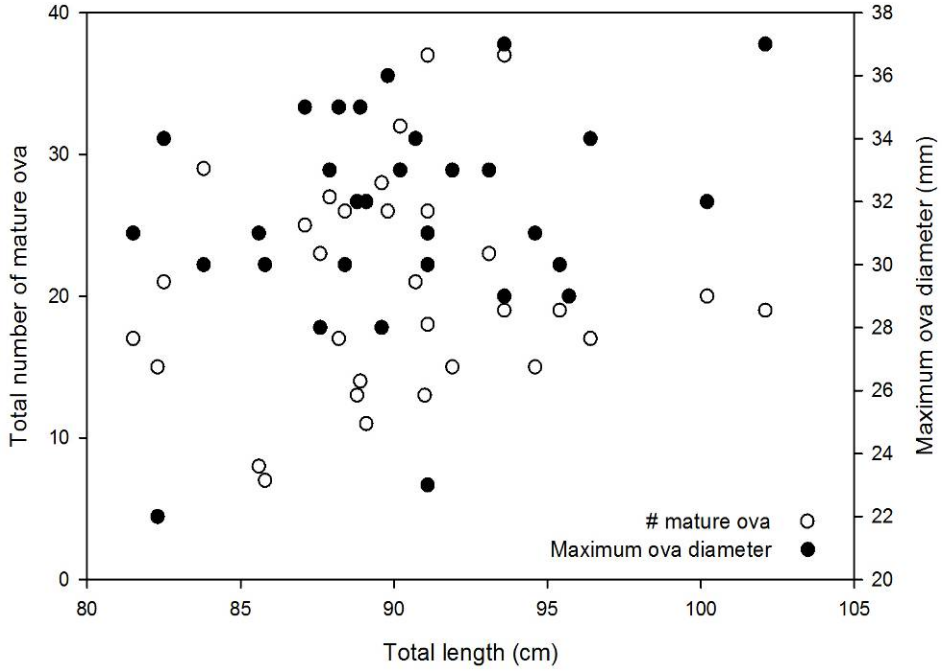

Figure 48.
The relationship between number of mature ova (n = 31) or maximum ova diameter (n = 30) and total length for *Bathyraja lindbergi*.

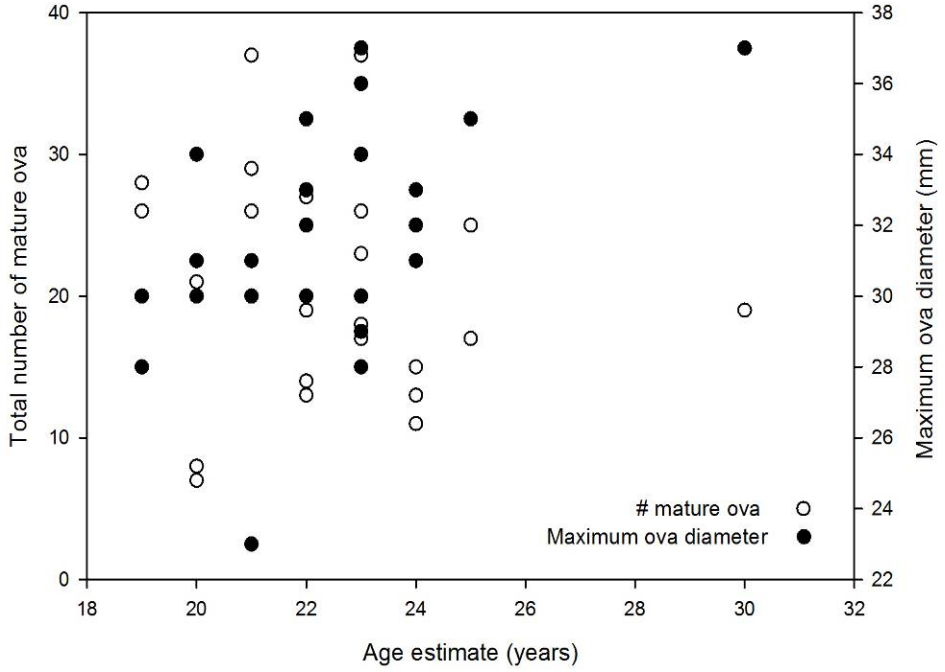

Figure 49.
The relationship between number of mature ova (n = 31) or maximum ova diameter (n = 30) and age estimate for *Bathyraja lindbergi*.

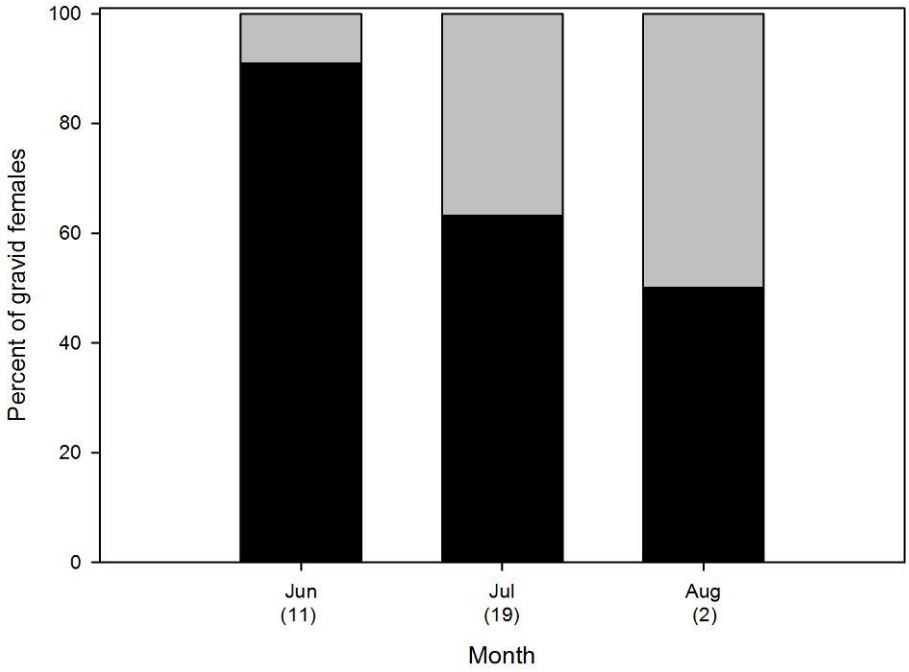

Figure 50.
The percent of gravid *Bathyraja lindbergi* among months sampled. Sample sizes are depicted below the month in parentheses. Black represents the proportion mature; grey represents the proportion gravid.

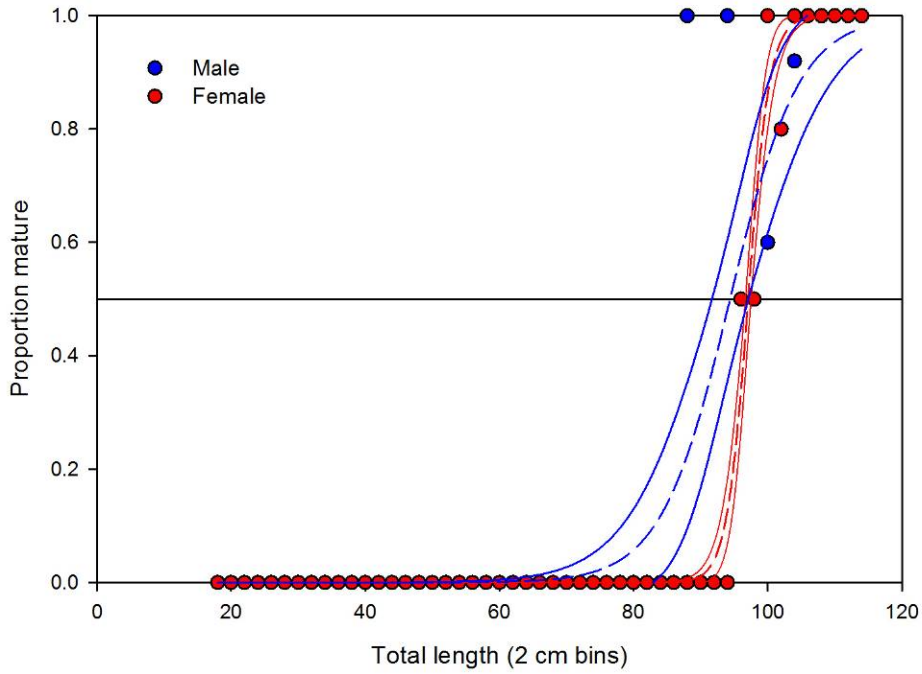

Figure 51.
Estimated median size at maturity for female and male *Bathyraja maculata*. Size at 50% maturity corresponds to 95.5 cm and 92.6 cm total length for females and males respectively.

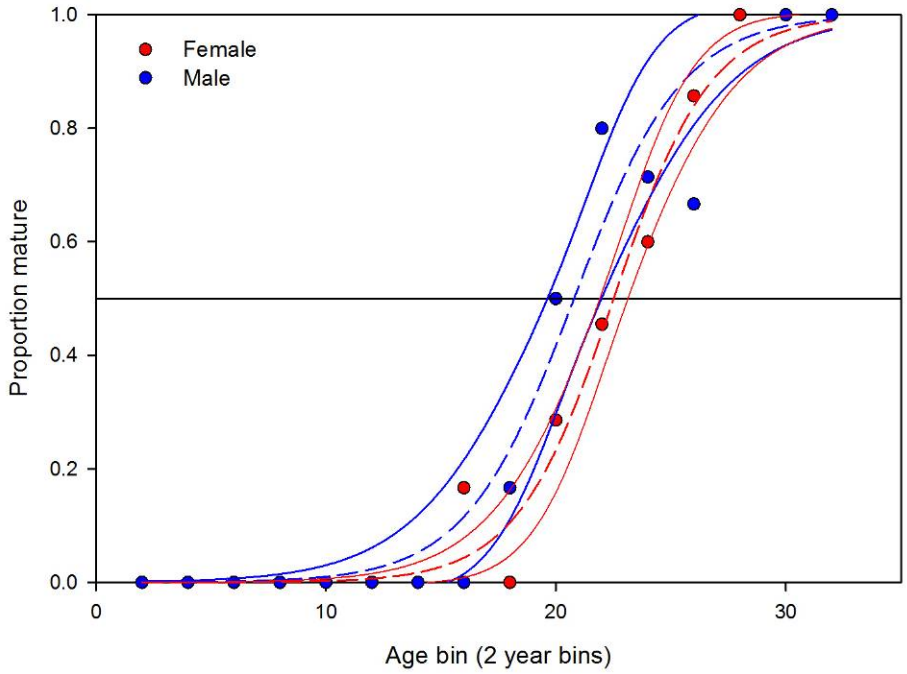

Figure 52.
Estimated median age at maturity for female and male *Bathyraja maculata*. Age at 50% maturity corresponds to 22.5 and 20.7 years for females and males respectively.

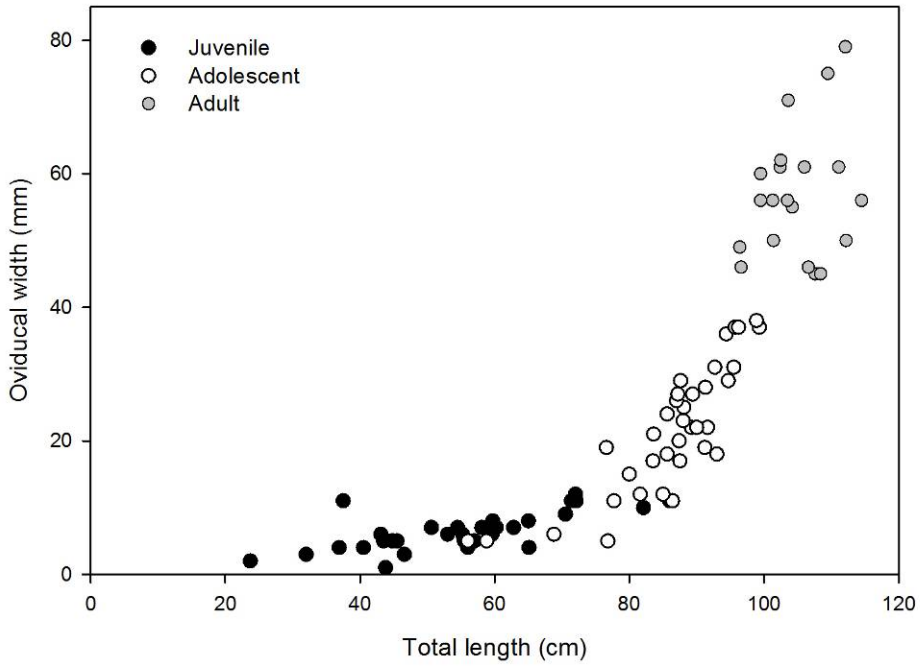

Figure 53.
Relationship between oviducal gland width (n = 88) and total length based on reproductive classifications of female *Bathyraja maculata*.

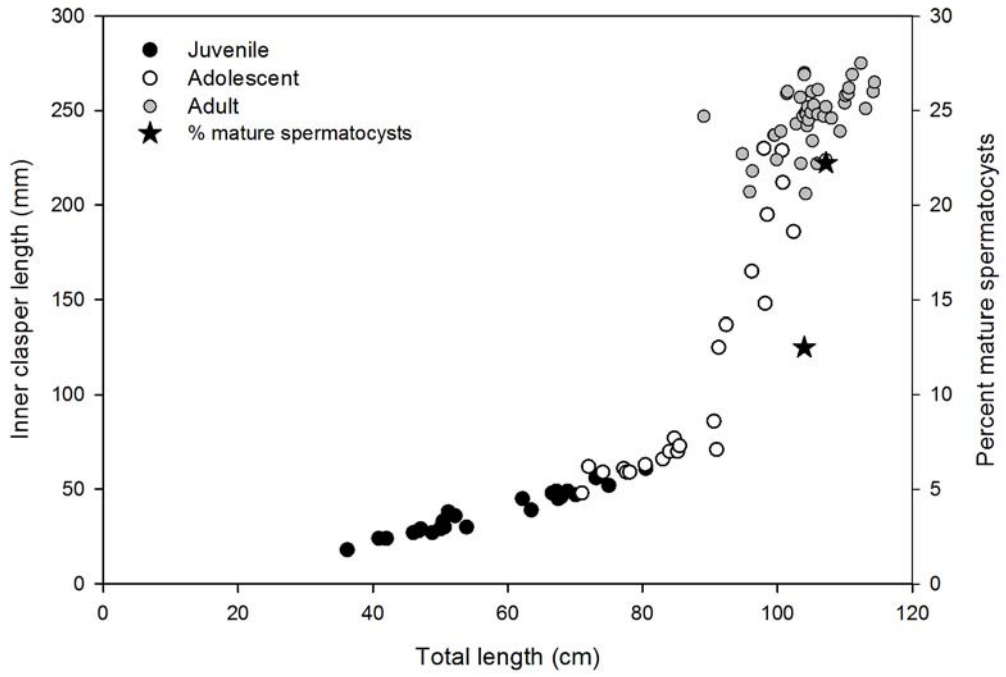

Figure 54.
Relationship between percent mature spermatocysts (n = 2), or inner clasper length (n = 92) based on reproductive classifications of male *Bathyraja maculata* and total length.

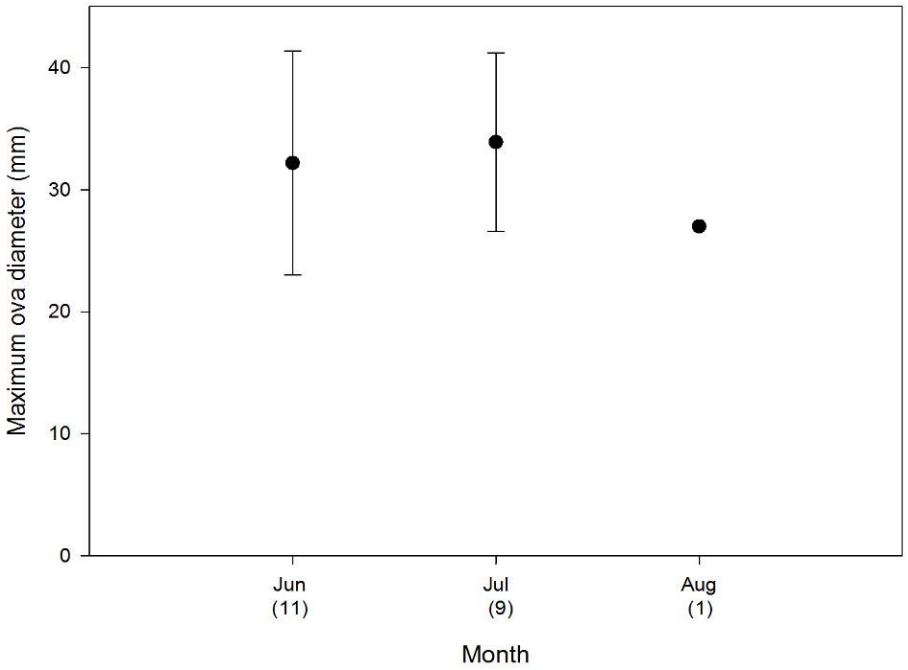

Figure 55.
Relationship between mean maximum ova diameter (n = 21) and month based on the examinations of mature female *Bathyraja maculata*. Sample sizes are depicted below the month in parentheses. Error bars represent ± one standard deviation.

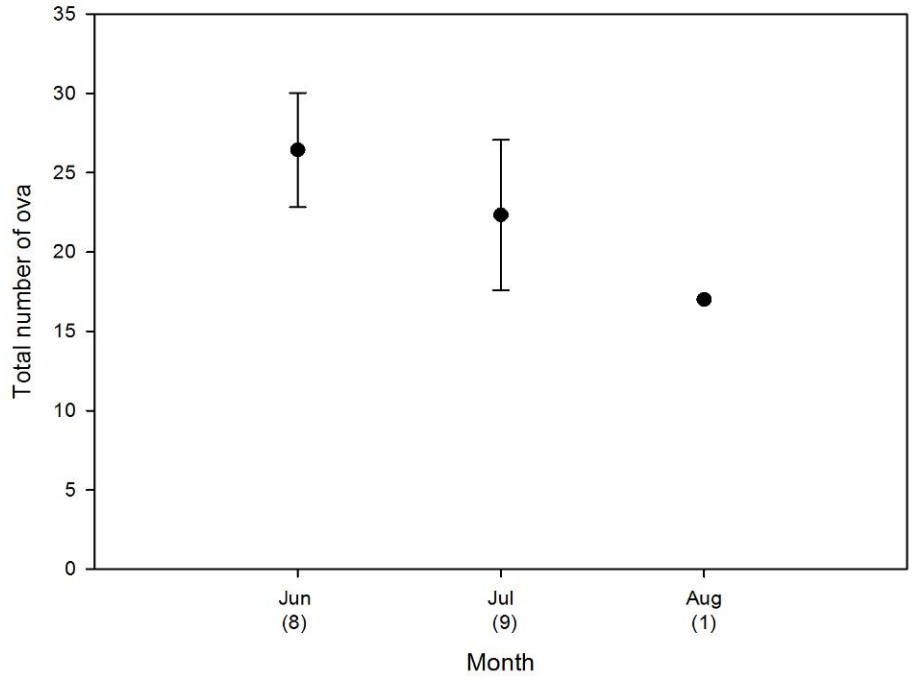

Figure 56.
Relationship between total number of ova (n = 18) and month based on the examinations of mature female *Bathyraja maculata*. Sample sizes are depicted below the month in parentheses. Error bars represent ± one standard deviation.

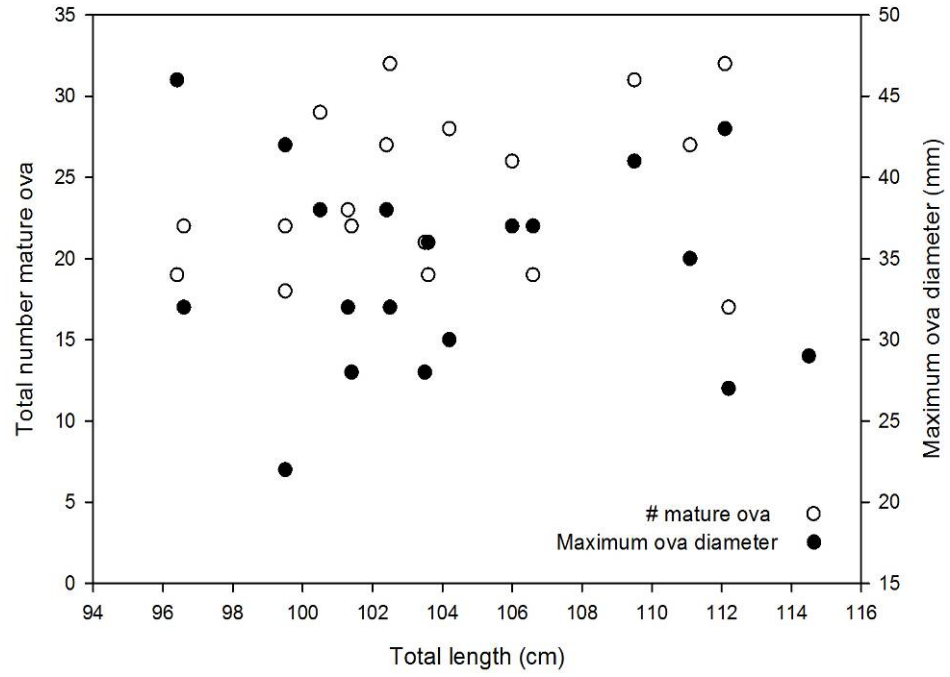

Figure 57.
The relationship between number of mature ova (n = 18) or maximum ova diameter (n = 21) and total length for *Bathyraja maculata***.**

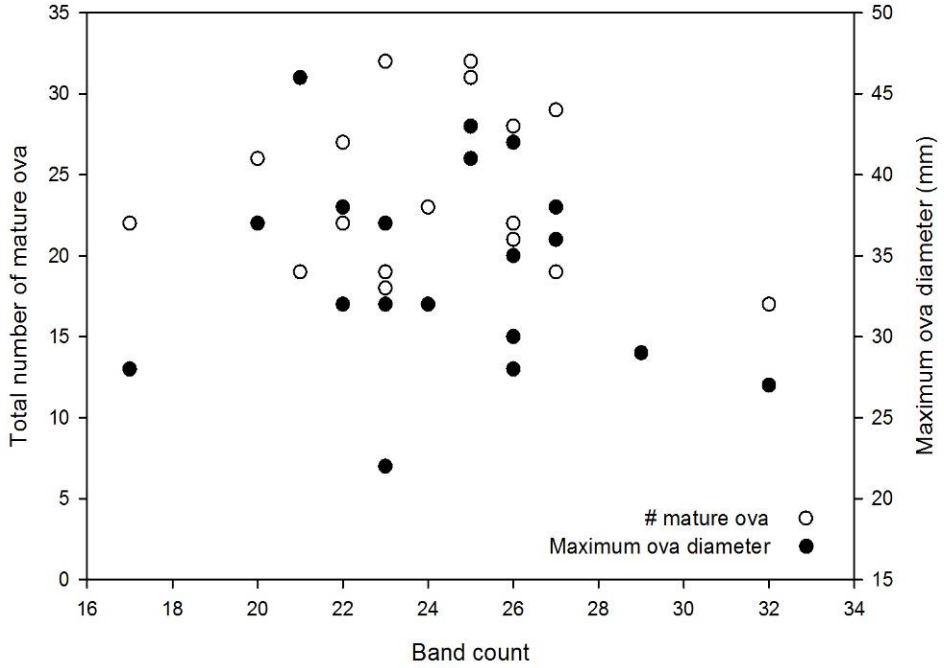

Figure 58.
The relationship between number of mature ova (n = 18) or maximum ova diameter (n = 21) and age for *Bathyraja maculata*.

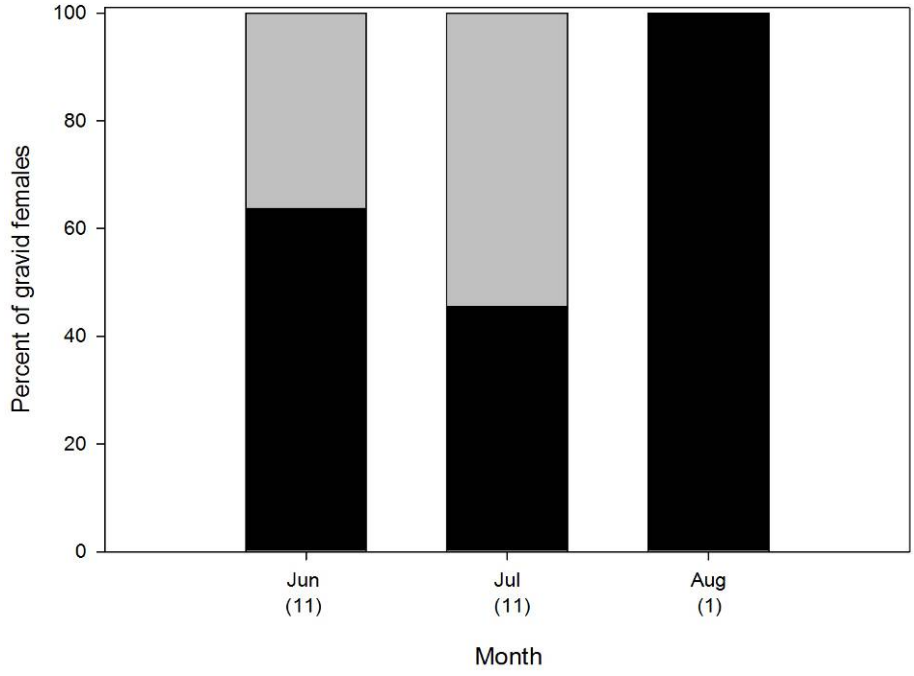

Figure 59.
The percentage of gravid *Bathyraja maculata* among months sampled. Sample sizes are depicted below the month in parentheses. Black represents the proportion mature; grey is the proportion gravid.

Only two testes of *B. maculata* were collected in 2004 both were prepared for histological examination. Both individuals had mature sperm present and were classified as mature males at the time of collection (Fig. 54). Examination of prepared oviducal glands did not show any evidence of sperm storage.

Number of mature ova in the left and right ovaries was not significantly different ($t = -0.911$, $p = 0.368$, $n = 18$). Ova diameter and number of mature ova did not differ among months (ova diameter: $t = -0.453$, $p = 0.656$, $n = 20$; number mature ova: $t = 2.239$, $p = 0.041$, $n = 17$: Figs. 55 & 56).

There was no detectable relationship between TL or age estimate and number of mature ova (TL: $r^2 = 0.034$; age: $r^2 < 0.001$; Figs. 57 & 58) or maximum ova diameter (TL: $r^2 < 0.001$; age: $r^2 < 0.001$ Figs. 57 & 58). A total of 10 gravid females were observed during the summer months, June-August (Fig. 59).

Bathyraja minispinosa. The size at first maturity occurred at 65.7 cm TL for males and 66.8 cm TL for females. The largest immature male was 79.5 cm TL, while the largest immature female was 73.3 cm TL. Male *B. minispinosa* reach TL_{50} at 70.1 cm and females at 67.4 cm (Males: $r^2 = 0.9597$, $p < 0.0001$, $n = 27$; Females: $r^2 = 0.9958$, $p < 0.0001$, $n = 28$; Fig. 60). Male *B. minispinosa* reach median age at maturity (Age_{50}) at 23 years (Males: $r^2 = 0.9535$, $p < 0.0001$, $n = 18$) and females at 23.5 years (Females: $r^2 = 0.9681$, $p < 0.0001$, $n = 19$; Fig. 61).

Inner clasper lengths ranged from 6 mm to 188 mm, with a sharp increase in clasper length at around 68 cm TL for males ($n = 125$; Fig. 62). Oviducal widths ranged from 1 mm to 59 mm with an increase in oviducal width at 65 cm TL for females ($n = 106$; Fig. 63).

While six testes of *B. minispinosa* were collected in 2004 and were prepared for histological examination, only one teste was useful for examining sperm development. The individual had mature sperm present and was classified as a mature male at the time of collection (Fig. 62). Examination of prepared oviducal glands did not show any evidence of sperm storage.

A one-sample Kolmogorov-Smirnov test found the distributions of ova counts in both ovaries of mature females were not significantly different from the normal distribution (Left: $Z = 0.788$, $n = 28$, $p = 0.564$; Right: $Z = 0.682$, $n = 28$, $p = 0.741$). A paired t-test found no significant difference between the mean numbers of mature ova in either ovary (paired $t = 0.143$, $df = 27$, $p = 0.887$). A total of 9 gravid females were encountered throughout the three months of the survey, three in June and six in July (Fig. 64). No difference was detected in number of mature ova among months (ANOVA: $F_{2,27} = 1.373$, $p = 0.272$, $n = 28$; Fig. 65). A significant difference in maximum ovum diameter was found among months (ANOVA: $F_{2,33} = 6.365$, $p = 0.005$, $n = 34$), and a Tukey's HSD post-hoc comparison found the mean maximum ovum diameter to be smaller in July than in June or August (Fig. 66).

No relationship was found between the total number of mature ova and the maternal TL (r^2 = 0.074, P = 0.088; Fig. 67). Additionally, no relationship was found between either the total number of mature ova (r^2 = 0.121, P = 0.223) or the maximum ovum diameter (r^2 = 0.057, P = 0.372) and the maternal age (Fig. 68). While a significant relationship was found between the maximum ovum diameter and maternal TL (r^2 = 0.114, P = 0.031; Fig. 67), with a small sample size and high variability these data do not indicate any biological relevance.

Bathyraja taranetzi. Reproductive data and maturity assessment was obtained for 82 females and 95 males of *B. taranetzi*. The largest immature female was 65.7 cm TL, and the smallest mature female was 62.0 cm TL. Of the males the largest immature individual was 63.3 cm TL and the smallest mature was 57.5 cm TL. Median sizes at maturity were 61.4 and 58.0 cm, for females and males respectively (Fig.69). Corresponding median age at maturity was 9.1 years for females and 9.6 years for males (Fig. 70).

Measurements of inner clasper length ranged from 8 to 180 mm, with a sharp size increase around 40 cm TL (Fig. 71). Oviducal width had a size range of 2 to 47 mm, and increased sharply in size around 51 cm TL (Fig. 72). No testes from *B. taranetzi* males were collected for histological processing.

There was no difference detected between counts of mature ova in the left and right ovaries (t = 649.5, p = 0.205, n = 24). There were only two females collected in August for which mature ova counts and maximum ova size width were available. As such only June and July were tested for difference in ova count and maximum ova count. No difference was detected in number of mature ova among months (t = 0.477, p = 0.66, n = 22; Fig. 73), however there was a significant difference in maximum ova size among months (t = 206.5, p = 0.028, n = 28; Fig. 74).

There was no detectable relationship between TL or age estimate and number of mature ova (TL: $r^2 < 0.001$; age: $r^2 = 0.0825$; Figs. 75 & 76) or maximum ova diameter (TL: $r^2 = 0.0475$; age: $r^2 < 0.001$ Figs. 75 & 76). A total of 9 gravid females were observed during the summer months, June-August (Fig. 77).

Demography

Indirect methods for estimating overall natural mortality rate produced survivorship values ranging from 0.70 to 0.97 (Table 8, 9). Jensen's (1996) methods generally produced the greatest estimates, with the least values predicted from the Campana *et al.* (2001) and Hoenig (1983) methods. The Chen and Watanabe (1989) method predicted some of the least age-specific survivorship probabilities.

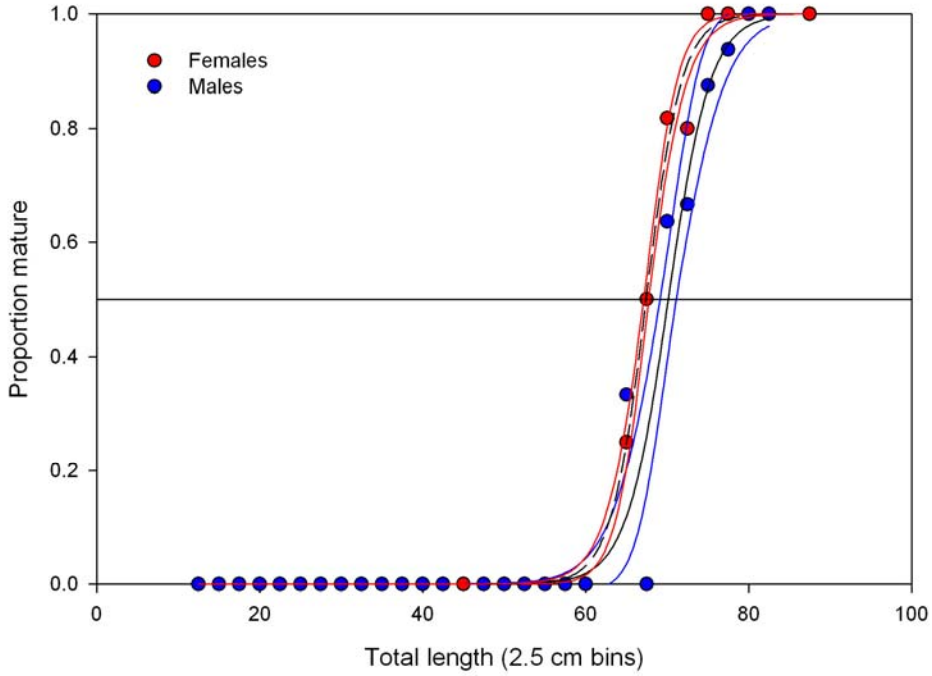

Figure 60.
Estimated median size at maturity for female and male *Bathyraja minispinosa* with 95% confidence intervals shown in red and blue respectively. Size at 50% maturity corresponds to 67.4 cm and 70.1 cm total length for females and males respectively.

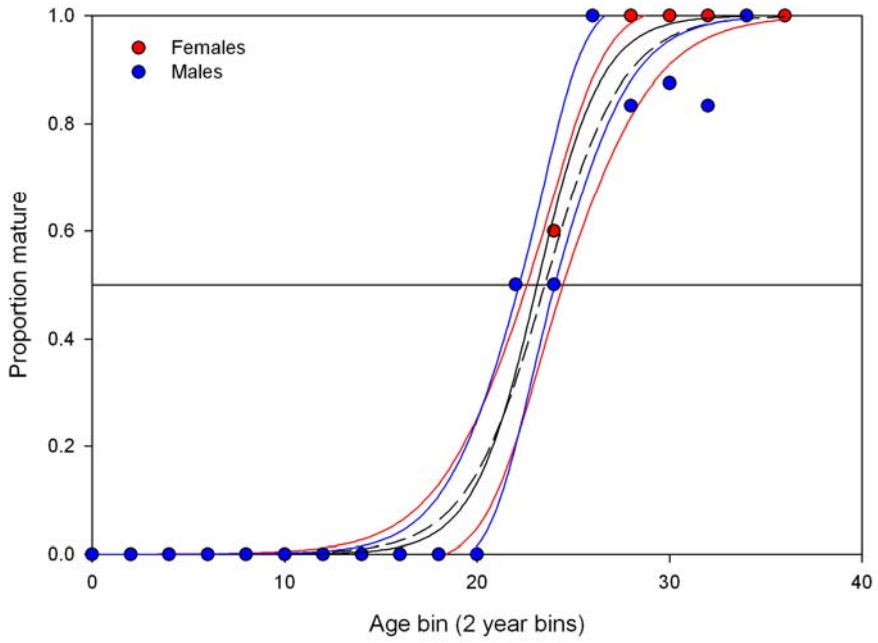

Figure 61.
Estimated median age at maturity for female and male *Bathyraja minispinosa* with 95% confidence intervals shown in red and blue respectively. Age at 50% maturity corresponds to 23.5 and 23.1 years for females and males respectively.

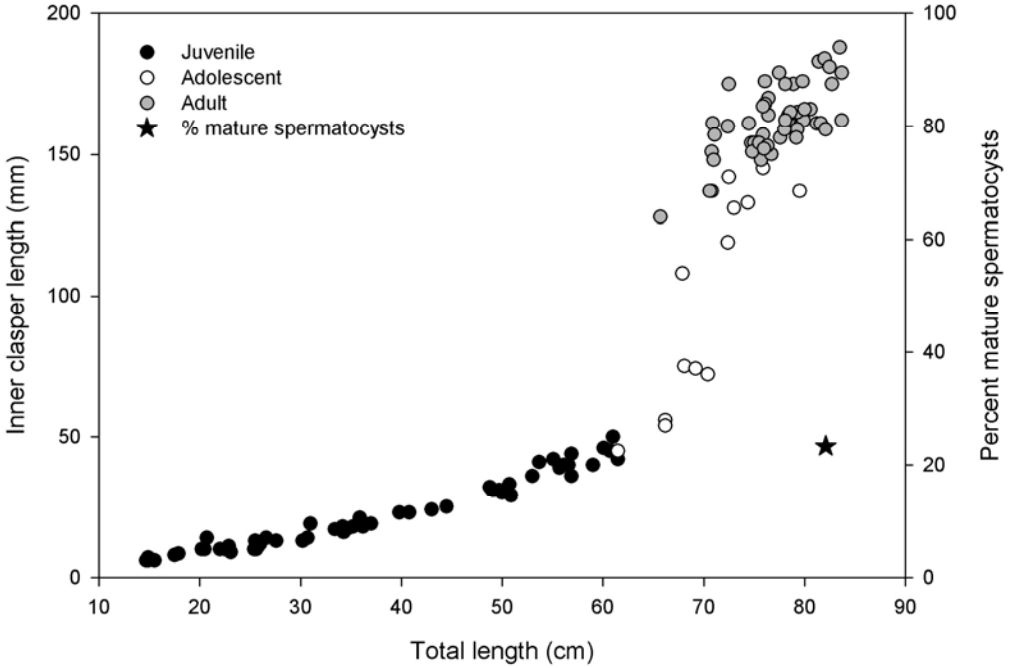

Figure 62.
Relationship between percent mature spermatocysts (n = 1), or inner clasper length (n = 125) based on reproductive classifications of male *Bathyraja minispinosa* and total length.

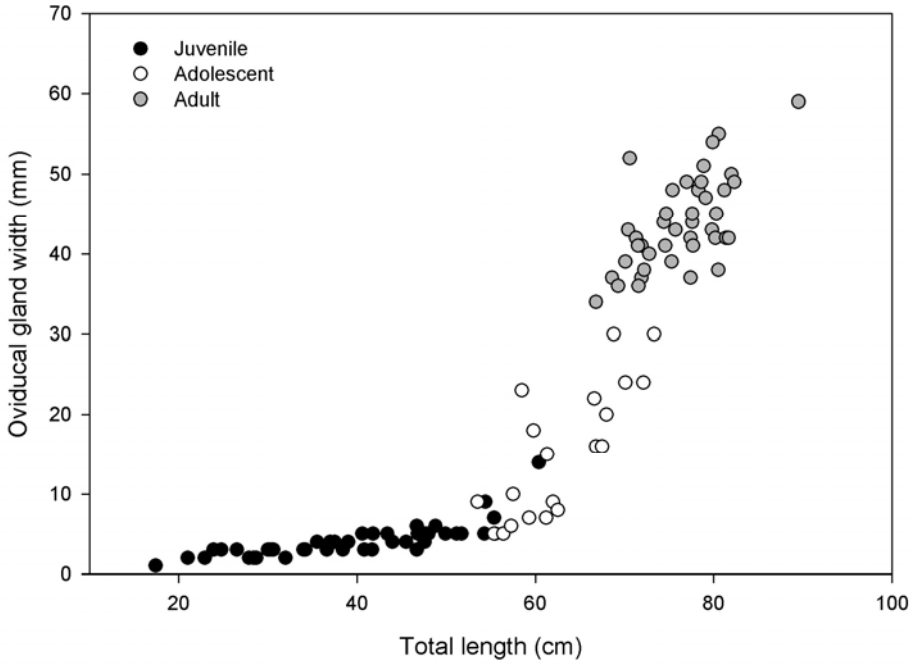

Figure 63.
Relationship between oviducal gland width (n = 106) based on reproductive classifications of female *Bathyraja minispinosa* and total length.

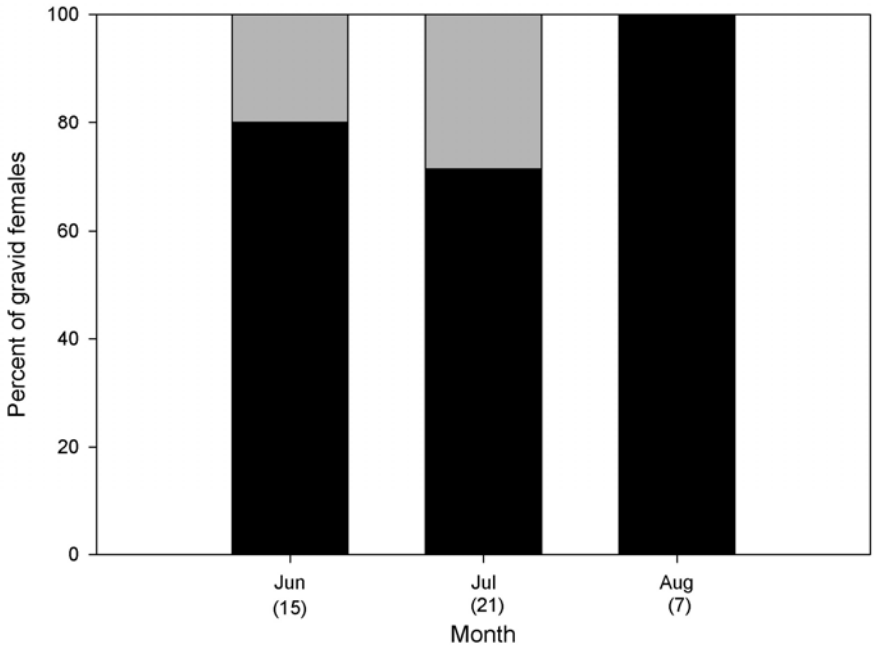

Figure 64.
The percent of gravid *Bathyraja minispinosa* among sampled months. Sample sizes are depicted below the month in parentheses. Black represents the proportion mature; grey represents the proportion gravid.

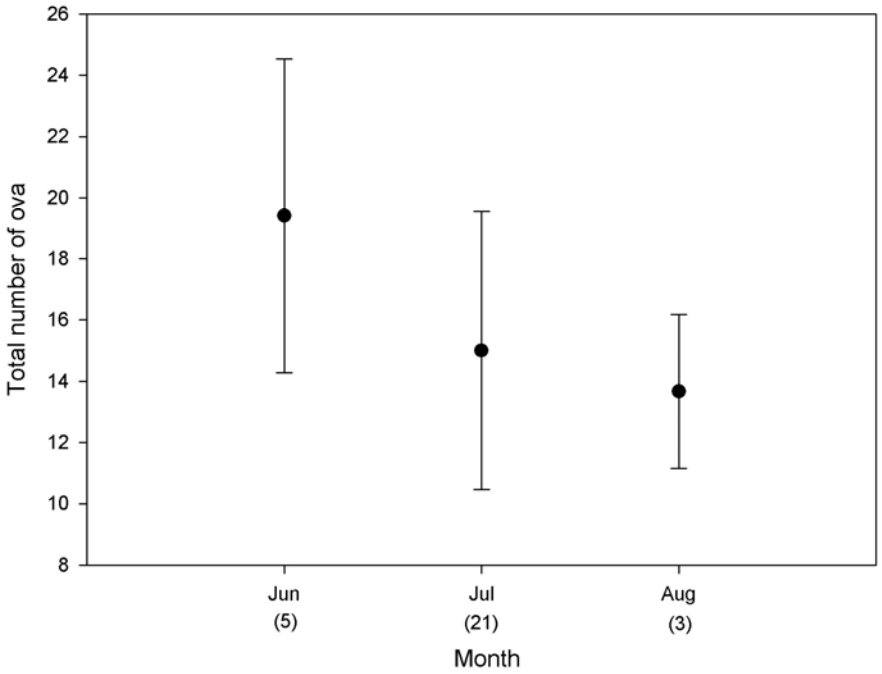

Figure 65.
Relationship between total number of ova (n = 28) and month based on the examinations of mature female *Bathyraja minispinosa*. Sample sizes are depicted below the month in parentheses. Error bars represent ± one standard deviation.

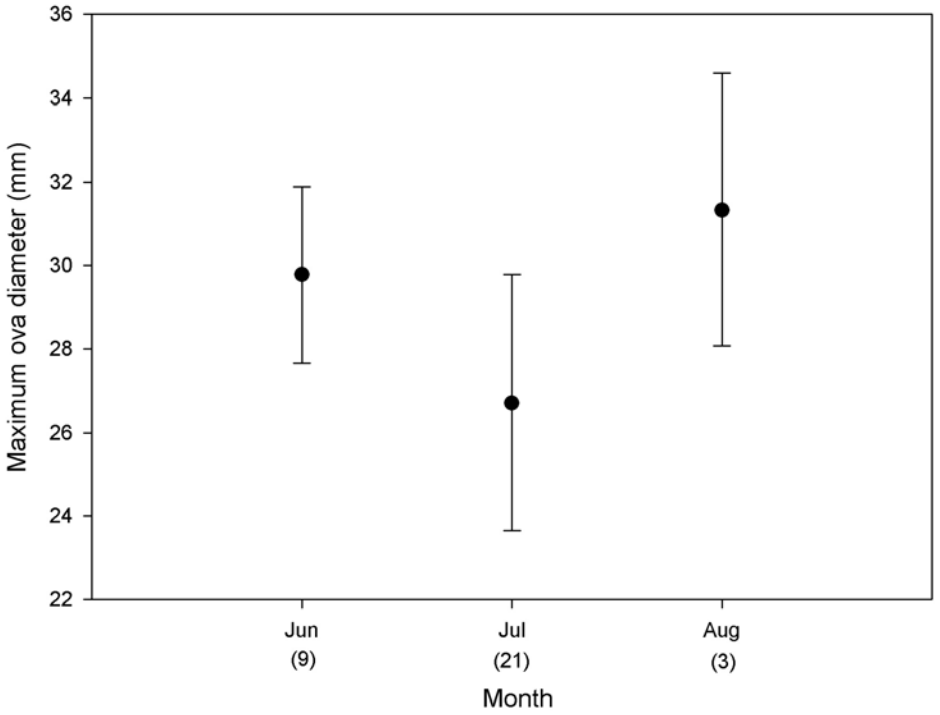

Figure 66.
Relationship between mean maximum ova diameter (n = 34) and month based on the examinations of mature female *Bathyraja minispinosa*. Sample sizes are depicted below the month in parentheses. Error bars represent ± one standard deviation.

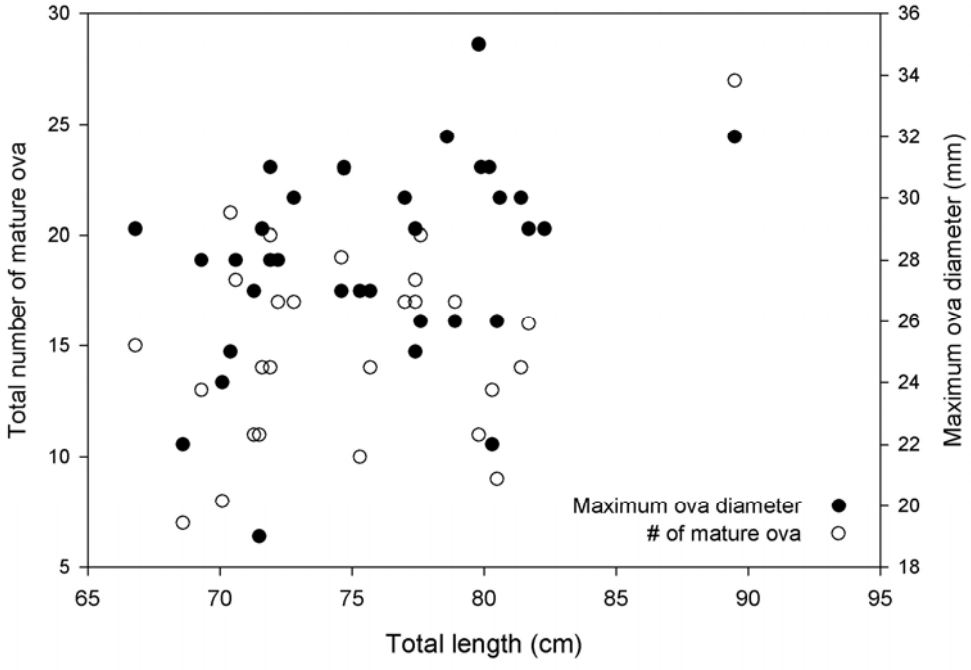

Figure 67.
The relationship between number of mature ova (n = 28) or maximum ova diameter (n = 33) and total length for *Bathyraja minispinosa*.

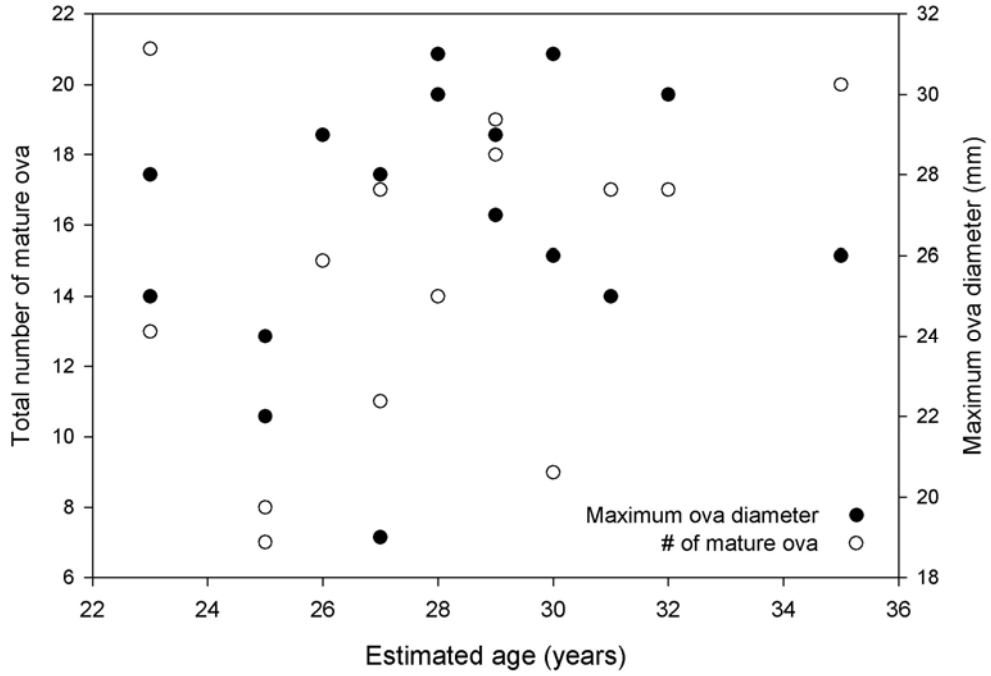

Figure 68.
The relationship between the number of mature ova (n = 14) or maximum ova diameter (n = 16) and age estimate for *Bathyraja minispinosa*.

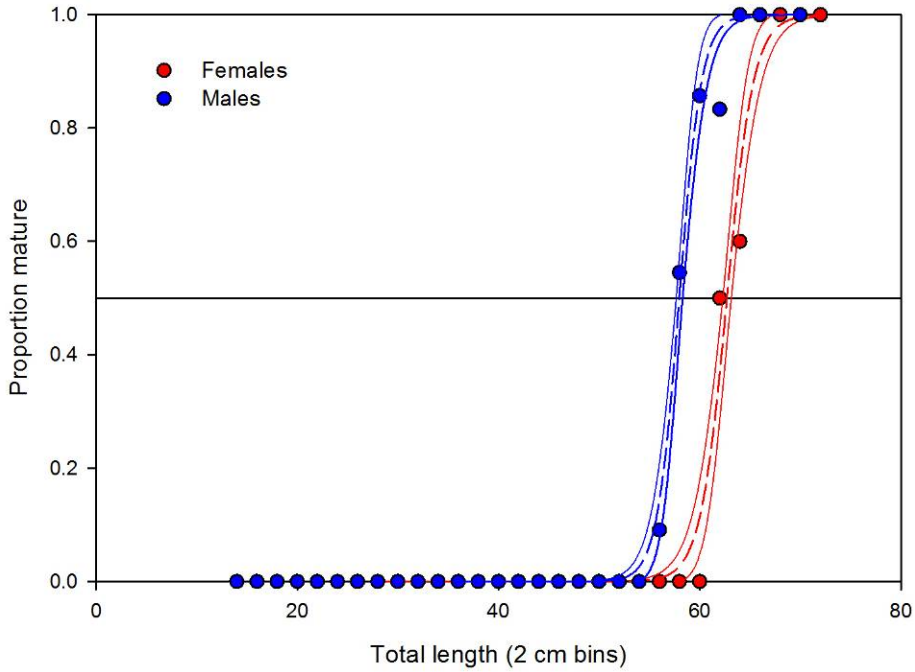

Figure 69.
Estimated median size at maturity for female and male *Bathyraja taranetzi*. Size at 50% maturity corresponds to 62.7 cm and 57.9 cm total length for females and males respectively.

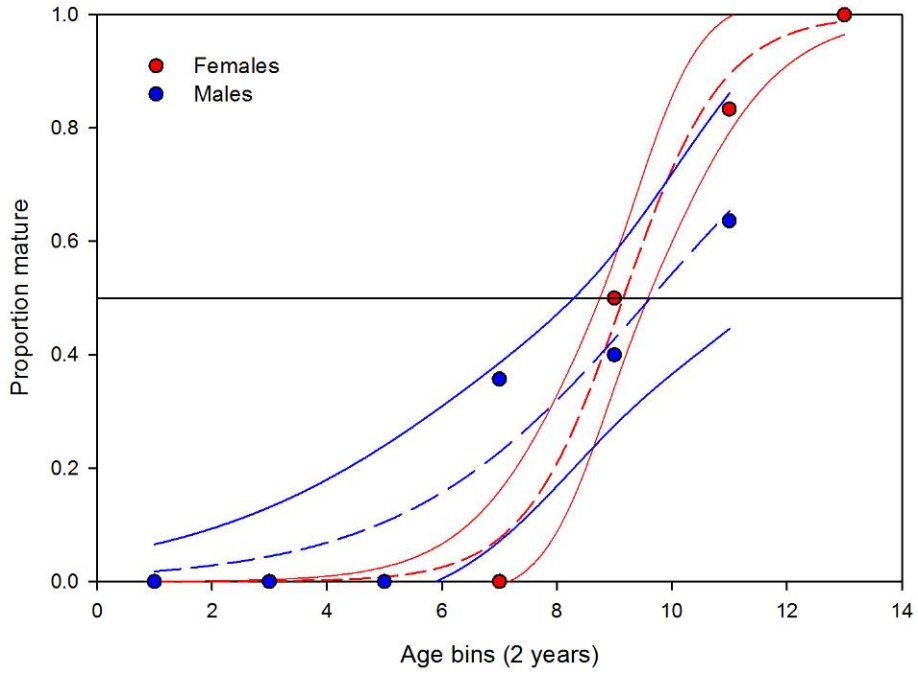

Figure 70.
Estimated median age at maturity for female and male *Bathyraja taranetzi*. Age at 50% maturity corresponds to 9.2 and 9.6 years for females and males respectively.

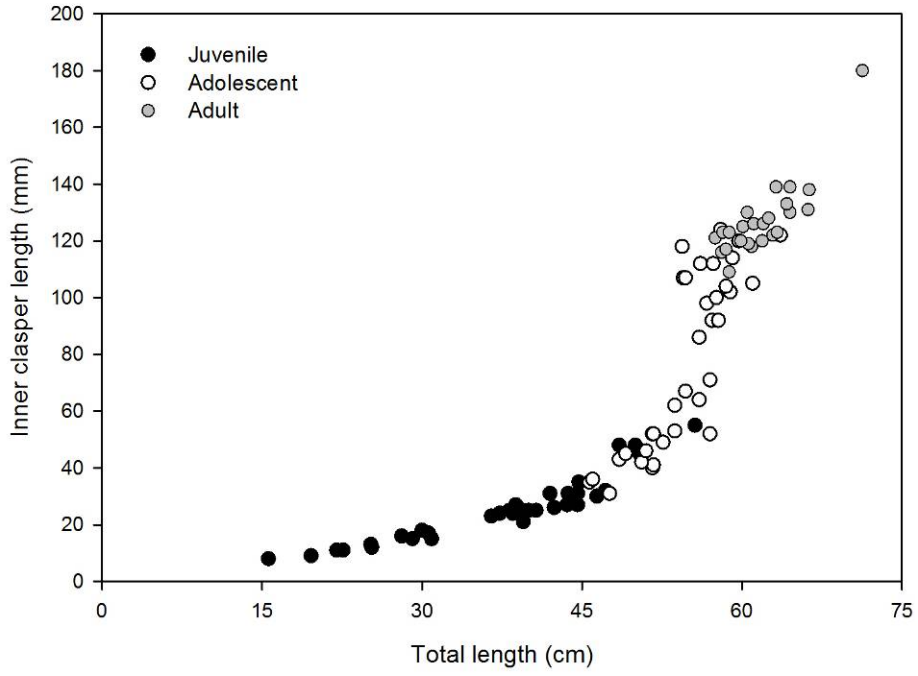

Figure 71.
Relationship between inner clasper length (n = 94) and total length based on reproductive classifications of male *Bathyraja taranetzi*.

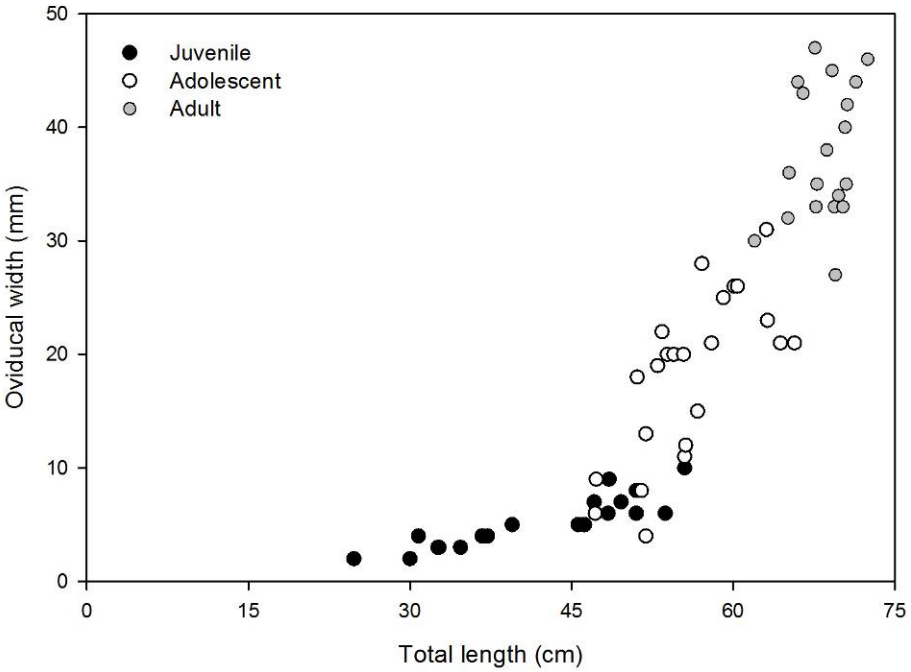

Figure 72.
Relationship between oviducal gland width (n = 62) and total length based on reproductive classifications of female *Bathyraja taranetzi*.

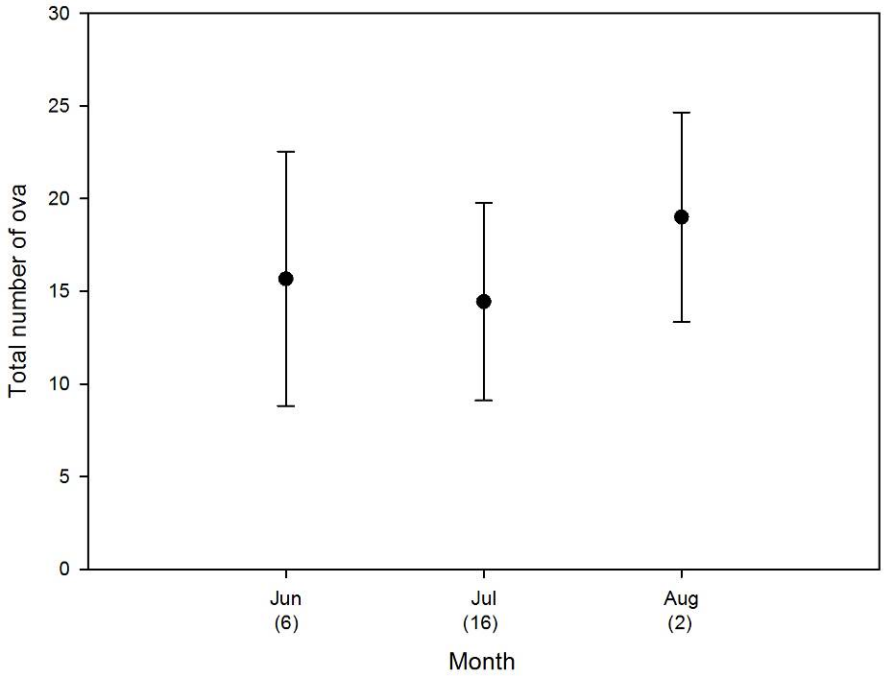

Figure 73.
Relationship between total number of ova (n = 24) and month based on the examinations of mature female *Bathyraja taranetzi*. Sample sizes are depicted below the month in parentheses. Error bars represent ± one standard deviation.

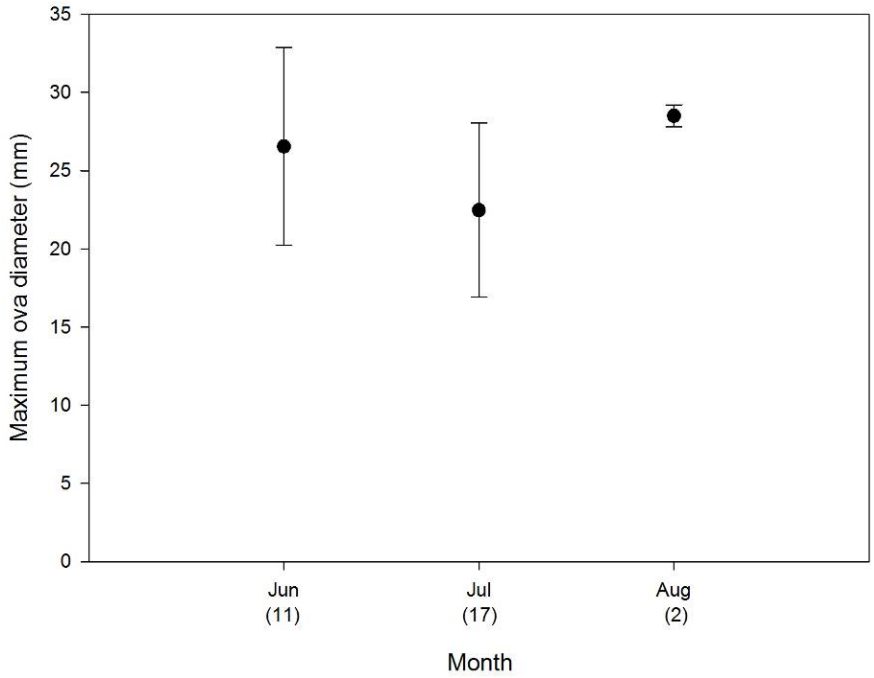

Figure 74.
Relationship between mean maximum ova diameter (n = 30) and month based on the examinations of mature female *Bathyraja taranetzi*. Sample sizes are depicted below the month in parentheses. Error bars represent ± one standard deviation.

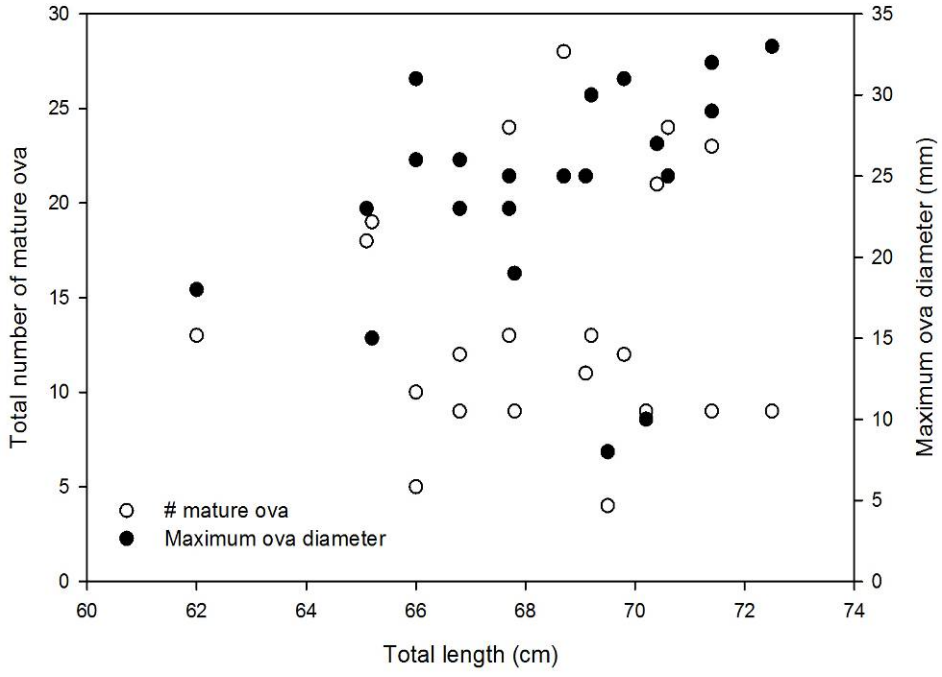

Figure 75.
The relationship between number of mature ova (*n* = 24) or maximum ova diameter (*n* = 30) and total length for *Bathyraja taranetzi*.

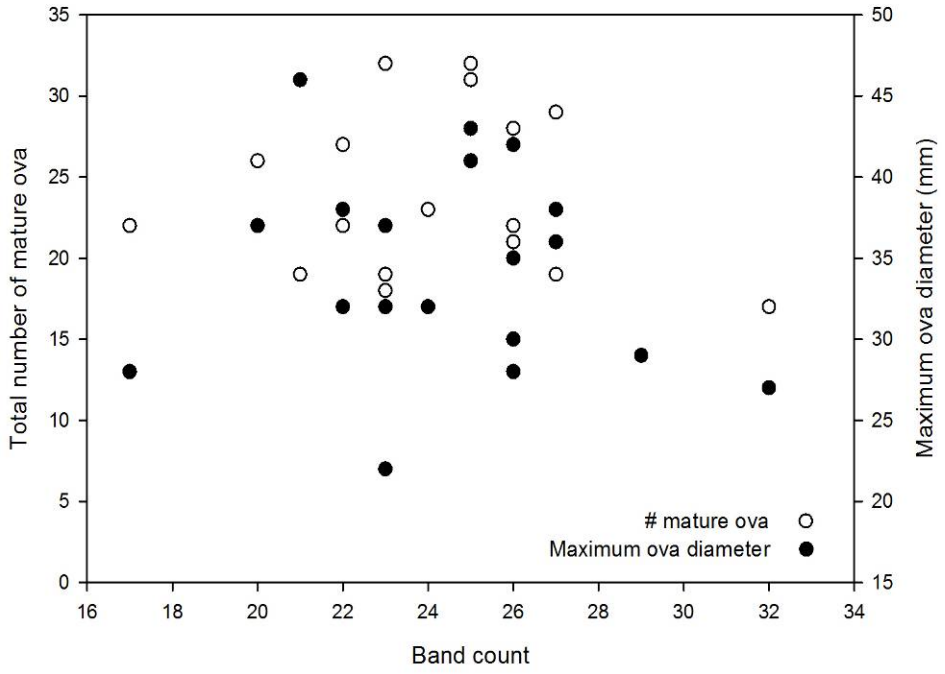

Figure 76.

The relationship between number of mature ova (n = 24) or maximum ova diameter (n = 30) and age for *Bathyraja taranetzi*.

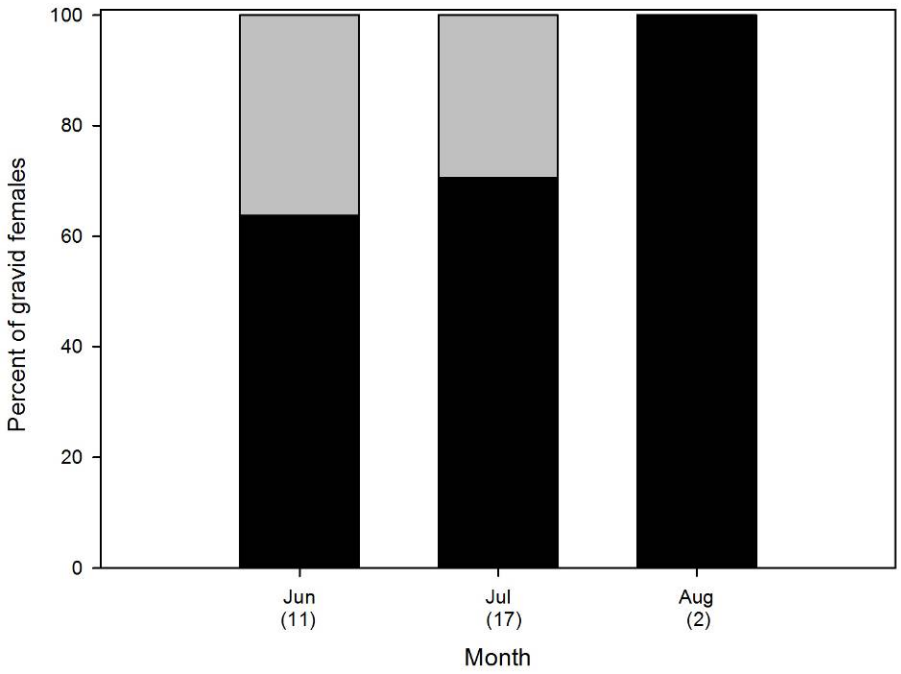

Figure 77.

The percent of gravid *Bathyraja taranetzi* among sampled months. Sample sizes are depicted below the month in parentheses. Black represents the proportion mature; grey is the proportion gravid.

The projected finite rates of population increase (λ) were similar among species (Table 10). Mean λ ranged from 1.08 (*B. maculata*) to 1.12 (*B. taranetzi*), with lower confidence limits greater than 1.05 for all species. Population growth rates were more sensitive to variation in α than any other parameter, with only minor changes in response to variation in longevity (Fig. 78). Mean $\overline{A}$ differed among all species, with *B. minispinosa*, *B. maculata*, *B. lindbergi*, and *B. taranetzi* in decreasing order. Mean μ_1 was lesser in *B. lindbergi* than *B. minispinosa*, and least in *B. taranetzi*. Means of rT and R_0 were least for *B. taranetzi*, but similar among all other species.

Juvenile survival had the greatest elasticity value for all species. Fertility had the least elasticity for all species. Adult survival to juvenile survival elasticity ratios was similar among species. The adult survival to fertility elasticity ratio was least in *B. taranetzi*, and similar among all other species. Juvenile survival to fertility ratios differed among all species, with *B. minispinosa*, *B. maculata*, *B. lindbergi*, and *B. taranetzi* in decreasing order.

Mean age-specific reproductive values (V_x) increased with increasing rate until approximately age at maturity, thereafter decreasing with increasing rate. Variability in V_x increased throughout the lifespan. *B. lindbergi* were most prolific at age 19, when they were expected to produce 137 female offspring, and their reproductive output decreased gradually with increasing age (Fig. 79). *B. maculata* had a more ephemeral period of maximum reproductive output than *B. lindbergi*, reaching an average of 151 female offspring by age 23, then rapidly decreasing to zero by age 35 (Fig. 80). *B. minispinosa* obtained a greater maximum reproductive value than any other species, 195 female offspring at age 24 (Fig. 81). *B. taranetzi* had lesser average reproductive output than any other species, increasing nearly linearly to an average of just 72 at age 9, and subsequently decreasing nearly linearly to an average of zero at age 15 (Fig. 82).

Discussion

Age determination

Several studies have investigated the utility of caudal thorns as an ageing structure in bathyrajid skates with varied results (Gallagher and Nolan 1999, Perez 2005, Davis et al. 2007, Ebert el al. 2007, Matta and Gunderson 2007, Serra-Pereira et al. 2008). For this study it was assumed that caudal thorns were present at the time of hatching and not replaced during an individual's life. *Bathyraja lindbergi* caudal thorns and vertebral centra increased in size proportional to TL. Thorn dimensions showed greater variability than vertebral centra with increasing TL. Caudal thorn age estimates were consistently lower than vertebral age estimates, with a maximum difference of 22 years. Similarly caudal thorns of

Method	*Bathyraja lindbergi*		*Bathyraja maculata*		*Bathyraja minspinosa*		*Bathyraja taranetzi*	
	M (year^{-1})	S_x (year^{-1})	M (year^{-1})	S_x (year^{-1})	M (year^{-1})	S_x (year^{-1})	M (year^{-1})	S_x (year^{-1})
Hoenig (1983)								
1. $\ln M = 1.46 - 1.010 \ln \omega$	0.13	0.88	0.13	0.88	0.12	0.89	0.30	0.74
2. $\ln M = 1.44 - 0.982 \ln \omega$	0.14	0.87	0.14	0.87	0.13	0.88	0.32	0.73
Jensen (1996)								
3. $M = 1.65/\alpha$	0.09	0.91	0.07	0.93	0.07	0.93	0.18	0.84
4. $M = 1.50k$	0.06	0.94	0.05	0.95	0.03	0.97	0.17	0.85
5. $M = 1.60k$	0.07	0.94	0.05	0.95	0.03	0.97	0.18	0.84
Campana *et al.* (2001)								
6. $M = -\ln 0.01/\omega$	0.14	0.87	0.14	0.87	0.13	0.88	0.33	0.72

Table 8.

Indirect estimates of overall natural mortality (M) and annual survival (S_x, where $S_x = \ln M$) used to parameterize demographic models in this study. The parameter k in the Jensen (1996) equations is the growth coefficient from a three-parameter von Bertalanffy growth function.

Age	*Bathyraja lindbergi*		*Bathyraja maculata*		*Bathyraja minspinosa*		*Bathyraja taranetzi*	
	M (year^{-1})	S_x (year^{-1})	M (year^{-1})	S_x (year^{-1})	M (year^{-1})	S_x (year^{-1})	M (year^{-1})	S_x (year^{-1})
0	0.26	0.77	0.24	0.78	0.18	0.83	0.51	0.60
1	0.21	0.81	0.20	0.82	0.16	0.85	0.37	0.69
2	0.18	0.83	0.17	0.84	0.14	0.87	0.30	0.74
3	0.16	0.85	0.15	0.86	0.12	0.88	0.25	0.78
4	0.14	0.87	0.14	0.87	0.11	0.89	0.22	0.80
5	0.13	0.88	0.12	0.88	0.10	0.90	0.20	0.82
6	0.12	0.89	0.11	0.89	0.10	0.91	0.19	0.83
7	0.11	0.89	0.11	0.90	0.09	0.91	0.17	0.84
8	0.10	0.90	0.10	0.91	0.08	0.92	0.16	0.85
9	0.10	0.91	0.09	0.91	0.08	0.92	0.16	0.86
10	0.09	0.91	0.09	0.92	0.07	0.93	0.15	0.86
11	0.09	0.92	0.08	0.92	0.07	0.93	0.14	0.87
12	0.08	0.92	0.08	0.92	0.07	0.93	0.14	0.87
13	0.08	0.92	0.08	0.93	0.06	0.94	0.08	0.92
14	0.08	0.92	0.07	0.93	0.06	0.94	0.08	0.92
15	0.08	0.93	0.07	0.93	0.06	0.94	0.08	0.92
16	0.07	0.93	0.07	0.93	0.06	0.94	0.09	0.92
17	0.07	0.93	0.07	0.94	0.06	0.95	0.10	0.91
18	0.07	0.93	0.06	0.94	0.05	0.95	0.11	0.89
19	0.07	0.94	0.06	0.94	0.05	0.95	0.15	0.86
20	0.07	0.94	0.06	0.94	0.05	0.95	0.27	0.76
21	0.06	0.94	0.06	0.94	0.05	0.95		
22	0.06	0.94	0.06	0.94	0.05	0.95		
23	0.06	0.94	0.06	0.95	0.05	0.95		
24	0.06	0.94	0.06	0.95	0.04	0.96		
25	0.06	0.94	0.05	0.95	0.04	0.96		
26	0.06	0.94	0.05	0.95	0.04	0.96		
27	0.06	0.94	0.05	0.95	0.04	0.96		
28	0.06	0.95	0.05	0.95	0.04	0.96		
29	0.06	0.95	0.05	0.95	0.04	0.96		
30	0.05	0.95	0.05	0.95	0.04	0.96		
31	0.05	0.95	0.05	0.95	0.04	0.96		
32	0.05	0.95	0.05	0.95	0.04	0.96		
33	0.05	0.95	0.05	0.95	0.04	0.96		
34	0.05	0.95	0.05	0.95	0.04	0.96		
35	0.05	0.95	0.05	0.95	0.04	0.96		
36	0.05	0.95	0.05	0.96	0.04	0.96		
37	0.05	0.95	0.05	0.96	0.04	0.97		
38	0.05	0.95	0.04	0.96	0.03	0.97		
39	0.05	0.95	0.04	0.96	0.03	0.97		
40	0.06	0.94	0.04	0.96	0.03	0.97		
41	0.07	0.94	0.04	0.96	0.03	0.97		
42	0.07	0.93	0.04	0.96	0.03	0.97		
43	0.09	0.92	0.04	0.96	0.03	0.97		
44	0.11	0.89	0.04	0.96	0.03	0.97		
45	0.16	0.85	0.04	0.96	0.03	0.97		
46	0.31	0.74	0.04	0.96	0.03	0.97		
47					0.03	0.97		
48					0.03	0.97		
49					0.03	0.97		
50					0.03	0.97		
51					0.03	0.97		
52					0.03	0.97		

Table 9.

Age-specific estimates of natural mortality (M) and annual survival (S_x, where $S_x = \ln M$) used to parameterize demographic models in this study. Calculations follow Chen and Watanabe (1989).

		λ	R_0	rT	$t_{\times 2}$	μ_1	$\overline{A}$
	2.5%	1.090	8.51	2.04	2.78	23.71	21.54
Bathyraja lindbergi	50.0%	1.112	13.00	2.48	2.93	25.21	22.49
	97.5%	1.132	18.95	2.91	3.15	27.35	24.35
	2.5%	1.063	5.45	1.57	3.04	26.64	24.71
Bathyraja maculata	50.0%	1.081	8.89	2.05	3.24	28.42	26.30
	97.5%	1.100	13.99	2.54	3.49	30.79	28.08
	2.5%	1.080	10.46	2.25	2.92	29.27	27.32
Bathyraja minispinosa	50.0%	1.097	16.47	2.73	3.07	31.23	28.74
	97.5%	1.114	25.10	3.22	3.25	33.93	30.60
	2.5%	1.063	2.13	0.60	2.55	11.30	9.31
Bathyraja taranetzi	50.0%	1.120	3.91	1.14	2.87	12.21	10.35
	97.5%	1.170	6.33	1.60	3.49	13.47	11.52

Table 10.
Predicted means (50th percentiles) and 95% confidence intervals (range bounded by upper 2.5th and lower 97.5th percentiles) of finite annual rates of population growth (λ), net reproductive rates (R_0), rates of increase per generation rT, theoretical population doubling times ($t_{\times 2}$), mean ages of females generating offspring produced by a cohort during its lifetime (μ_1), and mean ages of females generating offspring produced by a population at the stable-age distribution ($\overline{A}$). Values were estimated from 5000 Monte Carlo simulations.

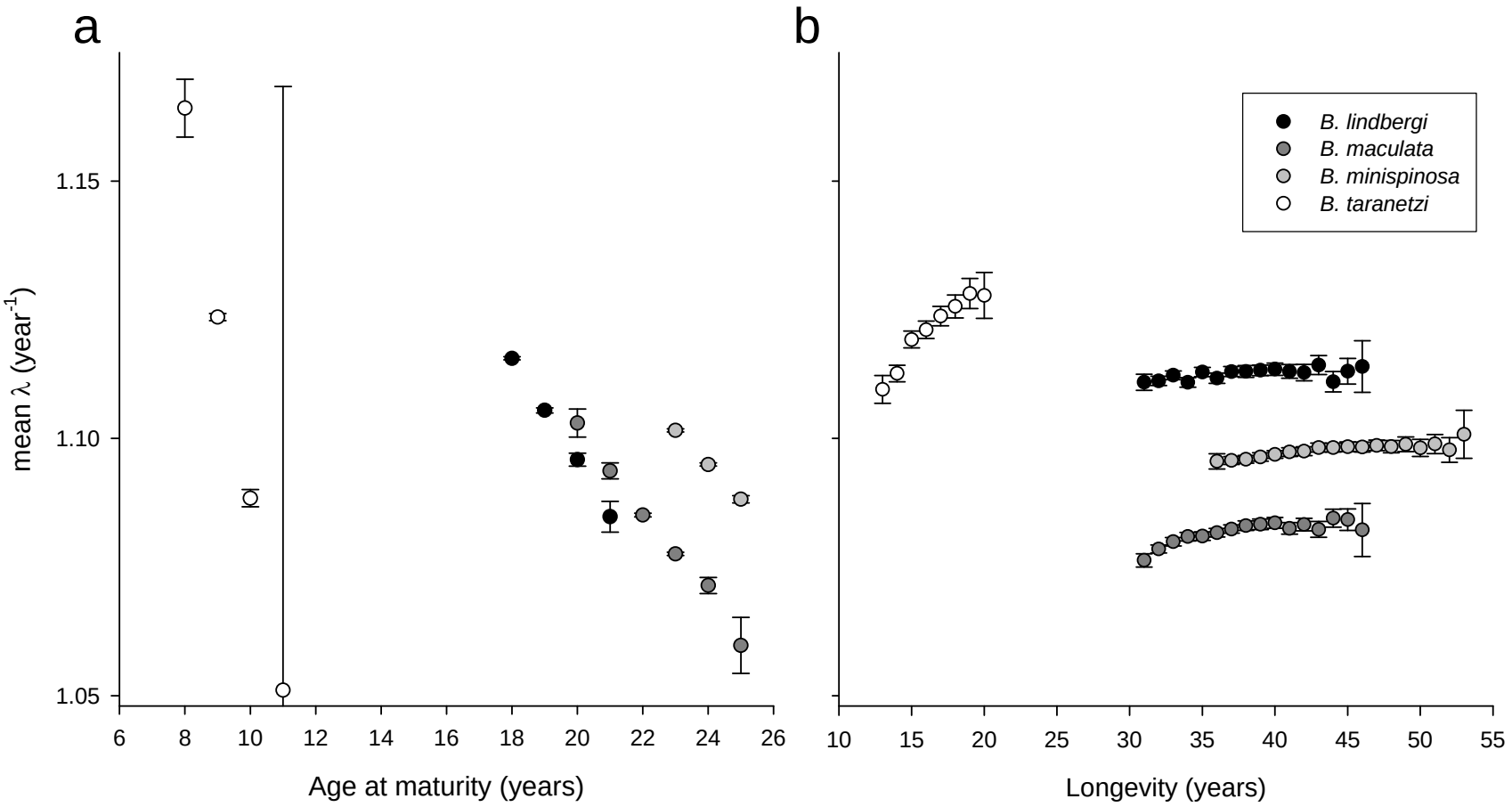

Figure 78.

Mean finite rates of population growth (λ) predicted from 5,000 Monte Carlo simulations by (a) age at maturity and (b) longevity. Error bars indicate 95% confidence interval.

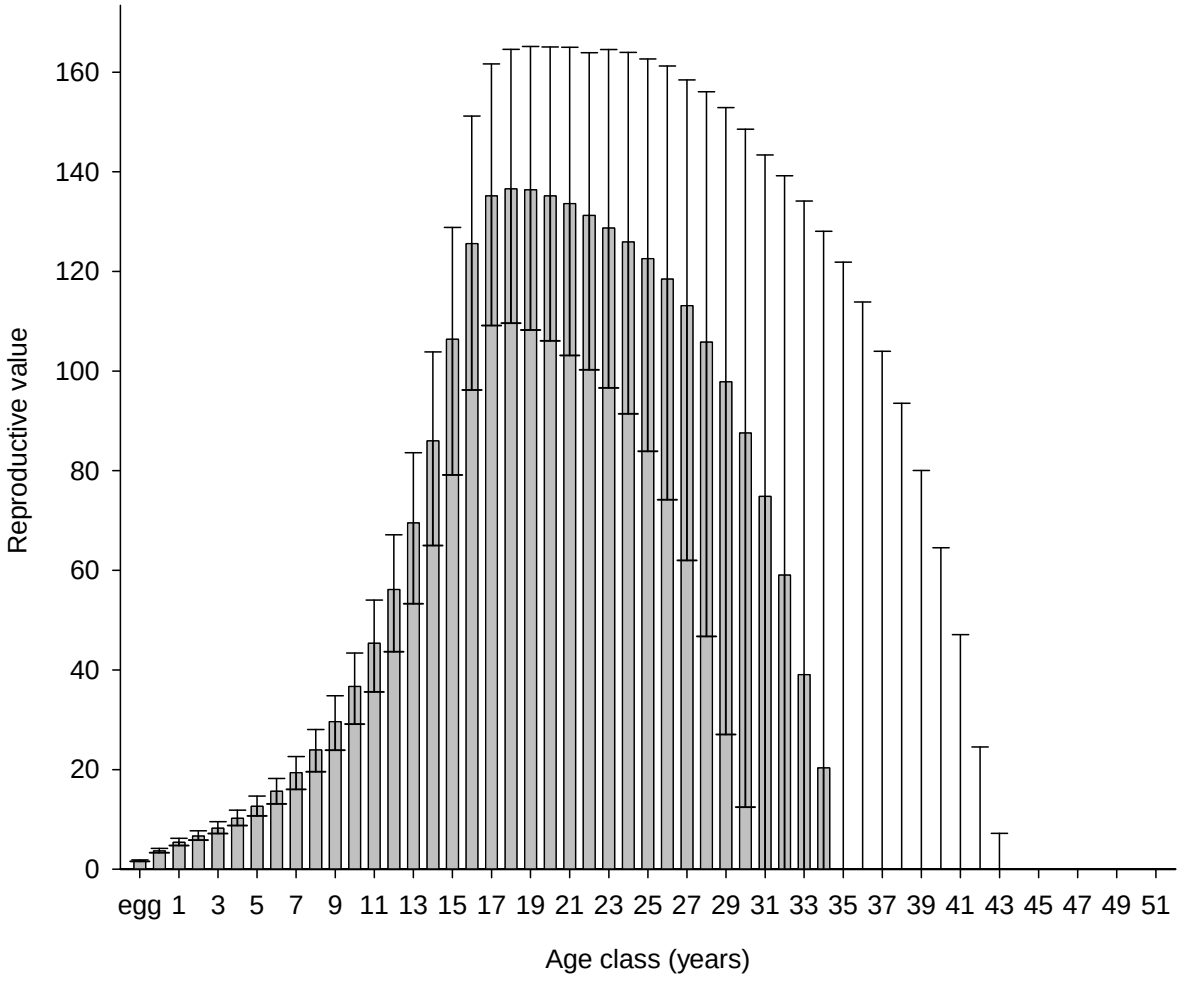

Figure 79.

Predicted mean age-specific reproductive values (V_x) for *Bathyraja lindbergi*. Error bars indicate 95% confidence intervals.

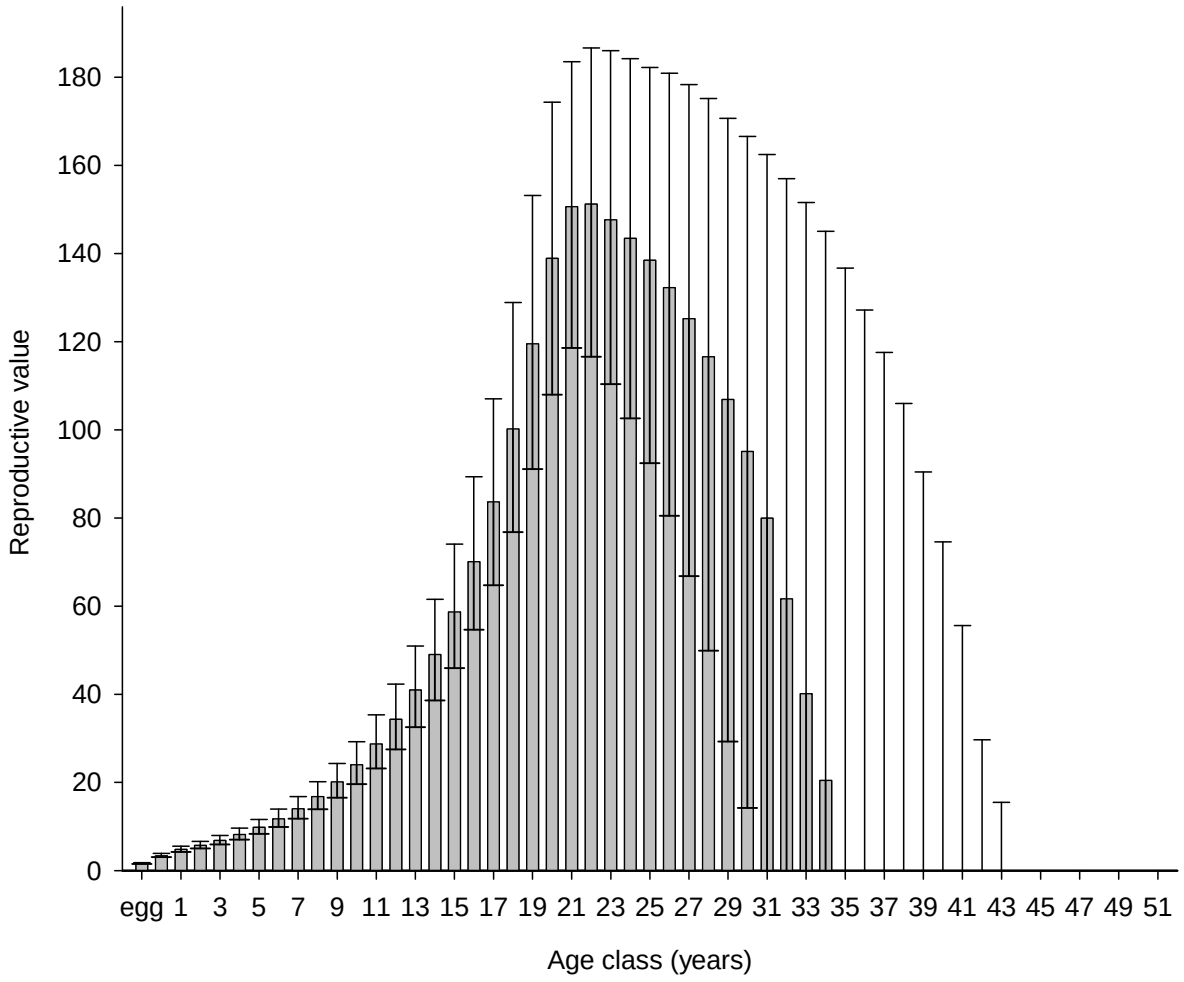

Figure 80.

Predicted mean age-specific reproductive values (V_x) for *Bathyraja maculata*. Error bars indicate 95% confidence intervals.

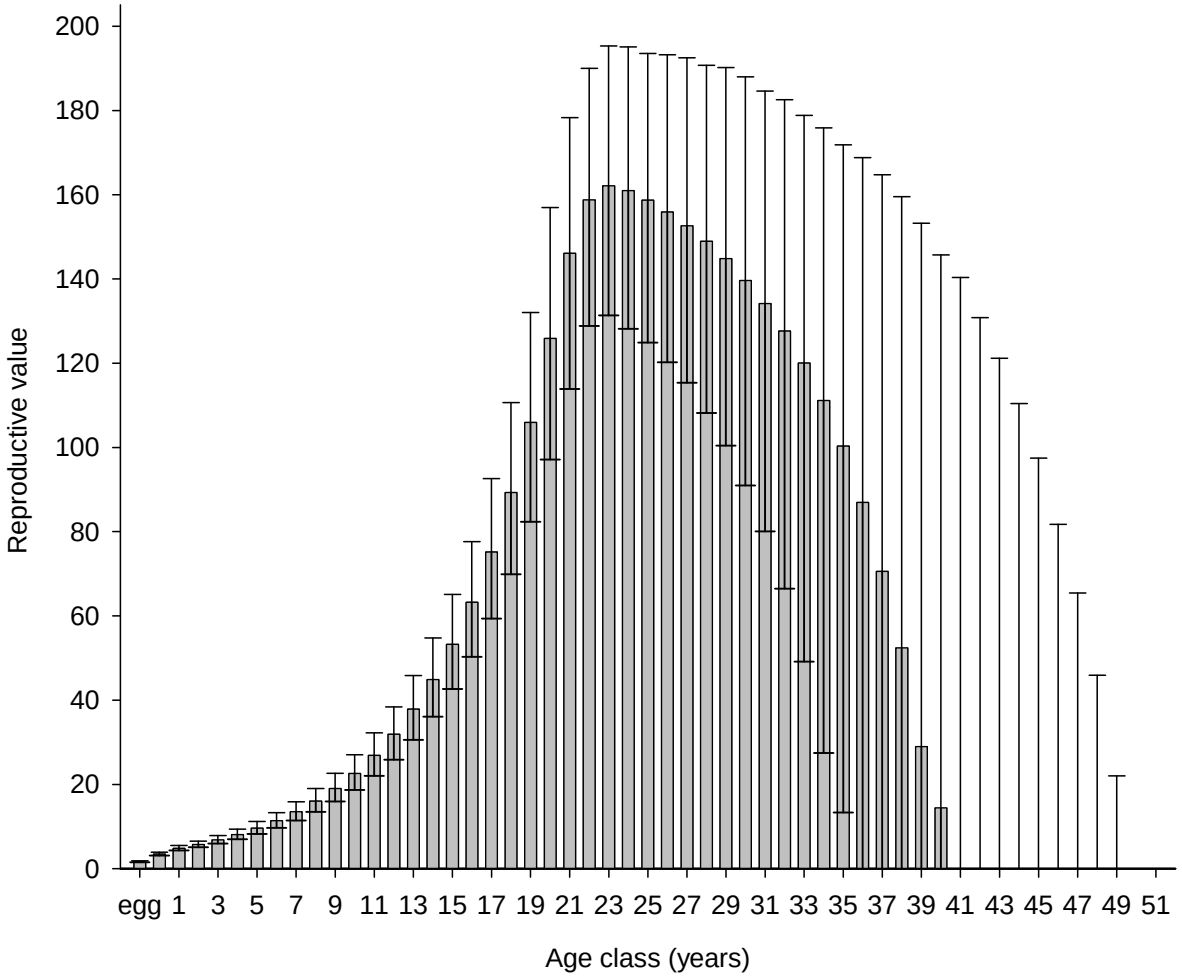

Figure 81.

Predicted mean age-specific reproductive values (V_x) for *Bathyraja minispinosa*. Error bars indicate 95% confidence intervals.

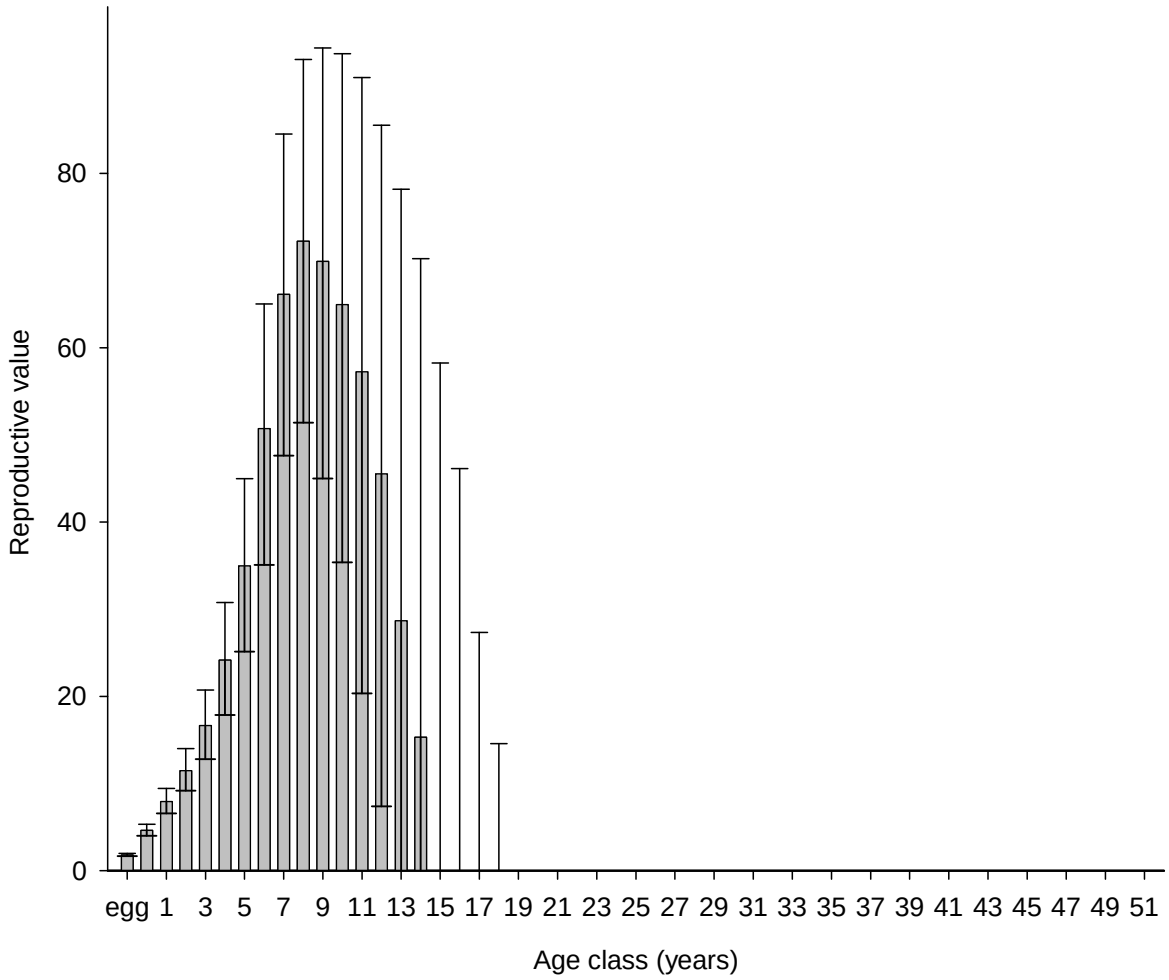

Figure 82.

Predicted mean age-specific reproductive values (V_x) for *Bathyraja taranetzi*. Error bars indicate 95% confidence intervals.

B. maculata grew proportional to TL; however the relationship was not as strong as MCD-TL relationship. There also was a significant bias between vertebral age estimates and caudal thorn age estimates, with vertebral centra producing greater age estimates in most individuals examined. Caudal thorn age estimate never exceeded 9 years; the greatest difference in age estimate between structures was 25 years. On the caudal thorns of *B. minispinosa* some bands appear thicker than others, in contrast to the examples shown as figures in both Gallagher and Nolan (1999) and Henderson et al. (2005), which displayed evenly spaced bands. Caudal thorn age estimates were consistently lower than vertebral age estimates after 5 years. The caudal thorns of *B. taranetzi* did not grow proportional to TL. Similarly, no detectable relationship was found between age estimates from caudal thorns and TL, verifying caudal thorns that were not an appropriate ageing structure for this species.

The results of this study indicate that caudal thorn band count is not in agreement with the banding on the vertebral centra of *B. lindbergi*, *B. maculata*, *B. minispinosa*, and *B. taranetzi*. There are several reasons why caudal thorns may not reflect the growth of a skate in the same way as the vertebral centra. Like centra, caudal thorns are present at the time of hatching, however they are subject to the erosive properties of water and substrate for the duration of the skate's life; this may wear down the thorn banding pattern used to estimate age causing under-age estimation. Additionally, thorns do not provide structural support and so do not need to grow in direct proportion with the overall growth of the individual.

The banding pattern of vertebral centra was not visible across the intermedialia for the majority of individuals of *B. lindbergi*, *B. maculata*, and *B. minispinosa*. For these three species the corpus calcareum was relied on for band counts. A bias was detected between reads 2 and 3 for *B. lindbergi*, ages 0-20, and *B. maculata*, ages 11-25, by McNemar's χ^2 test. The McNemar's test is sensitive to small levels of disagreement that reinforce each other upon pooling, and could be more reflective of low sample size rather than systematic bias (Evans and Hoenig 1998). Conversely the level of precision between reads was high (IAPE < 4%, both species) and percent agreement also was acceptable (80% ± 2, both species) thus it was determined that the bias detected by McNemar's test was acceptable and not biologically significant. For *B. maculata* an additional bias was detected by the Evans-Hoenig test for ages 16-20. Although not ideal, this bias only occurred within a 5 year age category, and reflects the difficulty in discerning the band pairs among certain individuals. No bias was detected between reads of *B. minispinosa* and *B. taranetzi*.

Species	TL_{max}(cm)	Age_{max}	L_∞	k	t_0	L_0	Study
B. aleutica	150.0	17	172.6	0.11	-1.78	29.7	Ebert et al. 2007
B. interrupta	86.0	13	126.4	0.08	-2.32	21.4	Ebert et al. 2007
B. lindbergi	102.1	33	119.3	0.04	-2.63	13.8	this study
B. maculata	134.0	36	169.6	0.02	-5.41	22.1	this study
B. minispinosa	89.5	37	147.0	0,02	-5.76	16.4	this study
B. parmifera	111.0	17	135.4	0.10	-1.60	20.0	Matta and Gunderson 2007
B. taranetzi	77.0	14	78.1	0.13	-1.90	17.3	this study
Raja binoculata	213.9	26	293.4	0.04	-2.01	NR	McFarlane and King 2006
R. rhina	124.6	26	133.8	0.07	-1.92	NR	McFarlane and King 2006

Table 11.

Comparison of parameters for 3-parameter von Bertalanffy growth function among Alaskan skate species; L_∞, asymptotic length; k, growth coefficient; t_0, theoretical age at 0 length; L_0, length at birth; g, instantaneous growth rate; NR, not reported

Maximum age estimates for *B. lindbergi*, *B. maculata*, and *B. minispinosa* are greater than all other skates aged to date in the North Pacific (Table 11). It is possible the maximum age estimates are under-estimates due to the long history of fishing on the EBSCS. Fishing mortality can alter life history parameters such as longevity by removing the larger, older individuals from the population. In some exploited fish populations it is possible that eventually individuals no longer attain maximum size or age because they are removed before they can reach either. In the case of *B. maculata* it is even more likely that this is an underage estimate as the maximum reported size for this species is 134 cm TL (Orlov et al. 2006) and the largest sample included in this study was 20 cm smaller at 114.5 cm TL. *Bathyraja taranetzi* maximum age estimate, 14 years, falls within the age range observed from previous age and growth studies of other eastern North Pacific skates (Table 11). However, the largest individuals of *B. taranetzi* collected for this study were ~71 cm TL, 6 cm smaller than the maximum reported size (Ebert 2005), so it is possible with the examination of larger individuals the maximum age estimate for *B. taranetzi* will be greater than 14 years.

Eastern North Pacific skates display a wide range of life history characteristics (Table 11). This will influence the way resource managers address the skate species complex in the eastern North Pacific and emphasizes the need for additional research including species specific: discard mortality rates, age validation, and fecundity.

Age estimates for *B. lindbergi*, *B. maculata*, and *B. minispinosa* are greater than those of any other skate species to date. Previous researchers estimated a maximum age at 50 years for *Raja batis*, however the maximum observed band count from the same study was only 23 (Du Buit 1972). These three species attain moderate size compared to other Alaskan species, *R. binoculata* and *R. rhina* which have maximum age estimate of 26 years (McFarlane and King 2006). These results indicate life history parameters of skates are varied and unpredictable based on size alone.

Age verification

Validation of annual band pair deposition was not possible for any of the four species. Only centra with high edge clarity were included in MIR and centrum edge analysis. For *B. lindbergi* and *B. maculata* samples were only collected from four months representing two seasons, summer and fall. Furthermore, low sample sizes for August and October prevented statistical comparison between all months; no difference was detected between MIR from June and July (both species). Although a greater number of months were represented for *B. minispinosa* and *B. taranetzi* the low sample size for most months prevented statistical comparison; no difference was detected in MIR among June, July August and October for *B. minispinosa* and between June and July for *B. taranetzi*. Visually there is some evidence of annual band formation in *B. taranetzi*, however low sample sizes prevent statistical verification of this

observation. In addition, sexes were combined for MIR analysis in all species, which may increase MIR variability or mask annual patterns. Recently, Natanson et al. (2007) found a difference between male and female MIR values of an Atlantic skate species, *Malacoraja senta*.

Although age verification was inconclusive in this study there is evidence of annual band deposition in skates including *B. parmifera* the Alaskan skate (Holden and Vince 1973, Matta and Gunderson 2007, Sulikowski et al. 2003, Natanson et al. 2007). Therefore, we assumed annual deposition of growth bands composed of one opaque and one translucent band for all four species. Future work to validate this assumption is needed for many skate species in the eastern North Pacific.

Growth parameter estimates

All of the growth models applied to *B. lindbergi* age-at-length data had high explanatory power. The Gompertz and logistic models were the best fit to age-at-length data producing realistic L_∞ values. The logistic model similarly was determined to have the best fit for *Raja rhina* (MacFarlane and King 2006), and *Carcharhinus brevipinna* the spinner shark (Carlson and Baremore 2005), while the Gompertz model, and forms of it, were the best fit model in other elasmobranch studies (Neer and Cailliet 2005, Neer and Thompson 2005, Matta and Gunderson 2007, Natanson et al. 2007).

The 3-parameter VBGF has received criticism (Knight 1968, Roff 1980), but is still the most commonly used growth function in chondrichthyan age and growth studies (Cailliet et al. 2006). The continued use of the 3-parameter VBGF facilitates comparison between species (Haddon 2001, Cailliet and Goldman 2004, Cailliet et al. 2006), and is used to develop fisheries growth models. *Bathyraja lindbergi* estimates of size at hatching and L_∞ values were greater than observed, decreasing the biological relevance of this model when compared to the logistic and Gompertz. Gamito (1998) clearly demonstrated the limited ability of the 3-parameter VBGF to describe early growth. The Richards model and polynomial model both closely matched the 3-parameter VBGF, however neither allow for direct biological interpretation of their calculated constants.

The 2-parameter VBGF provided a better biological fit to age-at-length data for *B. lindbergi* than the 3-parameter, although it had a slightly lower coefficient of determination (r^2). The disagreement between statistical and biological fit may be due to the lack of young of the year within the data set, from which the TL is used to set the length at time 0 in the model, biologically equivalent to size at hatching. The smallest individual in this study was 24.2 cm TL and assigned a band count of 0.5 years, in comparison to the observed size at hatching of 17 to 19 cm TL. The vertebral centra from individuals smaller than 25 cm TL are difficult to prepare for ageing using the method employed in this study, and often have poor clarity in their banding pattern. It may be useful in the future to investigate other

vertebral preparation techniques that could elucidate the banding pattern in these small individuals and more accurately describe early growth of all four species.

Bathyraja maculata age-at-length data were best described by the Gompertz and logistic models, although all models had high explanatory power. All models, except the 2-parameter VBGF, had greater estimates for size at hatching than has been observed. The inability of the growth models to determine size at hatching can be attributed to the lack of young of the year in the sample. The smallest individual collected was 23.7 cm TL and estimated to be 1 year old. Estimates of L_∞ also did not describe reported maximum TL for this species. The Gompertz model had the most accurate L_∞ value estimate at 127.7 cm, while the 2 and 3-parameter VBGF L_∞ values were greater than maximum observed TL. Finally, although the logistic estimates of L_∞ did not predict maximum observed size it did produce a reasonable value for this data set, indicating that with the addition of larger *B. maculata* individuals the logistic model may still produce the best fit for this species. The Richards model and polynomial model both closely matched the 3-parameter VBGF, however neither allow for direct biological interpretation of their calculated constants. Similar to *B. lindbergi* the 2-parameter VBGF provided a better biological fit to age-at-length data than the 3-parameter for *B. maculata*, although it had a slightly lower coefficient of determination (r^2).

All growth models fit the *B. minispinosa* data well, but the Gompertz model was the best fit. The Logistic and Richards models provided the lowest and most biologically reasonable estimates of L_∞ (89.6 cm TL and 96.5 cm TL, respectively). The Gompertz model estimated a much lower L_∞ (100.1 cm TL) than those of the 3 and 2-parameter VBGF models (146.9 and 130.8 cm TL), the L_0 was not as accurately estimated by. Conversely, the L_∞ estimates from the standard 3-paramter VBGF was much higher than the reported maximum sizes for the species, while the L_0 estimate was only slightly higher. Estimates of L_0 calculated from the growth curves were higher than expected given that five of the individuals included in the study that were assigned age 0 (13.6 to 15.5 cm TL) were right around the estimated size at hatching (14-15 cm). Results from this study support such claims that versions of the Gompertz model better characterize the growth of dorso-ventrally flattened elasmobranchs such as skates in comparison with the standard VB growth models (Cailliet and Goldman 2004, Neer and Thompson 2005).

Bathyraja lindbergi, *B. maculata*, and *B. minispinosa* have considerably lower growth coefficients than other Alaskan skates (Table 11). Although skates have a relatively wide range of growth coefficients, 0.05 to 0.5, reported from previous studies (Cailliet and Goldman 2004), all three of the species listed above fall outside of the previously reported range. The long lifespan coupled with relatively narrow distribution of these species could increase their susceptibility to fishing pressures.

Female and male growth curves for *B. taranetzi* were significantly different. The growth curves between the sexes differed in their growth coefficients and L_∞ values (Table 11). The largest male with suitable centra for age estimation was 66.3 cm TL, about 5 cm smaller than the largest individuals collected. Although other skate age and growth studies have found differences in male and female growth curves (Natanson et al. 2007) additional samples of larger *B. taranetzi* males are needed to confirm these observed difference between the sexes.

Despite the differences in growth parameters both sexes age-at-length data were best described by the logistic and Gompertz models ($r^2 > 0.83$ females, $r^2 > 0.79$ males; Figs. 40 & 41). The logistic model estimated a realistic L_∞ for females, while the Gompertz L_∞ estimation was greater than observed maximum TL. Both models estimated lower L_∞ values than observed for males. The calculated size at hatching from the Gompertz model was greater than observed size at hatching for both sexes.

The 3-parameter VBGF estimate did not describe early growth in females well, while in contrast estimated size at hatching for males was within the observed range. For both sexes 3-parameter VBGF L_∞ estimation did not reflect observed maximum TL. The 2 and 3-parameter VBGF as well as the Richards growth function were indistinguishable for males. The 3-parameter VBGF fit to female data was very similar to the polynomial and Richards growth functions, but differed from the 2-parameter VBGF during early growth.

Bathyraja taranetzi growth parameters and longevity are similar to other Alaskan skates falling within the previously observed age range of 12-17 years (e.g. Ebert et al. 2007, Matta and Gunderson 2007). The maximum size observed was 71.4 cm TL, which is smaller than the reported maximum TL for this species (Ebert 2005). The age estimates for *B. taranetzi* should be regarded as minimum longevity estimates until centra from larger individuals, female and male, can be examined for age estimation.

Maturity and reproduction

The maximum sizes of *B. lindbergi* and *B. minispinosa* found in this study exceeded that presently reported in the literature (Mecklenburg et al. 2002, Ebert 2005). Maximum sizes from this study were 102.1 cm TL for *B. lindbergi* and 89.5cm TL for *B. minispinosa* exceeding previous estimates by about 6 cm for both. The new *B. lindbergi* size record was a female specimen; all males collected were within the previously recorded size range. The maximum size for male *B. minispinosa*, of 83.7 cm TL found in this study also exceeded the size of the largest male reported in the literature (Mecklenburg et al. 2002, Ebert 2005). The maximum sizes observed for the other two species in this study were within previously reported ranges (Mecklenberg et al. 2002, Ebert 2005, Orlov et al. 2006).

In many elasmobranch species, including some skates, females attain and mature at larger sizes than males (Cortes 2004, McFarlane and King 2006, Ebert et al. 2007). McFarlane and King (2006) observed a size difference of 20 cm between male and female *Raja binoculata*. In contrast the largest females of *B. lindbergi* and *B. minispinosa* in this study were only ~10 cm longer than the largest males, not a striking difference. There was no size disparity observed between the sexes of *B. maculata* and *B. taranetzi*. In general it has been suggested that small and medium sized skates such as the *Bathyraja* species from this study (< 150cm) do not display sexual dimophism in maximum size (Ebert et al. 2008a & b).

Holden (1974) suggested 60-90% of asymptotic length as the range of mean length of maturity for female elasmobranchs. Cortés (2000) review of life history patterns concluded that, on average sharks reached maturity around 75% of their maximum size and 50% of maximum age, in comparison *B. lindbergi* matures slightly above that average classifying it as a mid-late maturing species. Each of the four species in this study followed this trend: *B. lindbergi* 77%, *B. maculata* 71.2%, *B. minispinosa* 81%, *and B. taranetzi* 81% (percentages based on female TL_{50}). These values are slightly lower than those calculated by Ebert (2005) for *B. lindbergi* and *B. maculata* where each of these species reached maturity at ≥ 80% of their maximum reported TL. Ebert (2005) used maximum reported TL of 96.5 cm for *B. lindbergi* and 120 cm *B. maculata*, which were the maximum reported sizes prior to Orlov et al. (2006) and this study, and may account for the disparity.

Visual assessment of maturity status may be unreliable or inconsistent, particularly during recovering phases of gonadal development (Gerristen and McGrath 2006, Vitale et al. 2006). Such errors may lead to systematic over- or underestimation of TL_{50}, skewing estimates of a population's reproductive potential. Although histological analysis of gonads was implemented, in part, as a secondary method of evaluation maturity status for a subset of samples, these analyses were only applied to males of *B. lindbergi*, *B. maculata*, and *B. minispinosa,* and small sample sizes limited their utility. Variability between TL, reproductive classification and/or gonad size was evident in each of the species examined in this study (e.g. Fig.45). Because reproductive classifications were assigned by multiple field personnel, biases or differential interpretations may have influences the observed variation. However, all personnel participation in field surveys received the same training. We note that the potential for misclassifying mature, but reproductively inactive specimens as immature was high given the criteria adopted for use in this study. Criteria for reproductive classifications frequently outline distinction for maturing individuals or distinguish categories for mature, active individuals, but lack descriptions or separate stages for resting and post-partum conditions or the possibility of senescence (e.g. Stehmann 2002, Ebert 2005). Thus, specimens that did not clearly fit into the adult or gravid categories used in this study because of recrudenscence of gonads or resorption of ova may have been inappropriately classified

as immature. These errors would result in overestimates of TL_{50} and median ages at maturity. Further verification of reproductive condition through histological, hormonal, or a combination of these assays is needed to confirm gonadal characteristics during spent, recovering, and resting phases. Future studies should consider the potential for these conditions as well the possibility of senescence by expanding reproductive classification criteria.

Size and age at maturity determined from logistic ogives were similar for both sexes of *B. lindbergi*, though maturity occurred over a greater size range for males. Median size (and age) at maturity occurred at 78.9 cm (18.5 years) for females and 80.4 cm (16.9 years) for males. This corresponds to 77.3% and 78.7% of maximum observed length, and 57.9% and 62.8% of maximum observed age for females and males, respectively.

Size at maturity estimates differ from previous estimates by Ebert (2005). The reported size at 50% maturity was 84.6 cm for females and 78.4 cm for males, greater and lesser values than this study found respectively. The difference can be accounted for by the use of different maximum TL between the two studies; other sources of variation may include variability between years, and sample size.

Bathyraja maculata size and age at maturity were similar for both sexes, though maturity occurred over a greater size range for males. Median size (and age) at maturity occurred at 95.4 cm (22.5 years) for females and 92.6 cm (20.7 years) for males. This corresponds to 71.2% and 69.1% of maximum observed length (Orlov et al. 2006), and 70.3% and 64.6% of maximum observed age for females and males respectively. Ebert (2005) reported greater size at median maturity for both sexes. Additionally, Ebert (2005) observed a much smaller range of size at maturity for males. As mentioned above these differences could be in part due to differences between years, and sample size. Age at maturity values for *B. maculata* in context with the review by Cortés (2000) indicates *B. maculata* is a late maturing species.

A difference was observed in size at maturity, but not age at maturity between male and female *B. minispinosa*. It is important to keep in mind that the crucial maturity parameter for demographic modeling of the populations, and therefore fisheries management, is the age at maturity, and in the case of *B. minispinosa*, there was no difference between sexes. Consequently, from a management perspective the difference in size at maturity may not be an important aspect of the reproductive biology of skates in general and specifically *B. minispinosa*.

Median size (and age) at maturity occurred at 67.4 cm (23.5 years) for female *B. minispinosa* and 70.1 cm (23 years) for males. This corresponds to 75.3% and 83.8% of maximum observed length, and 63.5% and 65.7% of maximum observed age for females and males respectively. The large discrepancy between males and females in size at maturity, as a percentage of maximum size, is due to the males maturing at a larger size than females, but growing to a smaller maximum size. This difference may

reflect a sampling bias rather than a biological difference between sexes. The estimates of size at maturity relative to maximum total length are lower than those of Ebert (2005) due to the larger maximum sizes included in this study as well as the different estimates of size at maturity.

Although median size and age determined from logistic ogives did not differ between female and male *B. taranetzi*, the males had a greater size range for maturity than females; the same pattern was observed in *B. lindbergi* and *B. maculata*. Median size (and age) at maturity occurred at 62.7 cm (9.1 years) for females and 57.9 cm (9.6 years) for males. This corresponds to 81.4% and 75.2% of maximum observed length, and 65.3% and 80.5% of maximum observed age for females and males respectively. Therefore, *B. taranetzi* is a late maturing species compared to the average maturation values for sharks, 50% maximum age and 75% maximum size (Cortés 2000).

In most skates, ovaries are paired and symmetrical, whereas other elasmobranchs often have one predominant and one rudimentary ovary (Lutton et al. 2005). The number of mature ova was not significantly difference between left and right ovaries for any of the four species in this study, which is consistent with other studies (Braccini and Chiaramonte 2002, Ebert 2005, Ruocco et al. 2006, Ebert et al. 2007, 2008b).

There was no consistent pattern in the relationship between mature ova diameter and maternal size among the four skates in this study. Ebert (2005) reported a "slight" increase in number of mature ova with TL for *B. taranetzi*, but sample size was small and no statistical tests were used to test the strength of the relationship.

Demographic analysis

Many demographic analyses attempt to estimate the level of fishing mortality (F) that will reduce λ to 1.0; however, these results can be misleading because classical demographic models do not account for density-dependence (Cortés, 2007). Though there are techniques being developed to incorporate density-dependent effects into demographic models (Au and Smith, 1997, Gedamke et al., 2007), we chose to keep the models as simple as possible because of the paucity of data available for fecundity. Without calculating F to reduce λ to 1.0, inference regarding the vulnerability of these populations to fishery overexploitation can be made by comparing λ among taxa. Comparisons of projected population parameters among taxa are most appropriate when similar vital rate estimation methods are used (Cailliet, 1992). For the latter reason we relied primarily on comparisons among probabilistic models.

Substantially lesser λ was predicted for all species in this study than for other Alaskan skates (Ebert et al., 2007). Compared to other elasmobranchs, these values were substantially lesser than the

midpoint of the range, but slightly greater than the median (Cortés, 2002, Frisk et al., 2002, Goldman, 2002, Beerkircher et al., 2003, Carlson et al., 2003, Smith et al., 2008, Romine et al., 2009). These results indicate that these four skates are vulnerable to population depletion by fishing mortality, based on the criteria of Musick (1999). Although the population growth rates predicted here are not among the least of elasmobranchs, they are low enough to indicate that these species are not likely candidates for sustainable directed fisheries, especially considering the magnitude and array of deleterious effects of fishing on North Atlantic skate populations (Walker and Hislop, 1998, Dulvy et al., 2000). Policy should be created to restrict mortality from incidental catch, and direct take should be prohibited or managed with great precaution.

Predicted rank order of elasticity values and ratios was similar to long-lived elasmobranchs (Cortés, 2002) and sea turtles (Heppell et al., 1999). Adult to juvenile survival elasticity ratios predicted in this study represent some of the least values for any vertebrate (Heppell et al., 1999, Heppell et al., 2000). Concordantly, juvenile survival to fertility ratios was greater than nearly all other vertebrates. These ratios, particularly the latter, were not as extreme for *B. taranetzi* as they were for the other three species. Adult survival to fertility ratios were more moderate, with values for *B. taranetzi* close to the median for mammals and elasmobranchs, and values for the other three species in the upper end of the range for teleost fishes (Heppell et al., 1999), sea turtles (Heppell et al., 1999), and elasmobranchs (Cortés, 2002). These results indicate that density-dependent compensation in the form of increased fecundity would not substantially increase λ, particularly for *B. lindbergi*, *B. maculata*, and *B. minispinosa*. The trend of great juvenile survival elasticities indicates that management efforts should be directed toward restriction of juvenile mortality.

In elasmobranchs, variability in α often affects λ with greater magnitude than other vital rates (Smith et al., 1998, Cortés, 2002). This generality held true for these skates, with variability in α impinging a much greater impact on λ than variability in ω. Age at maturity was particularly influential in the case of the shorter-lived *B. taranetzi*. Similarly, the affect of differing ω on λ was greater in *B. taranetzi* than the other species. These interspecific differences were likely caused by the presence of a greater proportion of individuals remaining in the reproductive and ultimate age classes of the shorter-lived species. The great sensitivity of λ to changes in α indicates that managers should place an emphasis on acquiring contemporary maturity estimates from populations on the same spatial scale of the management unit, because this character often varies intraspecifically with space (Parsons, 1993, Yamaguchi et al., 2000, Tovar-Ávila et al., 2007) and time (Olsen et al., 2004, Walker, 2007).

Shark life histories have been demonstrated to fall along a "fast-slow" continuum, with "slow" species defined as those with later age at maturity, greater generation times, and greater λ than "fast" species (Cortés, 2002). The relative position of skates along this life-history continuum remains unclear,

because few demographic analyses have been performed on this group. Values of $\overline{A}$ for all species except *B. taranetzi* were greater than other Alaskan skates (Ebert et al., 2007). Compared to other elasmobranchs, values for *B. taranetzi* were close to the median, but less than the midpoint of the range for $\overline{A}$ (Cortés, 2002) and μ_1 (Mollet and Cailliet, 2002, Smith, 2005), and both generation time measures for the other three species were in the upper end of the range. Rates of population increase per generation were greater than other Alaskan skates (Ebert *et al.*, 2007) and, except for *B. taranetzi*, greater than many other elasmobranchs (Mollet and Cailliet, 2002, Smith *et al.*, 2008). Net reproductive rates were lesser than those of most other Alaskan skates (Ebert *et al.*, 2007), with some similarity between *B. aleutica* and *B. minispinosa*. The value of R_0 for *B. taranetzi* was close to the lower end of the range of all elasmobranchs (Mollet and Cailliet, 2002, Smith, 2005). These comparisons indicate that the species analyzed here have moderately "slow" life histories compared to other elasmobranchs, substantially "slower" than other Alaskan skates. Skate life histories may represent a similar continuum to that of sharks, with significant interspecific variation present even within the North Pacific.

Conclusions

Bathyraja lindbergi

- Results of this study indicate that *B. lindbergi* is a slow growing, long lived, and mid-late maturing species. These life history parameters could be under-estimates given the long history of fisheries bycatch of skates on the EBSCS. More work is needed to elucidate species specific fishery mortality rates for EBSCS skates.
- Verification of vertebral centra band counts requires data from all months and was not possible in this study because samples were only available from four months.
- Caudal thorns are an unsuitable ageing structure for *B. lindbergi*.
- Assessing reproductive seasonality for *B. lindbergi* requires data from all months, including gonad measurements and histology. Future work incorporating steroid hormones would further enhance our understanding of reproductive patterns. Details on the annual fecundity of this and other Alaskan skate species are unknown and represent a critical area for continued research.
- *B. lindbergi* shared similar demographic parameters with *B. maculata*, but may be slightly more robust to increased mortality because generation times were lesser than those for *B. maculata* or *B. minispinosa*.

Bathyraja maculata

- *Bathyraja maculata* is a slow growing, long lived, and late maturing species. Additional samples of larger skates may improve fit of growth curves, and older ages may be found. Therefore, age estimates from this study should be considered minimum values.
- Verification of vertebral centra band counts requires data from all months and was not possible in this study because samples were only available from four months.
- Caudal thorns are an unsuitable ageing structure for *B. maculata.*
- As with *B. lindbergi*, more sample months are needed to accurately describe the reproductive cycle of *B. maculata*.
- Similar to the other species in this study *B. maculata*'s, predicted values of population growth were in the lower end of the range for elasmobranchs, however, great variation in the estimated age at maturity is cause for additional precaution in management.
- The life history aspects of *B. maculata* should be considered when setting bycatch limits for fisheries management as it is a common bycatch species within its range.

Bathyraja minispinosa

- The results of this study indicate that *B. minispinosa* is a slow growing, long lived, and late maturing species. It has the highest reported maximum band count of any Alaskan skate species, however it is likely, for the reasons stated above, that *B. maculata* has a similar estimated longevity.
- Verification of vertebral centra band counts requires data from all months and was not possible in this study due to the low sample size ($n < 5$) available for the majority of the 10 months sampled.
- Caudal thorns are an unsuitable ageing structure for *B. minispinosa.*
- While a difference in size-at-maturity was detected between sexes of *B. minispinosa*, there was no significant difference in the age-at maturity. The difference in size-at-maturity of 2.7 cm is statistical, but is likely not biologically significant as it is only 3% of the maximum total length.
- As in the case of *B. lindbergi* and *B. maculata*, additional sample months are needed to accurately describe the reproductive cycle of *B. minispinosa*.
- *B. minispinosa* is perhaps the most vulnerable of the species analyzed here to population depletion from increased mortality, primarily because it had the greatest generation time.

Bathyraja taranetzi

- Female and male *B. taranetzi* age estimates produced significantly different life history parameters. Although incorporation of age estimates from smaller females and larger males may prove the detected difference in this study false.
- This study shows that *B. taranetzi* longevity, growth rate, and maturity is within the range previously observed for other skates.
- Caudal thorns are an unsuitable ageing structure for *B. taranetzi.*
- Although samples were collected from 8 months low sample sizes prevent verification of centra band deposition and description of *B. taranetzi* reproductive cycle.
- *B. taranetzi* is likely the most robust to increased mortality, because this species had the greatest predicted upper confidence limit on rate of population growth, and drastically lesser generation time than the other species of this study.

Publications

Masters Thesis:

Maurer, J.R. Comparison of histology and gross sectioning techniques to determine age, growth, and reproduction of two Bering Sea skates, *Bathyraja lindbergi* and *B. maculata*. Expected completion date 2009.

Publications:

Manuscripts in preparation:

[1, 2] Comparison of histology and gross sectioning techniques to determine age, growth, and maturity of two Bering sea skates, *Bathyraja lindbergi* and *B. maculata*. Journal to be determined.

[1, 2]Age, growth, and maturity of the Alaskan mud skate *Bathyraja taranetzi.* Journal to be determined.

[1, 2]Age, growth, and maturity of the whitebrow skate *Bathyraja minispinosa.* Journal to be determined.

[1, 2]Comparative demography of four skates of the genus *Bathyraja*. Environmental Biology of Fishes.

[1, 2] Demographic patterns of Alaskan skates and the sustainability of emerging fisheries. Conservation Biology.

[1] Working titles

[2] Anticipate submissions in 2010

Outreach

Ebert, D.A. 2007. Skates of Alaska. An identification guide produced for the North Pacific Research Board. Additional print runs were made and distributed by Nora Deans, North Pacific Research Board, through various Alaskan agencies, and by personnel from the Pacific Shark Research Center at most of the below cited conferences.

Conference presentations:

Alaska Marine Science Symposium (2006)

Ebert, D.A., J.J. Bizzarro, D.L Haas, A.L. Neway, S.M. Ainsley, W.D. Smith, and G.M. Cailliet. Age, growth, and reproduction of four Alaskan softnose skates (Chondrichthyes: Rajiformes: Arhynchobatidae: *Bathyraja*).

American Elasmobranch Society (2006)

Ebert, D.A., J.J. Bizzarro, D.L. Haas, A.L. Neway, S.M. Ainsley, W.D. Smith, and G.M. Cailliet. Age, growth, and reproduction of six Alaskan skates (Chondrichthyes: Rajiformes: *Bathyraja* and *Raja*)

Western Groundfish Conference (2006)

Ebert, D.A., J.J. Bizzarro, D.L. Haas, A.L. Neway, S.M. Ainsley, W.D. Smith, and G.M. Cailliet. Age, growth, and reproduction of four Alaskan softnose skates (Chondrichthyes: Rajiformes: Arhynchobatidae: *Bathyraja*)

Alaska Marine Science Symposium (2008)

Ebert, D.A., J.R. Fry, S.M. Ainsley, and G.M. Cailliet
Preliminary results on the life history of four Bering Sea skate species, genus *Bathyraja* (Chondrichthyes, Rajiformes, Arhynchobatidae)

Western Groundfish Conference (2008)

Fry, J.R., D.A. Ebert, S.M. Ainsley, and G.M. Cailliet
Preliminary results on the life history of four Bering Sea skate species, genus *Bathyraja* (Chondrichthyes, Rajiformes, Arhynchobatidae)

American Elasmobranch Society (2008)

Maurer, J.R., S.M. Ainsley, D.A. Ebert, and G.M. Cailliet

Preliminary results on the life history of four Bering Sea skate species, genera *Bathyraja* and *Rhinoraja* (Chondrichthyes, Rajiformes, Arhynchobatidae)

Oceana Chondrichthyan Society (2008)

Ebert, D.A.

The Pacific Shark Research Center and chondrichthyan research in the North Pacific

*Keynote address at Conference

Department seminar California State University Long Beach (2008)

Ebert, D.A.

The Pacific Shark Research Center and chondrichthyan research in the North Pacific

*Invited seminar speaker

Hartnell Community College, Salinas, CA (2008)

Ebert, D.A.

The Pacific Shark Research Center and chondrichthyan research in the North Pacific

*Invited seminar speaker

Islands and Oceans Center public seminar, Homer, AK (2008)

Maurer, J.R.

Life history of two Bering sea skate species, Commander skate (*Bathyraja lindbergi*), and whiteblotched skate (*Bathyraja maculata*)

8th Indo Pacific Fish Conference (2009)

Ebert, D.A., Maurer, J.R., Ainsley, S.M., & Cailliet, G.M.

Preliminary results on the life histories of four Bering Sea skate species, genus *Bathyraja* and *Rhinoraja* (Chondrichthyes, Rajiformes, Arhynchobatidae)

American Elasmobranch Society (2009)

Ainsley, S.M., Ebert, D.A., & Cailliet, G.M.

Age, growth and maturity of the whitebrow skate, *Bathyraja minispinosa* (Ishiyama & Ishihara, 1977) from the eastern Bering Sea

Maurer, J.R., L.J. Natanson, D.A. Ebert, and G.M. Cailliet

Life history of two Bering sea skate species, Commander skate (*Bathyraja lindbergi*), and whiteblotched skate (*Bathyraja maculata*)

Moss Landing Marine Laboratories (2009)

Ebert, D.A.

Beyond Jaws: Shark Biodiversity and Conservation

Acknowledgements

We would like to thank the many people from the National Marine Fisheries Service Alaska Fisheries Science Center (NMFS-AFSC). In particular, we thank Jerry Berger, Lyle Britt, Sarah Gaichas, Jerry Hoff, Beth Matta, Jay Orr, and Duane Stevenson from NMFS-AFSC in Seattle for their input and cooperation in allowing us to participate on NMFS AFSC survey cruises in the eastern Bering Sea. Lisa Natanson of southeast NMFS provided critical feedback and analytical support throughout the project. James Sulikowski (University of New England) shared his knowledge on histological analysis. The help of students, alumni, and interns was of significant importance, and we thank the following individuals for their assistance: Joe Bizzarro, Chante Davis, Ashley Neway, Heather Robinson, Wade Smith, Megan Winton (Pacific Shark Research Center/ Moss Landing Marine Laboratories).

Additional funding was provided by NOAA/NMFS to the National Shark Research Consortium and Pacific Shark Research Center, American Elasmobranch Society, Western Groundfish Conference, Earl and Ethel Myers Foundation Grant, Signe memorial scholarship MLML Quilters Guild, and David and Lucille Packard Foundation.

Literature Cited

Au, D. W., and Smith, S. E. 1997. A demographic method with population density compensation for estimating productivity and yield per recruit of the leopard shark (*Triakis semifasciata*). Canadian Journal of Fisheries and Aquatic Sciences 54: 415-420.

Beamish, R.J., and Fournier, D.A. 1981. A method for comparing the precision of a set of age determinations. Canadian Journal of Fisheries and Aquatic Sciences 38:982-983.

Beerkircher, L., Shivji, M., and Cortés, E. 2003. A Monte Carlo demographic analysis of the silky shark (*Carcharhinus falciformis*): implications of gear selectivity. Fishery Bulletin 101: 168-174.

Beverton, R.J.H., and Holt, S.J. 1957. On the dynamics of exploited fish populations. Fishery Investigations Series II. Vol. XIX, Her Majesty's Stationery Office, London, England. 533 pp.

Braccini, J.M., and Chiaramonte, G.E. 2002. Reproductive biology of *Psammobatis extenta.* Journal of Fish Biology 61:272–288

Brander, K. 1981. Disappearance of common skate *Raja batis* from the Irish Sea. Nature 5801:48-49.

Cailliet, G.M. 1992. Demography of the central California population of the leopard shark (*Triakis semifasicata*). Australian Journal of Marine and Freshwater Research 43:183-189.

Cailliet, G.M., and Goldman, K. 2004. Age determination and validation in chondrichthyan fishes. *In* J.C. Carrier, J.A. Musick, and M.R. Heithaus (Editors) Biology of sharks and their relatives, pp. 399-447. Boca Raton, FL: CRC Press LLC.

Cailliet, G.M., Martin, L.K., Kusher, D., Wolf, P., and Welden, B.A. 1983. Techniques for enhancing vertebral bands in age estimation of California elasmobranchs. NOAA Technical Reports NMFS 8:179-188.

Cailliet, G.M., Smith, W.D., Mollet, H.F., and Goldman, K.J. 2006. Age and growth studies of chondrichthyan fishes: the need for consistency in terminology, verification, validation, and growth function fitting. Environmental Biology of Fishes 77:211-228.

Campana, S.E. 2001. Accuracy, precision, and quality control in age determination, including a review of the use and abuse of age validation methods. Journal of Fish Biology 59:197-242.

Campana, S.E., Annand, M.C., and McMillan, J.I. 1995. Graphical methods for determining the consistency of age determinations. Transactions of the American Fisheries Society 124:131-138.

Campana, S., Marks, L., Joyce, W., and Harley, S. 2001. Analytical assessment of the porbeagle shark (*Lamna nasus*) population in the Northwest Atlantic, with estimates of long-term sustainable yield. Canadian Stock Assessment, Research Document 2001/067, Ottawa, Ontario. 59 pp.

Carlson, J.K., and Baremore, I.E. 2005. Growth dynamics of the spinner shark (*Carcharhinus brevipinna*) off the United States southeast and Gulf of Mexico coasts: a comparison of methods. Fishery Bulletin 103:280-291.

Carlson, J.K., Cortés, E. and Bethea, D.M. 2003. Life history and population dynamics of the finetooth shark (*Carcharhinus isodon*) in the northeastern Gulf of Mexico. Fishery Bulletin 101:281-292.

Caswell, H. 2000. Prospective and retrospective perturbation analysis: their roles in conservation biology. Ecology 81: 619-627.

Caswell, H. 2001. Matrix Population Models: Construction, Analysis, and Interpretation. 2nd edition. Sinauer Associates, Inc., Sunderland, MA. 722 pp.

Caswell, H., Naiman, R. J., and Morin, R. 1984. Evaluating the consequences of reproduction in complex salmonid life cycles. Aquaculture 43: 123-134.

Chang, W.Y.B. 1982. A statistical method for evaluating the reproducibility of age determination. Canadian Journal of Fisheries and Aquatic Sciences 39:1208-1210.

Chen, S., and Watanabe, S. 1989. Age dependence of natural mortality coefficient in fish population dynamics. Bulletin of the Japanese Society of Scientific Fisheries 55: 205-208.

Conrath, C.L., Gelsleichter, J., and Musick, J.A. 2002. Age and growth of the smooth dogfish, *Mustelus canis*, in the northwest Atlantic. Fishery Bulletin 100:674-682.

Conrath, C.L, and Musick, J.A. 2002. Reproductive biology of the smooth dogfish. Environmental Biology of Fishes 64:367-377.

Cortés, E. 2000. Life history patterns and correlations in sharks. Reviews in Fisheries Science 8(4):299-344.

Cortés, E. 2002. Incorporating uncertainty into demographic modeling: Application to shark populations and their conservation. Conservation Biology 16(4):1048-1062.

Cortés, E. 2004. Life history patterns, demography, and population dynamics. *In* J.C. Carrier, J.A. Musick, M.R. Heithaus (Editors) Biology of Sharks and Their Relatives, pp. 449-469. Boca Raton, FL: CRC Press LLC.

Cortés, E. 2007. Chondrichthyan demographic modeling: an essay on its use, abuse, and future. Marine and Freshwater Research 58: 4-6.

Davis, C.D., Cailliet, G.M. and Ebert, D.A. 2007. Age and growth of the roughtail skate *Bathyraja trachura* (Gilbert 1892) from the eastern North Pacific. Environmental Biology of Fishes 80 (2-3), pp. 325-336

de Kroon, H., Plaisier, A., van Groenendael, J., and Caswell, H. 1986. Elasticity: The relative contribution of demographic parameters to population growth rate. Ecology 67(5):1427-1431.

Du Buit, M.H. 1972. Age et croissance de *Raja batis* et de *Raja naevus* en Mer Celtique. J. Cons. Int. Explor. Mer 37(3):261-265

Dulvy, N.K., Metcalfe, J.D., Flanville, J., Pawson, M.G., and Reynolds, J.D. 2000. Fishery stability, local extinctions, and shifts in community structure in skates. Conservation Biology 14(1):283-293.

Dulvy, N.K., and Reynolds, J.D. 2002. Predicting extinction vulnerability in skates. Conservation Biology 16(2):440-450.

Ebert, D.A. 2005. Reproductive biology of skates, *Bathyraja* (Ishiyama) along the eastern Bering Sea continental slope. Journal of Fish Biology 66:618-649.

Ebert, D.A., J.J. Bizzarro, W.D. Smith, H.J. Robinson, C.D. Davis, and A.L. Neway. 2006. Distribution and habitat associations of skates (Rajiformes: Arhychobatidae) slong the eastern Bering Sea continental slope. Western Groundfish Conference, abstract.

Ebert, D.A., Smith, W.D., Haas D.L., Ainsley, S.M. and Cailliet, G.M. 2007. Life history and population dynamics of Alaskan skate: providing biological information for effective management of bycatch and target species. North Pacific Research Board Final Report 510, 124p.

Ebert, D.A., Compagno, L.J.V., Cowley, P.D. 2008a. Aspects of the reproductive biology of skates (Chondrichthyes: Rajiformes: Rajoidei) from southern Africa. ICES Journal of Marine Science 65:81-102

Ebert, D.A., Smith, W.D., Cailliet, G.M. 2008b. Reproductive biology of two commercially exploited skates, *Raja binoculata* and *R. rhina*, in the western Gulf of Alaska
Fisheries Research 94 (1), pp. 48-57

Ebert, T.A. 1999. Plant and Animal Populations: Lessons in Demography. Academic Press, San Diego, CA. 312 pp.

Evans, G.T. and Hoenig, J.M. 1998. Testing and viewing symmetry in contingency tables, with applications to readers of fish ages. Biometrics 54:620-629

Fowler, C.W. 1988. Population dynamics as related to rate of increase per generation. Evolutionary Ecology 2:197-204.

Frisk, M.G., Miller, T.J., and Fogarty, M.J. 2002. The population dynamics of the little skate *Leucoraja erinacea*, winter skate *Leucoraja ocellata*, and barndoor skate *Dipturus laevis*: predicting exploitation limits using matrix analyses. ICES Journal of Marine Science 59:576-586.

Frisk, M.G., and Miller, T.J. 2006. Age, growth, and latitudinal patterns of two Rajidae species in the northwestern Atlantic: little skate (*Leucoraja erinacea*) and winter skate (*Leucoraja ocellata*). Canadian Journal of Fisheries and Aquatic Sciences 53:1078-1091.

Gaichas, S., Fritz, L., and Ianelli, J.N. 1999. Other species considerations for the Gulf of Alaska. *In* Stock assessment and fishery evaluation report for the groundfish resources of the Gulf of Alaska. Appendix D. North Pacific Fishery Management Council, 605 W. 4th Ave., Suite 306, Anchorage, AK 99501.

Gaichas, S., Ruccio, M., Stevenson, D., and Swanson, R. 2003. Stock assessment and fishery evaluation of skate species (Rajidae) in the Gulf of Alaska. *In* Stock assessment and fishery evaluation report for the groundfish resources of the Gulf of Alaska for 2004. North Pacific Fishery Management Council, 605 W. 4th Ave., Suite 306, Anchorage, AK 99501.

Gaichas, S., Sagalkin, N., Gburski, C., Stevenson, D., & Swanson, R. 2005. Gulf of Alaska skates. *In* Stock assessment and fishery evaluation report for the groundfish resources of the Gulf of Alaska. North Pacific groundfish stock assessment and fishery evaluation reports for 2006. Appendix B, Chapter 16, pp. 881-926.

Gallagher, M.J., Green, M.J., and Nolan, C.P. 2006. The potential use of caudal thorns as a non-invasive ageing structure in the thorny skate (*Amblyraja radiata* Donovan, 1808). Environmental Biology of Fishes 77:265-272.

Gallagher, M., and Nolan, C.P. 1999. A novel method for the estimation of age and growth in rajids using caudal thorns. Canadian Journal of Fisheries and Aquatic Sciences 56(3-4):1590-1599.

Gamito, S. 1998. Growth models and their use in ecological modeling: an application to a fish population. Ecological Modeling 113:83-94.

Gedamke, T., Hoenig, J. M., Musick, J. A., and DuPaul, W. D. 2007. Using demographic models to determine intrinsic rate of increase and sustainable fishing for elasmobranchs: pitfalls, advances, and applications. North American Journal of Fisheries Management 27: 605-618.

Gerristen, H.D., and McGrath, D. 2006. Variability in the assignment of maturity stages of plaice (*Pleuronectes platessa* L.) and whiting (*Merlangius merlangus* L.) using macroscopic maturity criteria. Fisheries Research 77:72-77.

Goldman, K. J. 2002. Aspects of age, growth, demographics and thermal biology of two lamniform shark species. Ph.D. thesis.Virginia Institute of Marine Science.

Haddon, M. 2001. Modeling and quantitative measures in fisheries. Chapman & Hall/CRC Press, Boca Raton, FL.

Hayashi, Y. 1976. Studies on the growth of the red tilefish in the East China Sea – I. A fundamental consideration for age determination from otoliths. Bulletin of the Japanese Society of Scientific Fisheries 42(11): 1237-1242.

Henderson, A. C., A. I. Arkhipkin, and J. N. Chtcherbich. 2005. Distribution, Growth and Reproduction of the White-spotted Skate *Bathyraja albomaculata* (Norman, 1937) Around the Falkland Islands. Journal of Northwest Atlantic Fishery Science. 35: 79-87.

Heppell, S.S., Crowder, L.B., and Menzel, T.R. 1999. Life table analysis of long-lived marine species with implications for conservation and management. *In* J.A. Musick (Editor) Life in the slow lane: ecology and conservation of long-lived animals, pp. 137-148. Bethesda, MD: American Fisheries Society Symposium 23.

Heppell. S.S., Caswell, H., and Crowder, L.B. 2000. Life histories and elasticity patterns: perturbation analysis for species with minimal demographic data. Ecology 81(3):654-665.

Hoenig, J.M. 1983. Empirical use of longevity data to estimate mortality rates. Fishery Bulletin 82(1):898-903.

Hoenig, J.M., Nirgab, M.J., and Brown, C.A. 1995. Analyzing differences between two age determination methods by tests of symmetry. Canadian Journal of Fisheries and Aquatic Science 52:364-368

Hoff, G. R. 2007. Reproductive biology of the Alaska skate *Bathyraja parmifera*, with regard to nursery

sites, embryo development and predation. Ph.D. Thesis. University of Washington.

Holden, M.J. 1974. Problems in the rational exploitation of elasmobranch populations and some suggested solutions. *In* F.R. Harden Jones (Editor) Sea Fisheries Research, pp. 117-137. New York: John Wiley & Sons.

Holden, M.J., and Vince, M.R. 1973. Age validation studies on the centra of *Raja clavata* using tetracycline. Journal du Conseil International pour l'Exploration de la Mer 35(1):13-17

Hood, G. M. 2005. PopTools. v. 2.6.9. http://www.cse.csiro.au/poptools.

Ishiyama, R. 1951. Studies on the Rays and Skates Belonging to the Family *Rajidae*, Found in Japan and Adjacent Regions. 2. On the Age-determination of Japanese Black-skate *Raja fusca* Garman (Preliminary Report). Bulletin of the Japanese Society of Scientific Fisheries 16(12):112-117

Jensen, A.L. 1996. Beverton and Holt life history invariants result from optimal trade-off of reproduction and survival. Canadian Journal of Fisheries and Aquatic Sciences 54:987-989.

Johnson, A.G. 1979. A simple method for staining the centra of teleost vertebrae. Northeastern Gulf Science 3:113-115.

Kimura, D.E. 1980. Likelihood methods for the von Bertalanffy growth curve. Fishery Bulletin 77(4):765-776.

Knight, W. 1968. Asymptotic growth: an example of nonsense disguised as mathematics. Journal of the Fisheries Research Board of Canada 25(6):1303-1307.

Krebs, C.J. 2001. Ecology: The Experimental Analysis of Distribution and Abundance. 5th edition. Benjamin Cummings, San Francisco. 695 pp.

LaMarca, M.J. 1966. A simple technique for demonstrating calcified annuli in the vertebrae of large elasmobranchs. Copeia 1966:351-352.

Laptikhovsky, V.V. 2004. Survival rates for rays discarded by the bottom trawl squid fishery off the Falkland Islands. Fishery Bulletin 102:757-759.

Leslie, P. H. 1945. On the use of matrices in certain population mathematics. Biometrika 33: 183-212.

Lutton, B.V., St. George, J., Murrin, C.R., Fileti, L.A., and Callard, I.P. 2005. The elasmobranch ovary. *In* W.C. Hamlett (Editor) Reproductive biology and phylogeny of Chondrichthyes: sharks, batoids, and chimaeras, pp. 237-281. New Hampshire: Science Publishers, Inc.

Maruska, K.P., Cowe, E.G., and Tricas, T.T. 1996. Periodic gonadal activity and protracted mating in elasmobranch fishes. Journal of Experimental Zoology 276:219-232.

Matta, M.E. 2006. Aspects of the life history of the Alaska skate, *Bathyraja parmifera*, in the eastern Bering Sea. MS Thesis, School of Aquatic and Fisheries Sciences, University of Washington, WA.

Matta, M.E., and Gunderson, D. 2007. Age, growth, maturity, and mortality of the Alaska skate, *Bathyraja parmifera*, in the eastern Bering Sea. Environmental Biology of Fishes 80:309-323

Matta, M.E., Gaichas, S., Lowe, S., Stevenson, D., Hoff, G., and Ebert, D. 2006. Bering Sea and Aleutian Islands skates. Stock assessment and fishery evaluation of skate species (Rajidae) in the Gulf of Alaska. *In* Stock assessment and fishery evaluation report for the groundfish resources of the Gulf of Alaska for 2007. North Pacific Fishery Management Council, 605 W. 4th Ave., Suite 306, Anchorage, AK 99501.

McFarlane, G.A., and King, J.R. 2006. Age and growth of big skate (*Raja binoculata*) and longnose skate (*Raja rhina*) in British Columbia waters. Fisheries Research 78:169-178.

McPhie, R. P., and Campana, S. E. 2009. Bomb dating and age determination of skates (family Rajidae) off the eastern coast of Canada. – ICES Journal of Marine Science 66: 546–560.

Mecklenburg, CW., Mecklenburg, T.A. and Thorsteinson, L.K. 2002. Fishes of Alaska. Bethesda, MD: American Fisheries Society. 104 pp.

Mollet, H.F., and Cailliet, G.M. 2002. Comparative demography of elasmobranchs using life history tables, Leslie matrices and stage-based matrix models. Marine and Freshwater Research 53:503-516.

Mollet, H.F., Ezcurra, J.M. and O'Sullivan, J.B. 2002. Captive biology of the pelagic stingray, *Dasyatis violacea* (Bonaparte, 1832). Marine and Freshwater Research 53:531-541.

Musick, J. A. 1999. Ecology and conservation of long-lived marine animals. *In* J.A. Musick (Editor) Life in the slow lane: ecology and conservation of long-lived marine animals, American Fisheries Society Symposium 23, pp 1–10. Bethesda, MD: American Fisheries Society.

Natanson, L.J., Sulikowski J.A., Kneebone, J.R., and Tsang, P.C. 2007. Age and growth estimates for the smooth skate, *Malacoraja senta*, in the Gulf of Maine. Environmental Biology of Fishes. 80(2-3):293-308

Neer, J.A., and Cailliet, G.M. 2001. Aspects of the life history of the Pacific electric ray, *Torpedo californica* (Ayers). Copeia 2001:842-847.

Neer, J.A., and Thompson, B.A. 2005. Life history of the cownose ray, *Rhinoptera bonasus*, in the northern Gulf of Mexico, with comments on geographic variability in life history traits. Environmental Biology of Fishes 73:321-331.

North Pacific Fisheries Management Council. 1999. DRAFT. Environmental assessment/regulatory impact review/initial regulatory flexibility analysis for amendments 63/63 to the fishery management plans for the groundfish fisheries of the Bering Sea/Aleutian Islands and Gulf of Alaska to revise management of sharks and skates. Prepared April 2, 1999, by the North Pacific Fishery Management Council and Alaska Department of Fish and Game, Juneau, AK. 72 pp.

Officer, R.A., Gason, A.S., Walker, T.I., and Clement, J.G. 1996. Sources of variation in counts of growth increments in vertebrae from the gummy shark, *Mustelus antarticus*, and school shark, *Galeorhinus galeus*: implications for age determination. Canadian Journal of Fisheries and Aquatic Sciences 53:1765-1777.

Olsen, E. M., Heino, M., Lilly, G. R., Morgan, M. J., Brattey, J., Ernande, B., and Dieckmann, U. 2004. Maturation trends indicative of rapid evolution preceded the collapse of northern cod. Nature 428: 932-935.

Orlov, A., Tokranov, A., and Fatykhov, R. 2006. Common deep-benthic skates (Rajidae) of the northwestern Pacific: Basic ecological and biological features. Cybium 30(4): 49-65.

Parsons, G. R. 1993. Geographic variation in reproduction between two populations of the bonnethead shark, *Sphyrna tiburo*. Environmental Biology of Fishes 38: 25-35.

Panfili, J., and Morales-Nin, B. 2002. Semi-direct validation. *In* Manual of fish sclerochronology (Panfili, J., Pontual, H. (de), Troadec, H., and Wright, P.J.,eds.), p. 129-134. Ifremer-IRD coedition, Brest, France.

Parent, S., Pepin, S., Genet, J.-P., Misserey, L., and Rojas, S. 2008. Captive breeding of the barndoor skate (*Dipturus laevis*) at the Montreal Biodome, with comparison notes on two other captive-bred skate species. Zoo Biology 27: 145-153.

Perez, C.R. 2005. Age, growth and reproduction of the sandpaper skate, *Bathyraja kincaidii* (Garman, 1908) in the Eastern North Pacific. MS Thesis, California State University, Monterey Bay, CA.

Richards, F.J. 1959. A flexible growth function for empirical use. Journal of Experimental Botany 10(29):290-300.

Ricker, W.E. 1979. Growth rates and models. *In* W.S. Hoar, D.J. Randall, J.R. Brett (Editors) Fish Physiology, Volume III, pp. 677-743. New York: Academic Press.

Roff, D.A. 1980. A motion to retire the von Bertalanffy function. Canadian Journal of Fisheries and Aquatic Sciences 37:127-129.

Romine, J. G., Musick, J. A., and Burgess, G. H. 2009. Demographic analyses of the dusky shark, *Carcharhinus obscurus*, in the Northwest Atlantic incorporating hooking mortality estimates and revised reproductive parameters. Environmental Biology of Fishes 84: 277-289.

Ruocco, N.L., Lucifora, L.O., Diaz de Astarloa, J.M., and Wöhler, O. 2006. Reproductive biology and abundance of the white-dotted skate, *Bathyraja albomaculata*, in the Southwest Atlantic. ICES Journal of Marine Science 63:105-116.

Serra-Pereira, B., Figueiredo, I., Farias, I., Moura, T., and Gordo, L. S. 2008. Description of dermal denticles from the caudal region of Raja clavata and their use for the estimation of age and growth. – ICES Journal of Marine Science, 65: 1701–1709.

Simpfendorfer, C.A., Chidlow, J., McAuley, R., and Unsworth, P. 2000. Age and growth of the whiskery shark, *Furgaleus macki*, from southwestern Australia. Environmental Biology of Fishes 58: 335-343.

Smith, S. E., Au, D. W., and Show, C. 1998. Intrinsic rebound potentials of 26 species of Pacific sharks. Marine and Freshwater Research 49: 663–678.

Smith, W.D. 2005. Life history aspects and population dynamics of a commercially exploited stingray, *Dasyatis dipterura*. MS Thesis, San Francisco State University, CA.

Smith, W.D., Cailliet, G.M., and Melendez, E.M. 2007. Maturity and growth characteristics of a commercially exploited stingray, *Dasyatis dipterura*. Marine and Freshwater Research 58:54–66.

Smith, W. D., Cailliet, G. M., and Cortés, E. 2008. Demography and elasticity of the diamond stingray, *Dasyatis dipterura*: parameter uncertainty and resilience to fishing pressure. Marine and Freshwater Research 59: 575-586.

Stehmann, M.F. 2002. Proposal of a maturity stages scale for oviparous and viviparous cartilaginous fishes (Pisces, Chondrichthyes). Archive of Fishery and Marine Research 50(1): 23-48.

Stevenson, D.E., Orr, J.W., Hoff, G.R., and McEachran, J.D. 2008. Emerging patterns of species richness, diversity, population density, and distribution in the skates (Rajidae) of Alaska. Fishery Bulletin 106:24-39.

Stobutzki, I.C., Miller, M.J., Heales, D.S., and Brewer, D.T. 2002. Sustainability of elasmobranchs caught as bycatch in a tropical prawn (shrimp) trawl fishery. Fishery Bulletin 100(4):800-821.

Sulikowski, J.A., Elzey, S., Kneebone, J., Jurek, J., Howell, W.H., and Tsang, P.C.W. 2007b. The reproductive cycle of the smooth skate, Malacoraja senta, in the Gulf of Maine. Marine and Freshwater Research 58: 98-103.

Sulikowski, J.A., Kneebone, J., Elzey, S., Jurek, J., Danley, P.D., Howell, W.H., and Tsang, P.C.W. 2005a. Age and growth estimates of the thorny skate (*Amblyraja radiata*) in the western Gulf of Maine. Fishery Bulletin 103:161-168.

Sulikowski, J.A., Morin, M.D., Suk, S.H., and Howell, W.H. 2003. Age and growth of the winter skate, *Leucoraja ocellata*, in the Gulf of Maine. Fishery Bulletin 101:405-413.

Tanaka, S. and Mizue, K. 1979. Age and growth of Japanese dogfish, *Mustelus manazo* Bleeker in the East China Sea. Bulletin of the Japanese Society of Scientific Fisheries 45(1):43-50.

Tovar-Ávila, J., Walker, T. I., and Day, R. W. 2007. Reproduction of *Heterodontus portusjacksoni* in Victoria, Australia: evidence of two populations and reproductive parameters for the eastern population. Marine and Freshwater Research 58: 956-965.

Tuljapurkar, S. 1997. Stochastic matrix models. *In* S. Tuljapurkar, H. Caswell (Eds.) Structured population models in marine, freshwater and terrestrial ecosystems, pp. 59-88. New York: Chapman and Hall.

Vitale, F., Svedäng, H., and Cardinale, M. 2006. Histological analysis invalidates macroscopically determined maturity ogives of the Kattegat cod *(Gadus morhua*) and suggests new proxies for estimating maturity status of individual fish. ICES Journal of Marine Science 63: 485-492.

Walker, P.A., and Hislop, G. 1998. Sensitive skates or resilient rays? Spatial and temporal shifts in ray species composition in the central and north-western North Sea between 1930 and the present day. ICES Journal of Marine Science 55: 392-402.

Walker, T. I. 2007. Spatial and temporal variation in the reproductive biology of gummy shark *Mustelus antarcticus* (Chondrichthyes:Triakidae) harvested off southern Australia. Marine and Freshwater Research 58: 67-97.

Walmsley-Hart, S.A., Sauer, W.H.H., and Buxton, C.D. 1999. The biology of the skates *Raja wallacei* and *R. pullopunctata* (Batoidea: Rajidae) on the Agulhas Bank, South Africa. South African Journal of Marine Science 21:165-179.

Yamaguchi, A., Taniuchi, T., and Shimizu, M. 2000. Geographic variations in reproductive parameters of the starspotted dogfish, *Mustelus manazo*, from five localities in Japan and in Taiwan. Environmental Biology of Fishes 57: 221-233.

Zar, J.H. 1999. Biostatistical Analysis. 4th Edition. Prentice Hall, Upper Saddle River, N.J. 663 pp.

Zeiner, S.J., and Wolf, P.G. 1993. Growth characteristics and estimates of age at maturity of two species of skates (*Raja binoculata* and *Raja rhina*) from Monterey Bay, California. *In* S. Branstetter (Editor) Conservation biology of elasmobranchs, pp. 87-90. NOAA Technical Report, NMFS 115.